

1-1-2012

Hdm2 Small-Molecule Inhibitors For Therapeutic Intervention In B-Cell Lymphoma

Angela Sosin
Wayne State University,

Follow this and additional works at: http://digitalcommons.wayne.edu/oa_dissertations

Recommended Citation

Sosin, Angela, "Hdm2 Small-Molecule Inhibitors For Therapeutic Intervention In B-Cell Lymphoma" (2012). *Wayne State University Dissertations*. Paper 622.

This Open Access Dissertation is brought to you for free and open access by DigitalCommons@WayneState. It has been accepted for inclusion in Wayne State University Dissertations by an authorized administrator of DigitalCommons@WayneState.

HDM2 SMALL-MOLECULE INHIBITORS FOR THERAPEUTIC INTERVENTION IN B-CELL LYMPHOMA

by

ANGELA M. SOSIN

DISSERTATION

Submitted to the Graduate School

of Wayne State University,

Detroit, Michigan

in partial fulfillment of the requirements

for the degree of

DOCTOR OF PHILOSOPHY

2012

MAJOR: CANCER BIOLOGY

Approved by:

Advisor

Date

© COPYRIGHT BY

ANGELA M. SOSIN

2012

All Rights Reserved

DEDICATION

All of my hard work, determination, and motivation to complete this doctoral degree would not have been possible without the inspiration of one of the greatest role models and influential mentors I have ever had. Therefore, I dedicate this dissertation to the memory of Dr. Angelika Burger. Although you passed away before this work was finished, it was a privilege to have you on my committee. Your words of encouragement and push for tenacity both as an individual and as a scientist will forever resonate with me.

To my amazing parents Rich and Carolyn Sosin, my brother Rick, the Ellerbrocks and the rest of my extended family for your unconditional love and support. I apologize immensely for missing so many family events during these past 5 years and promise I will do my best to make up for this time lost. My deepest expression of love and appreciation goes out to my remarkable boyfriend, Ryan Ellerbrock, for the sacrifices you made with me during this arduous endeavor. Without your patience, tolerance, and light-hearted attempts to understand my project by portraying it in poorly-drawn cartoons, none of this would have been possible.

ACKNOWLEDGMENTS

This dissertation project was achieved over the past several years from the advice, assistance, and expertise of many individuals. First, I am indebted to my mentor, Dr. Ayad Al-Katib. I will forever be appreciative and cannot thank you enough for your support, counsel, and willingness to let me make my own mistakes time in and time out to blossom into a highly independent investigator.

I would also like to acknowledge my amazing committee members, Dr. Rodney Braun, Dr. Ramzi Mohammad, and Dr. Gen Sheng Wu for your continuous support and constructive criticism. Thank you for your interest in this research, willingness to serve on my committee and for raising the bar and challenging me.

A special thanks to Dr. Judith Abrams for her exhausting efforts on the biostatistical analyses. To those at St. John VanElslander Cancer Center: Mary Ann Rubio for your help with, well, EVERYTHING; Mary Frances Walsh for editing this dissertation; and Mary Steigelman for corresponding with me on the patient samples. To Christine Cupps, for willingly helping me with the formatting and for your encouraging words of wisdom. To Amro (Omar) Aboukameel: Omar, thank you tremendously for being such an amazing friend to me and listening to me vent/cry on so many occasions, work related or not. I wish nothing but the best for you and the kids and there is no one that deserves happiness more than you do. Inshallah, you will find this very soon! I can never repay you for all you have done to help me make it through this endeavor alive. Thank you from the bottom of my heart.

To everyone else that made this possible. I wish I had the time and space to list off every single one of you, but I fear that list would surpass the length of this dissertation! Thank you all, I love you so very much.

TABLE OF CONTENTS

Dedication	ii
Acknowledgements	iii
List of Tables	vii
List of Figures	viii
List of Abbreviations	xi
CHAPTER I: THE ROLE OF p53 AND HDM2 IN LYMPHOMA	1
Introduction to lymphoma	1
Role of the ubiquitin-proteasome system (UPS)	8
p53: Guardian of the genome	9
E3 ubiquitin ligase HDM2	17
Targeting the UPS for cancer therapy	20
Specific aims of the study	25
CHAPTER II: MATERIALS AND METHODS	26
Experimental design	26
Cell lines and culture conditions	26
Human Investigation Committee (HIC) approval	27
Isolation and purification of patient-derived B-lymphocytes	28
Chemical synthesis, reagents, drug treatment, and competitive binding	31
Cell viability assays	31
Morphology	32
p53 sequencing	32
RNA extraction, cDNA preparation and real-time quantitative PCR (qRT-PCR)	34

Flow cytometric analysis.....	34
Western blots.....	35
Immunoprecipitation and co-immunoprecipitation.....	36
HDM2 autoubiquitination assay.....	36
Gel band quantification.....	36
Data and statistical analyses.....	37
CHAPTER III: BIOLOGICAL EFFECTS OF HDM2 SMIs IN LYMPHOMA CELLS.....	39
Introduction.....	39
Results.....	40
Summary.....	83
CHAPTER IV: NOVEL MECHANISM OF ACTION FOR MI-219.....	85
Introduction.....	83
Results.....	86
Summary.....	90
CHAPTER V: CONCLUSION, SIGNIFICANCE AND FUTURE STUDIES.....	92
Limitations of primary lymphoma cells.....	92
Appendix A: HIC APPROVAL.....	101
References.....	102
Abstract.....	121
Autobiographical Statement.....	123

LIST OF TABLES

Table 1.1 Projected New Cases and Estimated Deaths from Lymphoma in the U.S., 2012.....	1
Table 1.2 Cotswolds modified Ann Arbor staging system for NHL.....	3
Table 2.1 p53 primers used for sequencing.....	33
Table 2.2 p53 primer sets and PCR conditions.....	33
Table 2.3 List of antibodies.....	35
Table 3.1 Status of p53 in lymphoma cell lines.....	44
Table 3.2 Comprehensive list of lymphoma patients.....	50
Table 3.3 Biostatistical analyses of lymphoma patient samples.....	61
Table 3.4 Cell cycle arrest p values.....	68

LIST OF FIGURES

Figure 1.1 Age-adjusted SEER (Surveillance Epidemiology and End Results) incidence and mortality rates of NHL by sex.....	2
Figure 1.2. Age-adjusted SEER incidence and mortality rates in HL in both males and females.....	5
Figure 1.3. Secondary structure and functional domains of p53 tumor suppressor protein.....	10
Figure 1.4. The p53–HDM2 feedback loop.....	12
Figure 1.5. The enzymatic process contributing to the ubiquitin-proteasome system.....	16
Figure 1.6 Secondary structure of HDM2, its domains, and its E3 ligase activity	18
Figure 2.1. Isolation of PBMCs from a lymphoma patient in leukemic phase. A.....	29
Figure 2.2. Isolation of normal donor B-lymphocytes from post-leukoreduction apheresis cones.....	30
Figure 2.3. Location of p53 primers on p53 cDNA.....	33
Figure 3.1 Chemical structure of MI-319 and MI-219 and MDM2 protein binding assay.....	41
Figure 3.2 Amplification of p53 in four of the lymphoma cell lines used.....	43
Figure 3.3 Effect of MI-319 on cell proliferation <i>in vitro</i>	45
Figure 3.4 Effect of MI-319 on Toledo cell proliferation.....	46
Figure 3.5 HDM2 inhibitors reduce cell viability of wt-p53 lymphoma cells.....	47
Figure 3.6 Statistical significance of the ability of HDM2 inhibitors to inhibit wt-p53 lymphoma cellular growth.....	48
Figure 3.7 Treating with 20 μ M of inactive Nutlin-3b does not possess similar growth inhibitory effects as Nutlin-3 and MI-219, demonstrating the selectivity of active HDM2 SMIs binding to the p53 binding pocket of HDM2.....	49
Figure 3.8 Optimization of HDM2 inhibitors in Primary Lymphoma cells.....	51
Figure 3.9 Flow cytometric assessment of the purity of CD19+ patient-derived B lymphocytes.....	52

Figure 3.10 FACS analysis of B lymphocyte purity after pan CD2+ T cell depletion in normal blood donors.....	53
Figure 3.11 Effects of HDM2 inhibition in samples from lymphoma patients.....	55
Figure 3.12 Cumulative effect of HDM2 inhibition on the viability of primary B lymphoma cells.....	56
Figure 3.13 Effect of HDM2 SMIs on the cell viability of peripheral B lymphocytes from normal blood donors.....	59
Figure 3.14 Cumulative time- and dose-dependent reduction of cell viability of primary B lymphoma cells after HDM2 inhibition.....	60
Figure 3.15 HDM2 inhibition reduces cell survival in patient-derived lymphoma cells...	61
Figure 3.16 HDM2 antagonists activate the p53 pathway and MI-219, but not Nutlin-3, stimulates HDM2 self-ubiquitination and degradation in primary B lymphocytes.....	63
Figure 3.17 Upregulation of p53 protein predicts efficacy and biological response to MI-219 in primary lymphoma cells.....	64
Figure 3.18 Lack of effect of HDM2 SMIs on the cell viability of peripheral B lymphocytes from normal blood donors.....	65
Figure 3.19 Biological response of lymphoma cell lines to HDM2 SMIs.....	67
Figure 3.20 Assessment of apoptosis after HDM2 inhibition in lymphoma cell lines.....	69
Figure 3.21 MI-219 induces greater apoptosis than Nutlin-3 in wt-p53 WSU-FSCCL cells.....	69
Figure 3.22 Kinetics of p53 reactivation upregulates p53 and its targets upon HDM2 inhibition in lymphoma cell lines.....	71
Figure 3.23 Effect of HDM2 inhibition on p53-dependent gene expression.....	73
Figure 3.24 MI-219 enhances the stability of p53 to a greater extent than Nutlin-3.....	75
Figure 3.25 HDM2 inhibition results in disruption of the HDM2-p53 protein-protein interaction.....	76
Figure 3.26 HDM2 inhibition causes cell cycle arrest in wt-p53 lymphoma cell lines.....	77
Figure 3.27. HDM2 inhibition induces apoptosis in WSU-FSCCL, but not KM-H2 lymphoma cells.....	78
Figure 3.28 KM-H2 does not undergo apoptosis upon exposure to HDM2 SMIs.....	79

Figure 3.29 HDM2 SMIs reduce cell growth of wt-p53 HL cells.....	81
Figure 3.30 Biological effects of HL cell lines to HDM2 SMIs after a 24 hour treatment.....	82
Figure 3.31 HDM2 antagonism in HL cell lines reactivates wt-p53, but are resistant to p53-induced apoptosis.....	82
Figure 4.1 HDM2 SMIs do not inhibit E3 ligase function of HDM2.....	87
Figure 4.2 A higher concentration of zinc ejector D24 induces autoubiquitination and degradation HDM2.....	88
Figure 4.3 HDM2 autoubiquitination and degradation is detected in whole cell lysates from treated wt-p53 WSU-FSCCL (A) and KM-H2 cells (B).....	89
Figure 4.4 MI-219 enhances endogenous HDM2 self-ubiquitination and degradation.....	90

LIST OF ABBREVIATIONS

a.a.	Amino acid
ABVD	Doxorubicin, bleomycin, vinblastine, decarbazine
AMP	Adenosine monophosphate
Ara-C	Cytosine arabinoside
ARF-BP1	ADP ribosylation factor binding protein 1
ATM	Ataxia-telangiectasia mutated kinase
ATP	Adenosine triphosphate
BAX	Bcl-2-associated X protein
BCA	Bicinchoninic acid
Bcl2	B cell lymphoma 2
Bcl-xl	B-cell lymphoma-extremely large
BL	Burkitt's lymphoma
BLAST	Basic Local Alignment Search Tool
bp	Base pair
cDNA	Copy deoxyribonucleic acid
cHL	Classical Hodgkin lymphoma
CHOP	Cyclophosphamide, doxorubicin, vincristine, prednisone
CHX	Cycloheximide
CITI	Collaborative Institutional Training Initiatives
CLL	Chronic lymphocytic leukemia
CO ₂	Carbon dioxide
Cop1	Coat protein complex 1
CT	Computed tomography
$\Delta\Delta Ct$	Delta delta cross-over threshold
DBD	DNA-binding domain
DLBCL	Diffuse large B-cell lymphoma
DMSO	Dimethyl sulfoxide
DNA	Deoxyribonucleic acid
DSMZ	Deutsche Sammlung von Mikroorganismen und Zellkulturen
DUB	De-ubiquitinating enzyme
EFS	Event free survival
FACS	Fluorescence-activated cell sorting
FBS	Fetal bovine serum
FISH	Fluorescent in situ hybridization
FITC	Fluorescein isothiocyanate
FL	Follicular lymphoma
FLIPI	Follicular Lymphoma International Prognostic Index
g	Gravity
GAPDH/GAP3DH	Glyceraldehyde 3-phosphate dehydrogenase
h	Hours
HA	Human influenza hemagglutinin
HAUSP	Herpesvirus-associated ubiquitin-specific protease
HDM2	Human double minute 2
HIC	Human Investigation Committee

HL	Hodgkin lymphoma
HRP	Horseradish peroxidase
IC ₅₀	Inhibitory concentration (50%)
IgG	Immunoglobulin G
IHC	Immunohistochemistry
IP	Immunoprecipitation
IPI	International Prognostic Index
IRB	Institutional Review Board
kDa	Kilodalton
LDH	Lactate dehydrogenase
Leu	Leucine
M PER	Mammalian protein extraction reagent
MDM2	Murine double minute 2
MDM4	Protein Mdm4
Min	Minutes
mL	Milliliter
mM	Millimolar
mRNA	Messenger ribonucleic acid
Mt	Mutant
MTT	3-(4, 5-dimethylthiazol-2-yl)-2, 5-diphenyl-tetrazolium bromide
Mule	Mcl-1 ubiquitin ligase E3
MZL	Marginal zone lymphoma
NCBI	National Center for Biotechnology Information
NES	Nuclear export signal
NF-κB	Nuclear factor kappa B
NHL	Non-Hodgkin's lymphoma
NK	Natural killer
NLS	Nuclear localization signal
nM	Nanomolar
NoLS	Nucleolar localization signal
p53	Protein 53
p53AIP1	p53 apoptosis inducing protein 1
PARP	Poly (ADP-ribose) polymerase
PBL	Peripheral blood lymphocytes
PBMC	Peripheral blood mononuclear cells
PBS	Phosphate buffered saline
PCR	Polymerase chain reaction
Phe	Phenylalanine
PI	Propidium iodine
Pirh2	p53-induced RING-H2
PUMA	p53 upregulated modulator of apoptosis
PVDF	Polyvinylidene fluoride
qRT-PCR	Quantitative reverse transcription polymerase chain reaction
RBC	Red blood cell
R-CHOP	Rituximab, cyclophosphamide, doxorubicin, vincristine, prednisone
RING	Really interesting new gene

RITA	Reactivation of p53 and induction of tumor cell apoptosis
RPMI medium	Roswell Park Memorial Institute medium
RS	Reed-Sternberg
SCT	Stem cell transplantation
SDS-PAGE	Sodium dodecyl sulfate polyacrylamide gel electrophoresis
SEER	Surveillance epidemiology and end results
SLL	Small lymphocytic lymphoma
SMI	Small molecule inhibitor
SNP	Single nucleotide polymorphism
SV40	Simian virus 40
TdT	Terminal deoxynucleotidyl transferase
TIGAR	TP53-induced glycolysis and apoptosis regulator
TP53	Tumor protein 53
Trp	Tryptophan
TUNEL	Terminal deoxynucleotide transferase dUTP nick end labeling
Ubc	Ubiquitin conjugating enzyme
UPS	Ubiquitin proteasome system
UV	Ultraviolet
WCL	Whole cell lysate
WHO	World Health Organization
WM	Waldenström's macroglobulinemia
WSU-DLCL ₂	Wayne State University diffuse large cell lymphoma 2
WSU-FSCCL	Wayne State University follicular small cleaved lymphoma
WSU-WM	Wayne State University Waldenström's macroglobulinemia
Wt	Wild-type
µg	Microgram
µL	Microliter

CHAPTER I

THE ROLE OF p53 AND HDM2 IN LYMPHOMA

Introduction to Lymphoma

Lymphoma, a complex, heterogeneous set of lymphocyte malignancies, is the most common hematological malignancy in the United States. Lymphomas are classified into one of two major groups: Hodgkin lymphoma (HL) and non-Hodgkin's lymphoma (NHL), the former being less common than the latter (Table 1.1). Both HL and NHL display variable behavioral characteristics and respond differently to treatment. It is estimated that over 660,000 people in the United States are currently living with, or are in remission from, lymphoma.

Table 1.1 Projected New Cases and Estimated Deaths from Lymphoma in the U.S. 2012.

Type	New Cases			Deaths		
	Total	Male	Female	Total	Male	Female
Hodgkin Lymphoma	9,060	4,960	4,100	1,190	670	520
Non-Hodgkin's Lymphoma	70,130	38,160	31,970	18,940	10,320	8,620
Total	79,190	43,120	36,070	20,130	10,990	9,140

Source: *Cancer Facts and Figures, 2012*. American Cancer Society: 2012.

Non-Hodgkin lymphoma

Over 70,000 new cases of NHL will afflict individuals in the U.S. in 2012, 5% of all cancer cases and 3% of all cancer related deaths (1). The incidence of NHL in the U.S. has risen more than 82.5% from 1975-2008, an average of 3% annually (2). Cancer rates increase with age of the population but age is not the only factor contributing to these increases (Figure 1.1) (2). Despite the alarmingly high incidence, mortality rates have decreased dramatically since the turn of the century (Figure 1.1) (2). This could be attributed to detection of differences in the biology of the tumor as a

result of scientific advancements, and more personalized therapy.

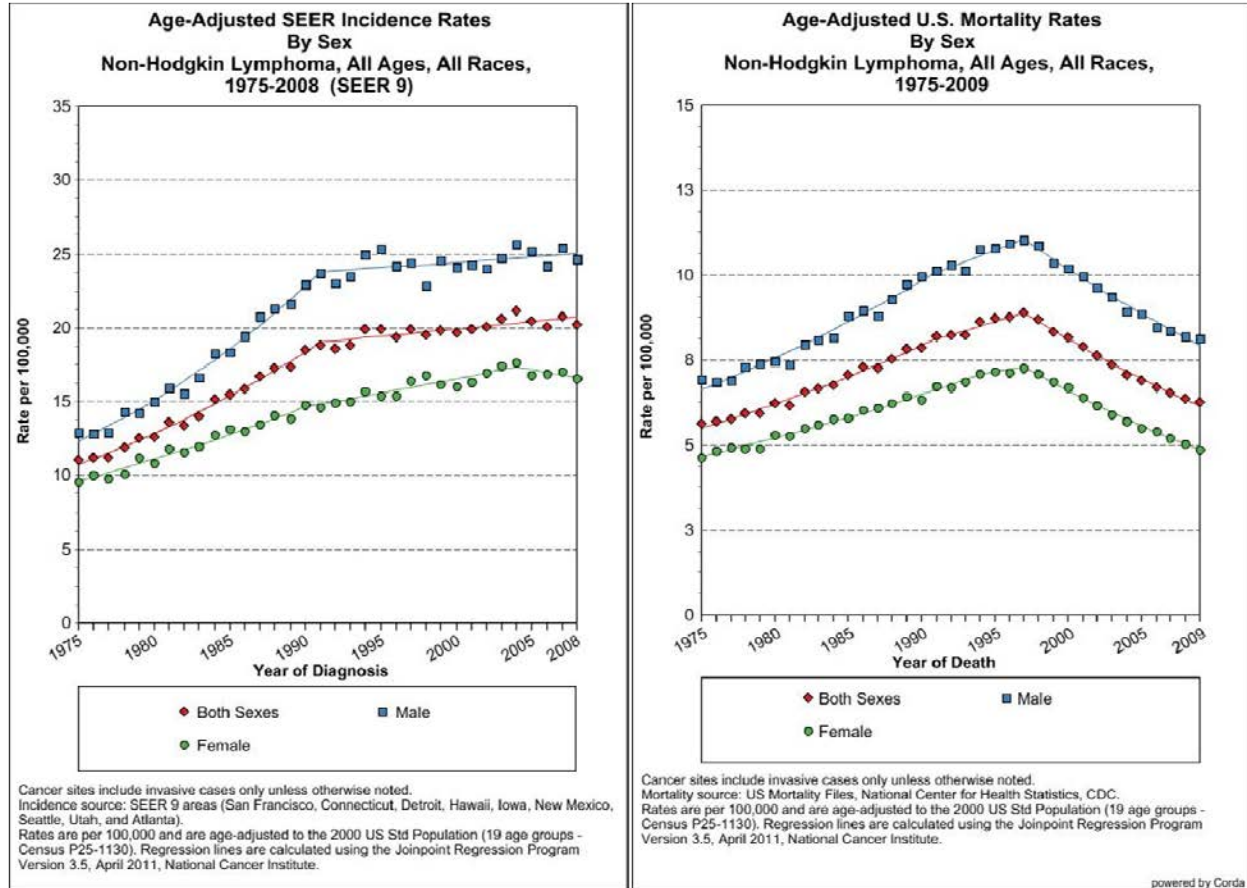


Figure 1.1 Age-adjusted SEER (Surveillance Epidemiology and End Results) incidence and mortality rates of NHL by sex (2).

Since NHL comprises many disease subtypes each with different biological characteristics and prognosis, classifying lymphomas is essential to diagnosis and subsequent treatment strategy. NHL was initially classified based on histopathologic appearance and placed into 1 of 3 subtypes in 1966 (3, 4). More sophisticated diagnostic tests have been implemented as research has progressed resulting in frequent modification of classification systems. Currently, the World Health Organization (WHO) has classified more than 60 subtypes based on a combination of morphology, immunophenotype, genetic and clinical features (5). Approximately 85% derive from B lymphocytes where the origin of disease can be located at a certain stage of B cell

differentiation within precursor or peripheral cells. The rest comprise T cell and natural killer (NK) cell lymphomas. This study focused primarily on B cell NHL.

NHL cells contain antigenic markers that are identified by immunohistochemistry (IHC) and flow cytometry. Genetic abnormalities are often associated with lymphomas, particularly chromosomal translocations, insertions, or deletions detected by karyotyping or fluorescent in situ hybridization (FISH). These abnormalities may play a role in the pathogenesis of specific subtypes of NHL and some are currently important prognostic factors.

The stage, or extent of the spread of disease, is established after diagnosis and determines the prognosis and treatment. In 1966, lymphoma was the first disease for which a tumor staging system was recommended, as exemplified by the Rye staging (6). The Cotswolds modified Ann Arbor staging system is in use at the current time (7, 8) Table 1.2 (9, 10).

Table 1.2. Cotswolds modified Ann Arbor staging system for NHL. (7)

Stage	Definition
I	The tumor is located to a single region, usually 1 lymph node and the surrounding area.
II	The tumor is located in multiple regions on the same side of the diaphragm.
III	The disease has spread to the lymph nodes on both sides of the diaphragm (III ₁) or the disease has spread into an area or organ next to the lymph node (III ₂).
IV	Diffuse involvement of extranodal sites beyond those designated in E, including bone marrow, liver, brain, or pleura.
Suffixes: E , involvement of one extranodal site, contiguous or proximal to identified nodal site of disease. X , presence of bulky disease >10 cm. Stage followed by A or B where: A - no disease symptoms B - presence of disease symptoms; >10% body mass reduction in 6 month period, fevers of $\geq 38^{\circ}\text{C}$ for 3 consecutive days or more, recurrent drenching night sweats.	

The behavior of NHL may be characterized as indolent, aggressive or very aggressive. Aggressive lymphomas are fast growing and high grade, but are potentially

curable. The cure rate depends on a number of prognostic factors as outlined in the International Prognostic Index (IPI) and can vary from 26% to 73% (11). Diffuse large B-cell lymphoma (DLBCL) accounts for 31% of all NHL (12) and serves as a paradigm for the treatment of aggressive lymphomas whereas very aggressive lymphomas are exemplified by Burkitt's lymphoma (BL). These are some of the most curable forms and are expected to be more responsive since current chemotherapies target actively dividing cells (13). Indolent lymphomas are slow growing and relatively low grade, and are currently incurable with existing treatment regimens. Follicular lymphoma (FL) constitutes 30-35% of all NHL and is considered to be the prototypical indolent type (14). Because of their slow growing nature, it is difficult to predict treatment outcome for indolent NHL. The Follicular Lymphoma International Prognostic Index (FLIPI) has established 5 factors that assist in outcome prediction and is a modification of the IPI for less aggressive NHL (15). These prognostic factors are age, stage III or IV, low hemoglobin levels (<12 gm/dL), greater than 4 lymph node sites affected, and elevated LDH levels. Other indolent subtypes include chronic lymphocytic leukemia/small lymphocytic lymphoma (CLL/SLL), marginal zone lymphoma (MZL), and Waldenstrom's macroglobulinemia (WM) which is a lymphoplasmacytic lymphoma.

Hodgkin lymphoma (HL)

Over 9,000 new cases of HL are predicted to occur in the U.S. in 2012 resulting in an estimated 1,000 deaths (1) (Table 1). Overall incidence rates of HL have decreased, but there has been a slight increase in young adults (16). As with NHL, mortality rates in the U.S. have decreased from 1975-2009 (Figure 1.2).

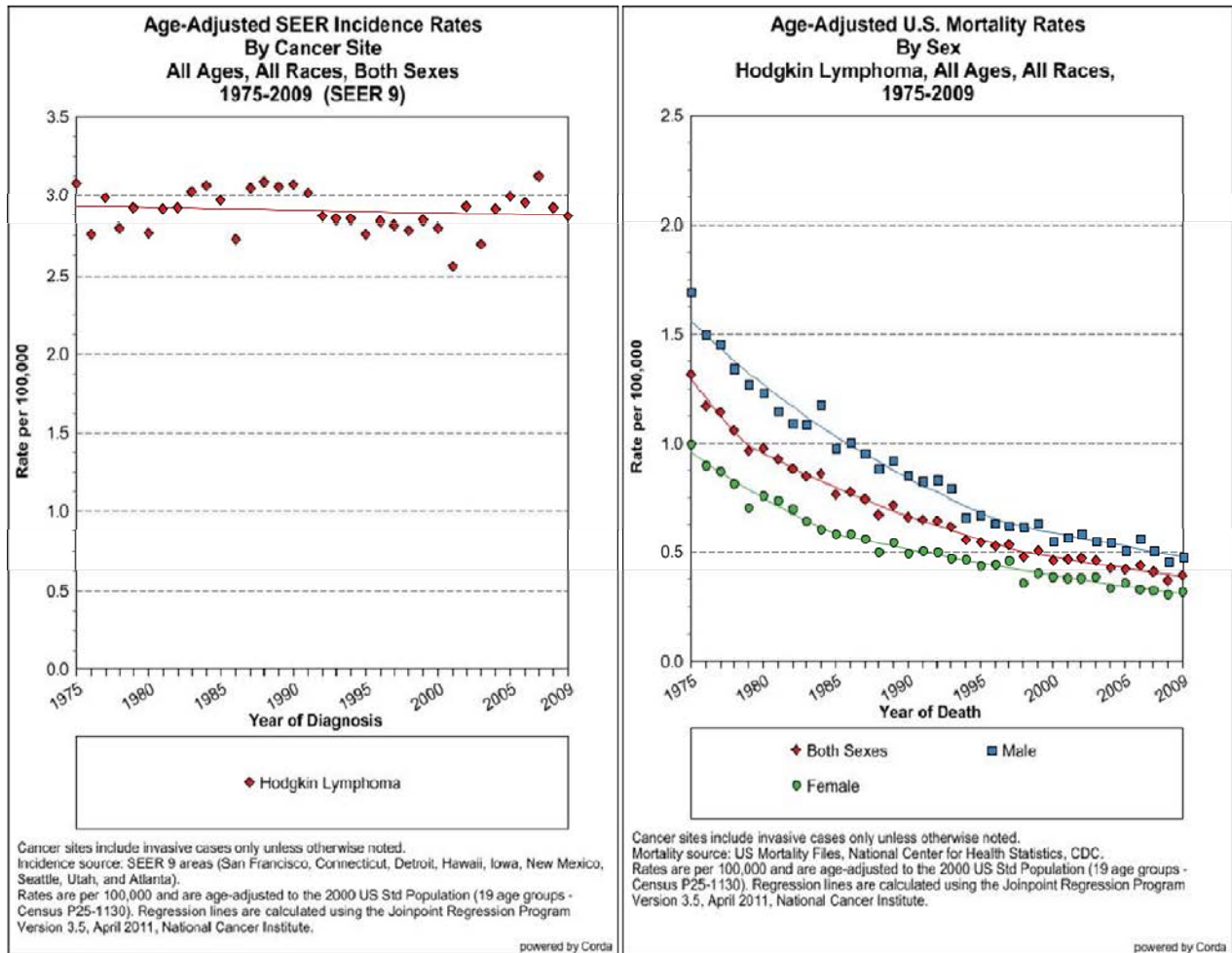


Figure 1.2. Age-adjusted SEER incidence and mortality rates in HL in both males and females (2).

HL was initially described by Thomas Hodgkin in 1832 and the disease was later named after him (17). Giant, multinucleated Reed-Sternberg (RS) cells are a characteristic feature of HL. RS cells typically contain two nuclei but can be multinucleated or mononuclear and are thought to be of B cell origin. Infiltration of reactive cell types with the RS cells defines specific HL subtypes. HL is broadly divided into two categories: 1.) nodular lymphocyte-predominant HL (approximately 5% of all HL cases) (18) and 2.) classical HL (cHL) (the remaining 95%) consisting of nodular sclerosis, mixed cellularity, lymphocyte-rich, and lymphocyte depleted types.

Treatment of lymphomas

Treatment for lymphomas is generally based on stage of disease and histologic subtype and varies from NL to NHL. Therapeutic options for B-cell lymphomas consist of conventional cytotoxic chemotherapeutics, radiation therapy, immunotherapy or stem cell transplantation (SCT). Since the 1970's, a combination of cyclophosphamide, doxorubicin, vincristine and prednisone (CHOP) has been the standard form of cytotoxic therapy for NHL. Indolent lymphomas frequently undergo initial 'watch and wait' approach since they are incurable. Although very aggressive lymphomas are curable with intensive chemotherapy, there is no standard treatment. Alternative chemotherapy regimens incorporating higher doses of additional cytotoxic agents like methotrexate and cytosine arabinoside (Ara-C) were shown to improve therapeutic efficacy. The cure rate with chemotherapy alone has reached a plateau of approximately 40% for aggressive NHL subtypes (19). Radiation can be used in conjunction with chemotherapy or at relapse, with or without SCT. Despite the initial activity of these regimens, overall efficacy is limited due to high toxicity or disease resistance.

A combination of doxorubicin, bleomycin, vinblastine, and decarbazine (ABVD) has been the standard chemotherapy regimen for HL with or without radiotherapy, depending on stage and histological grade. In use since the mid-1970's, this regimen has been shown to provide patients with the highest efficacy and the lowest toxicity (20-22). Although the majority of HL patients are cured with current treatment modalities, relapse can, and does, occur with a worse outcome (23, 24). Long-term toxicity such as infertility, development of secondary tumors, premature menopause, and cardiopulmonary complications are also major concerns and a challenge to overcome.

Extensive recent research efforts have paved the way to a better understanding

of the molecular pathobiology of lymphomas. This has provided new clues on how to exploit the underlying pathogenesis for therapeutic intervention. One such approach is the development of a monoclonal antibody, rituximab, specifically targeting the CD20 antigen expressed on B-cell neoplasms. When added to CHOP (i.e. R-CHOP), the event free survival (EFS) in patients with aggressive NHL was increased approximately 16% (25), and 18% in patients with indolent NHL (26). However, the overall survival of indolent lymphoma has not significantly improved even with the success of rituximab as a targeted therapy (26, 27), suggesting that the underlying biology of the disease largely dictates outcome.

As in the majority of human cancers, levels and activation of tumor suppressors and proto-oncogenes are deregulated in lymphomas (28). However, in contrast to most solid tumors, the course of proto-oncogene activation, at least in NHL, is via chromosomal translocations. Regardless, presence of a translocation alone is not sufficient to drive lymphomagenesis as they are infrequently found in HL (29). Indeed, a number of different genetic lesions and alterations to signal transduction pathways appear to be important in defining events implicated in the pathogenesis of lymphomas (28). Many of these alterations are becoming more and more useful as prognostic predictors in both NHL and HL, particularly the p53 pathway, which is part of the ubiquitin proteasome system (UPS), and an important focus of this study.

Most importantly, identification of molecular defects has led to the development of novel targeting agents. This is reflected by the numerous preclinical and clinical trials investigating targeted therapeutics to several different molecular targets. The challenge is to identify highly selective agents that will complement conventional chemotherapy to reduce toxicity and improve survival rates when managing both HL and NHL.

Of particular interest and primary focus of this study is the p53-HDM2 protein-protein interaction, a pathway within the ubiquitin proteasome system (UPS), and the preclinical assessment of novel anti-cancer agents to target p53-HDM2 disruption in lymphoma cells.

Role of the ubiquitin-proteasome system

The ubiquitin-proteasome system (UPS) is perhaps the most important pathway for monitoring eukaryotic cell proteolytic activity. An estimated 80-90% of protein degradation is thought to be regulated by the UPS. Both short- and long-lived proteins are continually destroyed at variable half-lives and restored by *de novo* synthesis (30, 31). The UPS causes rapid substrate proteolysis which inactivates and eliminates damaged, oxidized, or misfolded proteins before they aggregate (32), serving an essential role in the maintenance of physiologic function of intracellular proteins.

Because the UPS serves to sustain cellular homeostasis and critical mechanisms exist to regulate its function precisely and with high specificity, it should come as no surprise that alterations to components of the UPS have been associated to a variety of human diseases, including cancer. Many deregulated signaling pathways in cancer cross-talk with the UPS by undergoing ubiquitination and proteasomal degradation. Some of the proteins targeted for degradation include transcription factors, cell cycle regulators, and signal transducers that are involved in numerous signaling pathways and biological processes such as cell division, apoptosis, DNA repair, cell cycle arrest, transcriptional regulation, differentiation and endocytosis (33, 34). In fact, p53 is heavily regulated by various components of the UPS, particularly by its predominant negative regulator, HDM2.

p53: Guardian of the genome

In 1979, the T-antigen of simian virus 40 (SV40) was found to be associated with a 53 kilodalton (kDa) protein (35). Protein 53 (p53, protein product of the TP53 gene), was initially identified as an oncogene (36). However, extensive studies determined that the T-antigen of SV40, a viral oncogene, was blocking p53 activity and not vice versa since wt-p53 was unable to transform cells in culture. It later became clear that the function of p53 was tumor suppressive rather than oncogenic (37-39), a paradigm shift that occurred more than a decade after its discovery. Today, p53 is cited in over 62,000 literature publications and is viewed as the 'guardian of the genome' due to its role in conservation of genomic stability and its involvement in development, aging, and numerous diseases, particularly cancer. Furthermore, it is found in all cells, although p53 expression and activity is both cell type and context specific.

More genetic errors arise with the loss of p53 function, leading to a higher susceptibility to cancer. This was demonstrated in genetically engineered p53 null mice (40). These mice developed spontaneous tumors at an early age and had a significantly shorter life-span compared to heterozygous or wild-type p53 mice (40). Interestingly, 45-70% of these spontaneous tumors were lymphomas in p53 null mice from two different strains. This highlighted the possibility that there may be underlying predisposing cell- or tissue-specific factors in lymphoma and other cancers. Therefore, the integrity of functional p53 activity is vital to the development and protection of normal cells from cancer development.

Detection of p53 mutations and their alteration of tumor suppressor function were initially discovered in most colon cancers in 1989 (38). Today, the importance of p53's function is underscored by its frequent mutation rate found in at least 50% of all cancers

(41, 42). Interestingly, however, p53 mutations are far less prevalent in hematological malignancies compared to solid tumors suggesting that p53 loss-of-function is important to the course of cancer progression.

Structure and function

The human TP53 gene is located on the short arm of chromosome band 17p13.1, encoding a pleiotropic transcription factor (43). The predominant p53 mRNA transcript consists of 11 exons, although the coding sequence lacks the 1st exon. The resulting p53 protein product is composed of 393 amino acids (a.a) in length, divided into five evolutionarily conserved domains that reflect a specific function (Figure 1.3).

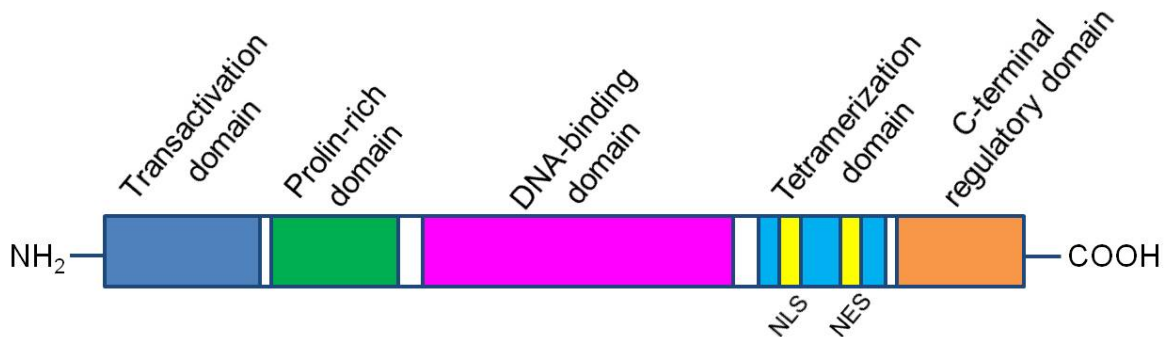


Figure 1.3 Secondary structure of p53 tumor suppressor protein. Human p53 protein is composed of five domains, each corresponding to specific functions.

These domains and their residues include: the transactivational domain (1-42 a.a), a proline-rich domain (63-97 a.a), a DNA-binding domain (DBD) (98-292 a.a), a tetramerization domain (324-355 a.a), and a C-terminal regulatory domain (363-393 a.a) (44). Additionally, p53 contains a nuclear localization signal sequence (NLS) and three nuclear export signal sequences (NES) located within the tetramerization domain (44). The transactivation domain is located at the N-terminus which interacts with co-transcription factors that aid in modulating gene expression. The proline-rich domain is

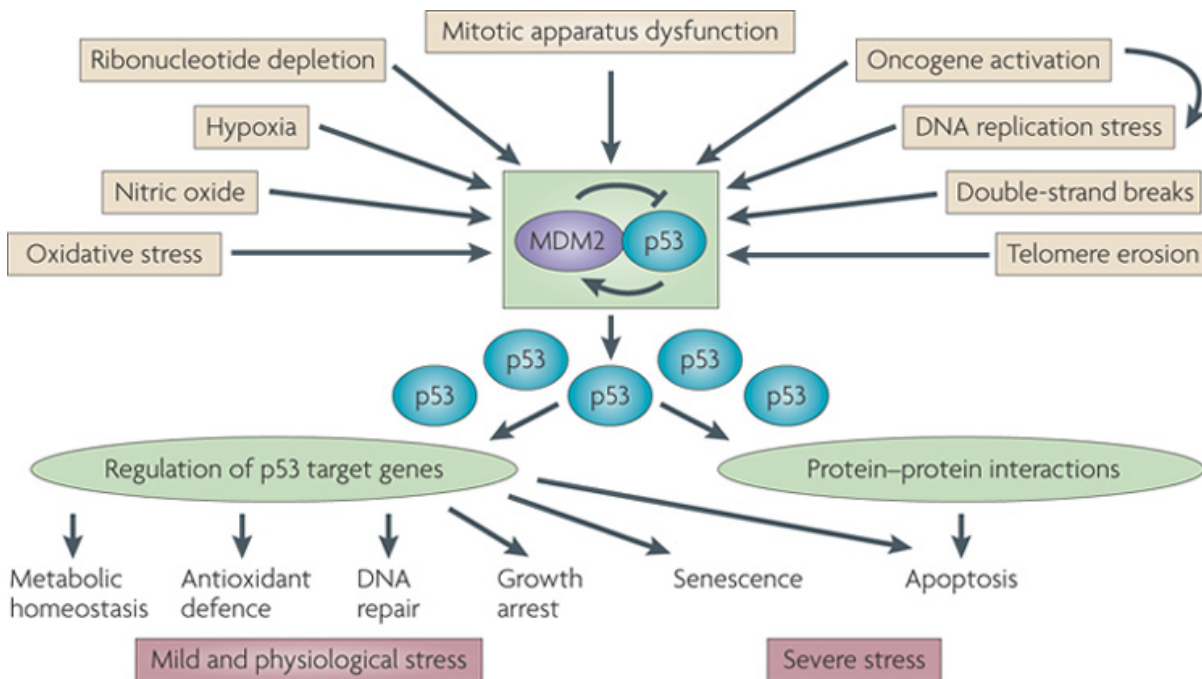
also located at the N-terminus. Its function, which once was poorly characterized, has been shown to be critical for a complete p53 apoptotic response to genotoxic DNA-damaging agents (45). The DBD is located at the central core and binds to consensus sequences of DNA often in the promoter region of p53 target genes. Mutations in the DBD account for 90-95% of all p53 mutations, and encompass exons 5-9 (46, 47). Most of these are single a.a. substitution point mutations and are quite often located at 'hot spots', or frequently mutated spots in p53. Codons 248, 273, and 175 are some of the most frequently mutated, corresponding to the distribution pattern in other cancers (48). Transcription of p53 target genes is abrogated 81% of the time by the inability of p53 to bind to DNA (49). Interestingly, not all p53 mutations are considered to be equal and depending on their location, some have been shown to possess partial transcriptional activity (49). Less than 5% of all p53 mutations takes place outside of the DBD and occurs very rarely in lymphomas (50). Lastly, the C-terminal domain binds to DNA non-specifically and acts as a sensor to numerous posttranslational modifications. Of note, additional p53 isoforms do exist and are generated by alternative splicing of transcript variants.

p53 becomes activated in response to various cellular stresses to elicit multiple biological responses. Upon activation, p53 primarily acts in a transcription-dependent manner, forming a tetrameric complex that binds to DNA using its DNA-binding domain in the nucleus. This transactivates a plethora of target genes that regulate biological outcomes such as cell cycle, DNA damage and repair, apoptosis, senescence, and differentiation (51-54). Recent studies have also demonstrated p53 involvement in the regulation of autophagy, glycolysis, and metastasis (55-57). It can also act in a p53-transcription-independent manner in the cytosol to facilitate biological responses such

as apoptosis via direct action at the level of the mitochondria and autophagy.

Levels of active p53 are tightly regulated, although the precise mechanisms of this regulation are not entirely understood. Regulatory pathways involving posttranslational modifications are thought to predominantly mediate control over p53 activity and stabilization, some of which are shown in Figure 1.4 (58).

p53 posttranslational modifications determine biological outcome (59, 60). DNA damage or genotoxic stress can stabilize p53 by inhibiting HDM2 (MDM2 or E3 ubiquitin ligase)-directed p53 ubiquitination (reviewed below) (61). A variety of DNA-damaging agents, including UV and ionizing radiation, induce phosphorylation of p53 residues



Nature Reviews | **Cancer**

Figure 1.4 The p53–HDM2 feedback loop. p53 is maintained at low levels by its negative regulator, HDM2. p53 becomes activated upon various stress signals that release it from HDM2-mediated inhibition and results in elevated protein levels. Once released and depending on the severity of stress, p53 is subjected to interaction with other proteins and posttranslational modifications that can influence the p53-dependent response. p53 can act in a transcription-dependent manner upregulating target genes to carry out cellular response or in a transcription-independent way by acting as a cytosolic pro-apoptotic facilitator at the mitochondria. Reprinted by permission from Macmillan Publishers Ltd: Nature Reviews Cancer. (62) Copyright 2009.

within its N-terminal domain. Phosphorylation reduces p53 affinity for HDM2 and inhibits the ubiquitination and degradation of p53. ATM (ataxia-telangiectasia mutated kinase) is also capable of reducing ubiquitination and degradation of p53 by phosphorylating HDM2 (63). The most studied mode of regulating p53 ubiquitination is that of the p14 tumor suppressor that also binds to HDM2, preventing HDM2-mediated degradation of p53 (64). Thus, p53-HDM2 binding is central to the regulation of p53 activity (Figure 1.4).

Clinical significance

Inactivation of p53 promotes lymphomagenesis, although how it functions to prevent lymphoma remains unclear. Evidence suggests that p53-dependent apoptosis is required for cellular homeostasis of B cells (65, 66). Moreover, p53 has been shown to play a role in B cell differentiation. A recent *in vivo* study demonstrated that wt-p53 was capable of preventing the accumulation of incorrectly differentiating B cells, thereby suppressing the development of lymphoma (67). More recently, Mcl-1 ubiquitin ligase E3 (Mule), was shown to be crucial for B lymphocyte development, proliferation, immune response and homeostasis through a feedback loop with p53 in both normal and stressful conditions, adding an additional layer of complexity to p53 function in B cells.

The incidence of p53 mutations varies depending on the lymphoma type, subtype and stage of disease. Considering that the frequency of p53 mutations in hematological malignancies as a whole ranges from 5-20 percent (47, 68), lymphomas must share similar features that are cell-type specific. The p53 pathway is often compromised by alternative mechanisms. Defects upstream or downstream in the p53 pathway are typically observed in lymphoma and greatly contribute to the loss of wt-p53 functional

activity.

Response to radiation and chemotherapeutics is typically mediated through the induction of apoptosis, which is heavily governed by transcription of pro-apoptotic genes by p53. Therefore, p53 activation is considered to be favorable to the success of these treatments. Consequently, inactivation of p53 is often associated with a poor prognosis, relapse, and chemoresistance (65, 69).

Deletion of 17p, the short arm of chromosome 17, is currently used as an independent prognostic factor in patients diagnosed with NHL, particularly CLL (70). In many cases, heterozygous deletion of 17p is thought to correspond with p53 mutations, although this is now starting to become a topic of debate.

The presence of wt-p53 usually signifies a more favorable prognosis. However, the biological mechanisms activated by wt-p53 can actually hinder the apoptotic response and protect the cell, enhancing antioxidant activity or facilitating DNA repair (66, 71). In wt-p53 lymphocytes where downstream effectors are deregulated, p53 activation has been shown to slow lymphoma progression by prolonged or permanent cell cycle arrest or senescence rather than apoptosis (72). Recent evidence suggests that autophagy also contributes to inconsistencies in prognosis in wt-p53 tumors, although it remains to be determined how exactly p53 functions in autophagy. Autophagy has just been reported to be cytotoxic as well as cytoprotective and to be associated with resistance to chemotherapeutic agents in various lymphoma subtypes (73, 74). It is possible that induction of autophagy by wt-p53 contributes to lymphoma cell survival contrary to the popular belief that it acts as a precursor- or in a coordinated effort to induce apoptotic cellular death.

Therapeutic targeting

The prolific tumor suppressor activity of p53, particularly its apoptotic function, has gained considerable interest as a potential therapeutic strategy. Although there are numerous ways to reactivate wt-p53 or restore function to mt-p53, such methods have not made it far enough into the drug development process to become FDA approved.

Considering the importance of the p53 pathway in the pathogenesis of nearly every lymphoma subtype, there is a crucial need to expand our understanding of the role of p53 activation in lymphoma cells. The functional role of activated p53 is variable and has yet to be fully elucidated. Cell type, posttranslational modifications, as well as other survival factors may influence the extent of p53 activation. Thus, understanding the role of p53 in lymphoma will enable enhanced targeting of this 'guardian of the genome' in future therapies.

Proteasomal degradation of targeted substrates

In normal, unstressed cells, p53 protein is present at low levels and has a short half-life (75). HDM2 (human double minute 2, homolog of murine double minute, or MDM2) is a RING finger E3-ubiquitin ligase that acts as the predominant negative regulator of p53. HDM2 is also a transcriptional target gene of p53, creating an autoregulatory feedback loop that regulates p53 activity and stability (Figure 1.3) (76). One of the most important functions of HDM2 is its ability to target p53 for proteasomal degradation by a process called ubiquitination.

Ubiquitin is a highly conserved 8.5 kDa protein composed of 76 amino acids that is ubiquitously found in all cells in the human body (77). The process of ubiquitination entails covalent attachment of ubiquitin to any one of seven lysine residues within the target protein, forming mono- or polyubiquitinated polypeptide chains (78).

Ubiquitination not only provides a specific signal for protein degradation, but also functions in a degradation-independent manner as well, illustrating that this process is intricately complex. This three-step procedure is ATP-dependent and mediated by enzyme family members E1, E2, and E3 (Figure 1.5). First, ubiquitin is activated in the presence of ATP and E1 ubiquitin-activating enzyme. The C-terminal carboxy group of ubiquitin and sulfhydryl group of an E1 cysteine residue form a thioester bond upon release of AMP (79). Second, ubiquitin is transferred to a cysteine residue of an E2 ubiquitin-conjugating enzyme (Ubc). Third, the ubiquitin-bound E2 Ubc binds to an E3

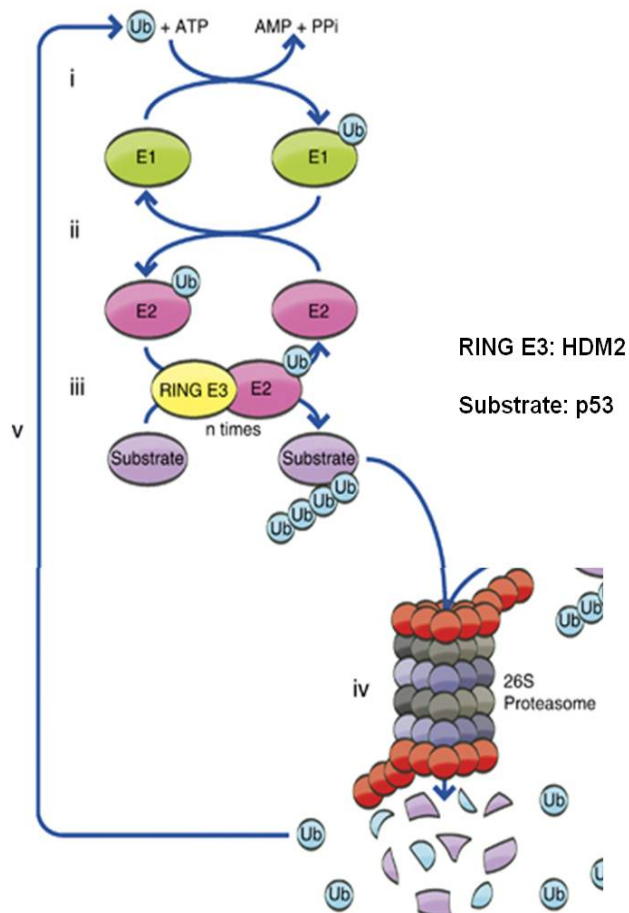


Figure 1.5 Ubiquitination is an enzymatic process that plays a role in the ubiquitin-proteasome system. Ubiquitin is catalytically conjugated to proteins by means of an E3 ubiquitin ligase. HDM2 is used as an example of a RING finger E3 ubiquitin ligase. (*i*) Ubiquitin-activating enzyme, E1, initiates ATP-dependent catalysis of ubiquitin. (*ii*) Activated ubiquitin is transferred to ubiquitin-conjugating enzyme, E2. E2 binds to HDM2 and transfers the ubiquitin moiety directly to a Lysine residue within the substrate (in this case, p53) that is also bound to the HDM2 (*iii*). The conjugated substrate is degraded to small amino acid residues by the 26S proteasome (*iv*). Ubiquitin is released and free to be reused by DUBs (*v*). Figure and figure legend are modified and reprinted with permission from Macmillan Publishers Ltd: Cell Death and Differentiation (80) Copyright 2011.

ubiquitin ligase, in this case, HDM2, capable of recognizing specific target proteins. E2 Ubc transfers the activated ubiquitin to the HDM2: target protein (p53) complex, where

E3 ligase forms an isopeptide bond between glycine 76 of ubiquitin and a lysine residue of the p53. This process is repeated, in most cases, adding ubiquitin monomers to the first ubiquitin to form polyubiquitinated chains. Typically, polyubiquitination is associated with degradation and the target protein is escorted to the proteasome for degradation. Far less frequently ubiquitinated proteins are trafficked to the lysosome for degradation (81). The 26S proteasome is an intracellular protease complex consisting of a 20S catalytic core and two 19S regulatory subunits and is present in the nucleus and cytosol of eukaryotic cells (82). Here, the proteasome unfolds and degrades the protein into various-sized peptide fragments. Ubiquitin monomer units that have been released are recycled for future use.

Ubiquitination can also be reversed by de-ubiquitinating enzymes (DUB), which facilitate the removal of ubiquitin from their substrates (83). The balance of ubiquitination and deubiquitination modifies enzymatic activity, stabilization, and sub-cellular localization of signaling proteins (84). One such example is HAUSP/USP7 (herpesvirus-associated ubiquitin-specific protease), which has been shown to de-ubiquitinate p53 and HDM2 in a concentration-dependent manner (85) and is yet another critical modulator of p53 stability.

The E3 ubiquitin ligase HDM2

Structure and function of HDM2

The hdm2 gene spans approximately 33kb of genomic DNA and consists of 12 exons. Exons 3-12 encode the coding sequence of full-length HDM2, which display both tumor suppressive and oncogenic properties. mRNA transcripts can arise from two different promoters. Transcripts from the P1 promoter in normal, unstressed cells lack exon 2, whereas the p53-inducible promoter generates transcripts lacking exon 1 (86).

The predominant HDM2 transcript encodes a protein 491 a.a. in length and is comprised of an N-terminal domain containing a hydrophobic binding pocket for p53, a central acidic domain, a putative zinc finger domain, and the C-terminal RING finger domain (Figure 1.6) HDM2 also contains a NLS, NES, and nucleolar localization signal (NoLS) (87). Over 40 alternatively spliced transcript variants of HDM2 mRNA have been identified in a variety of cancers, including lymphoma, and are often found together with full-length HDM2 transcripts. Many are also found in normal tissues, indicating that spliced forms may have normal physiological functions. Little is known

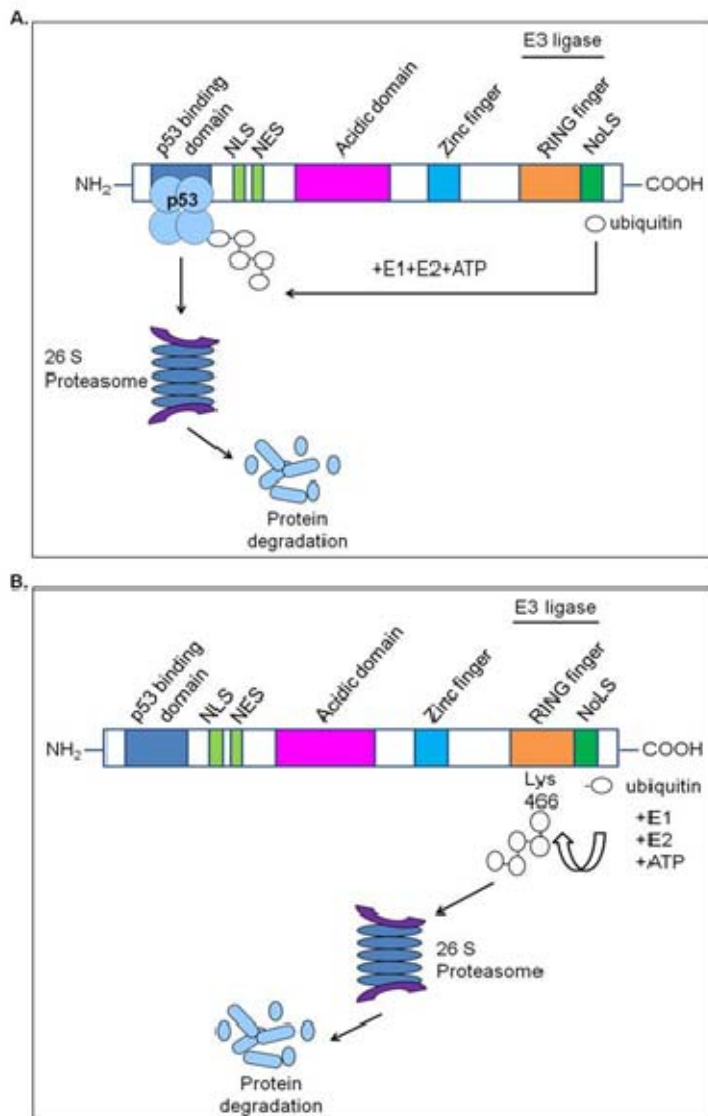


Figure 1.6 Secondary structure of HDM2, its domains, and its E3 ligase activity. **A**, Interaction of p53 and HDM2 occurs at the N-terminus where p53 binds to a pocket within the p53 binding domain. Also shown is the ubiquitination process and proteasomal degradation of p53. **B**, Autoubiquitination and self-degradatory activity of HDM2. Addition of ubiquitin moieties occurs at Lysine residue 466 within the RING finger domain at the C-terminus.

about the functions of alternatively spliced HDM2 transcripts and whether they are translated into protein, since the propensity for alternative splicing could differ from each promoter as well as their translatability. Some studies indicate that splice variants encode proteins that display transforming ability *in vitro* and *in vivo*. However, in different model systems, these splice variants have been shown to release p53 from full-length HDM2, acting as tumor suppressors by inducing wt-p53 activity. Alternatively spliced isoforms may regulate the activity of full-length HDM2 and p53. The implications of these isoforms and how their functions are controlled are not well-known (88-90).

Increased HDM2 protein levels attenuate p53 activity and stability by: 1.) blocking transcriptional activity of p53 by physically associating with its N-terminal domain; 2.) exporting p53 out of the nucleus, thereby modulating subcellular localization; and 3.) ubiquitinating p53, marking it for proteasomal degradation (87, 91, 92). Other negative regulators of p53 exist, including Cop1, Pirh2, and ARF-BP1, but they are unable to compensate for the loss of HDM2 (93).

HDM2 is capable of ubiquitinating its own lysine residue 466 and is thought to degrade itself by means of the proteasome (94, 95). Although this self-regulatory function of HDM2 is well-documented, the control and activation of this function still remains highly elusive. Importantly, HDM2 destabilization is required for proper p53 response. In fact, an early step in the accumulation of p53 in response to stress, DNA damage in particular, is an associated increase in HDM2 autoubiquitination and degradation (96, 97).

There is mounting evidence supporting the notion that p53-independent functions of HDM2 exist through the interaction of HDM2 with additional proteins, which can have

therapeutic implications. Their function and significance are not fully understood, although they have been shown to play a role in cellular responses such as transcriptional regulation, apoptosis and cell cycle (98, 99).

Expression in lymphoma and clinical significance

Overexpression of HDM2 has been shown to facilitate cancer development and progression in several tumor types and is often noted in hematological malignancies. Haploinsufficiency, or a single copy due to deletion or loss of the HDM2 allele inhibits lymphomagenesis, further supporting the role of its contributing to the development of lymphoma. In fact, HDM2 was found to be overexpressed in CLL and NHL. Its expression was found more frequently in low grade NHL (56.5%) compared with aggressive NHL (10.8%) and more in patients with advanced clinical stage (100). Abnormal expression of HDM2 has also been shown in HL (101). Little is known about the prognostic value of HDM2 in lymphomas.

Targeting the UPS for cancer therapy

There is considerable interest in members of the UPS as potential targets for therapeutic intervention in the treatment of cancer (102-105). The validity of exploiting the UPS for therapy has been demonstrated by the discovery of the proteasome as an anticancer target and the development of proteasome inhibitors. Proteasome inhibitors prevent degradation of polyubiquitinated proteins by inhibiting the proteolytic activity of the proteasome (106). Considering the ubiquity and essential role of the proteasome to all cells, it would appear that its inhibition would have profound adverse side effects. However, increased proteasomal activity is found in highly proliferative cancer cells compared to normal cells (107, 108), suggesting that these inhibitors may promote antitumor activity by targeting fast-growing cancer cells. The reason for

enhanced proteasomal activity in cancer is not understood.

Limitations of Bortezomib

As a single agent, the proteasomal inhibitor bortezomib has demonstrated preclinical cytotoxic activity in human tumor xenograft models and primary cultures of a broad spectrum of cancer types (109, 110). It elicits numerous effects on tumor cells although its predominant mechanism of action is thought to be via interference of the nuclear translocation of NF- κ B and its transcriptional activation (111). However, proteasomal inhibition also attenuates the degradation of substrates (i.e. p53) that disrupts the cell cycle and initiates cell death by multiple pathways. Hematological malignancies, such as lymphomas, appear to be particularly sensitive to the pro-apoptotic effects of bortezomib.

Several clinical trials have shown promising therapeutic merit in hematological malignancies. Currently, bortezomib is approved for treatment in multiple myeloma and mantle cell lymphoma patients (112, 113). Interestingly, not all subtypes of lymphoma respond to bortezomib. It is plausible that different mechanisms contribute to this subtype-specific activity of proteasomal inhibition, although the precise mechanisms underlying this activity are unknown (114, 115).

Bortezomib cannot be considered a targeted therapeutic agent due to its broad activity. Although the drug was shown to be well-tolerated in many clinical trials while producing clinical responses, it was still associated with side effects, most commonly nausea, chronic fatigue, and diarrhea but neutropenia, lymphopenia, hyponatremia, thrombocytopenia and peripheral neuropathy were also observed (116, 117). Although many patients do not respond to bortezomib, those that do, eventually develop resistance, suggesting that there is considerable room for improvement. Targeting

components of the UPS involved in deregulation of a subset of cellular proteins in a signaling pathway may offer tumor selectivity while achieving anti-tumor response with limited toxicity.

Design of SMIs to disrupt p53-HDM2

Physical interaction between HDM2 and p53 occurs at the N-terminal transactivation domain of p53 and the N-terminal domain of HDM2 (118). More specifically, 4 key residues (Phe 19, Leu 22, Trp 23, Leu 26) of p53 bind to the hydrophobic binding pocket of HDM2. This interaction induces a conformational change in both proteins which may allow other proteins to interact with the structural domains of either HDM2 or p53 under physiological conditions. Stressful conditions add additional levels of complexity to HDM2-p53 interactions (99).

The UPS provides additional targets for possible therapeutic intervention upstream of the proteasome. The importance of the E3 ligase HDM2 in the regulation of cellular processes, suggests that targeting the UPS to treat lymphomas warrants investigation. Exploiting the HDM2-p53 interaction in an attempt to restore wt-p53 activity is an attractive therapeutic strategy. Antisense oligonucleotides, peptide inhibitors, ribozymes and RNA interference have all been used to target cancer cells (119-122). HDM2 inhibition by antisense oligonucleotides was previously shown to stimulate p53 and to reduce tumor growth in mouse xenograft models (123, 124). Unfortunately, it is difficult to utilize such strategies for therapeutic intervention in the clinic. As a result, nongenotoxic p53 reactivating small-molecule inhibitors (SMIs) have been developed. SMIs are designed to penetrate the cell membrane and disrupt the physical interaction of proteins associated with deregulated signaling pathways. They work by sequestering and blocking overexpressed molecules, or by allowing negatively

regulated proteins to regain their functional activity. Theoretically, such SMIs should be highly potent, specific, cell permeable and possess pharmacokinetically feasible profiles (125). HDM2 SMIs should provide optimal tumor selectivity and target specificity while limiting toxicity.

Considerable effort has been expended into the development of therapeutic strategies to disrupt the HDM2-p53 protein-protein interaction to reactivate the functional activity of wt-p53. Nutlins were the first class of SMI to HDM2 to be reported (126). They were discovered in a high throughput screening of synthetic chemical libraries and possess a *cis*-imidazoline structure. Newer improved generations have now been formulated. Spiro-oxindoles were discovered using a structure-based de novo computational design (127). Both classes specifically bind to the p53 binding pocket of HDM2 by mimicking four key hydrophobic peptide residues in wt-p53. Crystal structure studies indicate that Trp 23 seems to be the most important residue for the binding of p53 to HDM2 since it is buried deep inside the hydrophobic binding cleft (128). However, spiro-oxindoles possess a greater affinity and specificity for HDM2 than *cis*-imidazolines, perhaps due to the differences in the chemical structure that binds to the HDM2 hydrophobic pocket. Where Nutlins bind to this region using a bromophenol moiety, spiro-oxindoles mimic the bulky Trp 23 by an indole ring. Homologs of HDM2, such as HDMX and proteins containing deep hydrophobic pockets, such as Bcl-2 and Bcl-xl, bind with much weaker affinity to these SMIs, indicating specificity for HDM2. Along with high potency and specificity, these two classes of SMIs also exhibit outstanding cell permeability and pharmacokinetic properties (118, 125, 126). Studies using HDM2 SMIs have generated sufficient data to demonstrate that these inhibitors can effectively be used to elicit antitumor response. However, the precise mechanisms

of susceptibility to HDM2 SMI induced cancer cell death are not completely understood. The extent that HDM2 SMIs influence p53-independent functions of HDM2 remains to be determined.

Although inhibition of HDM2 acts in a p53 dependent manner, the regulatory mechanisms mediating this effect are still uncertain. For example, it was initially thought that HDM2 inhibition completely abrogated all functionality of the protein after release of p53. HDM2 appears to be capable of retaining its p53-independent functions in the presence of Nutlin-3, even when p53-dependent activity is the primary effect seen. Of importance is the E3 ubiquitin ligase activity of HDM2. The effects of HDM2 inhibition on HDM2 auto-ubiquitination and p53 ubiquitination are currently unknown. Further, the precise mechanisms regulating the balance of ubiquitination and de-ubiquitination on protein-protein interactions such as p53 and HDM2 are not entirely well-defined in the presence of HDM2 SMIs. Elucidating some of these mechanisms can enhance our understanding of the therapeutic potential and limitations of HDM2 inhibitors in B-cell lymphoma.

Although preclinical assessment of many HDM2 SMIs has demonstrated great promise, it is becoming clearer that multiple distinct molecular mechanisms influence anticancer activity of each agent. Inadequate mechanistic studies will continue to prevent their successful utilization for therapy. More importantly, novel HDM2 SMIs are currently under clinical evaluation in phase I studies, demonstrating the significant impact and clinical relevance of these agents (129).

The UPS, p53 and lymphoma

Deregulation of the UPS is likely to contribute to the pathogenesis of lymphoma. Inactivating mutations or deletions in the TP53 gene are found in approximately 50% of

all cancers. However, this frequency is much lower in hematological malignancies, particularly indolent lymphomas, accounting for less than 10% of cases at diagnosis (130). p53 mutations become more prevalent as the disease progresses, indicate poor prognosis, and predict aggressive disease that is likely to develop chemoresistance (131, 132). Therefore, tumor cells containing a wt-p53 are typically more sensitive than those bearing mt-p53. Overall, mutations in p53 are not a common molecular characteristic driving lymphomagenesis with the exception of disease progression.

The p53 pathway is often compromised by alternative mechanisms. Aberrant signaling by other defects upstream or downstream in the pathway, such as HDM2 overexpression, is typically observed in lymphoma and greatly contributes to the loss of wt-p53 functional activity. Targeting components of the UPS, such as HDM2 using small-molecule inhibitors, to reactivate p53 is as an attractive therapeutic strategy and lymphomas are an ideal disease model to test this approach.

Specific aims of the study

Aim 1: To determine the biological effect of spiro-oxindole HDM2 inhibitors on B-cell lymphoma with WT & mutant p53 *in vitro* & *ex vivo*.

Aim 2: To examine the involvement of p53-dependent molecular mechanisms upon inhibition of HDM2 in B-cell lymphoma.

Aim 3: To investigate additional molecular effects of spiro-oxindole HDM2 SMIs on HDM2 upon physical disruption of HDM2-p53.

CHAPTER II

MATERIALS AND METHODS

Experimental design

The use of cell lines as a drug screening model is a valuable tool for assessing preclinical activity of newly developed anticancer agents. However, successful translation into phase I clinical studies are frequently marred by their questionable relevance to patient outcomes. Immortalized cell lines may undergo alterations and lose authenticity of cell and tissue-specific characteristics which complicates the validation of drug treatments. An advantage of using cell lines is the convenience they provide to researchers. Cell lines offer a continuous source of cells where multiple independent experiments can be repeated to verify results. They also provide an opportunity for in-depth investigations that could lead to novel mechanistic findings.

Primary cells obtained from patients provide the most physiological relevance possible. Therefore, access to malignant B lymphocytes derived from lymphoma patients was of particular importance to this study. This would allow us to compare and validate results from patient derived cells with those obtained in cell lines. Furthermore, patient samples also validate the clinical relevance of the cell lines if results are consistent, particularly when determining mechanisms of action or performing investigations that cannot be logistically conducted on patient samples. We reasoned that results from the *in vitro* cell line data would be similar to the results obtained using patient samples. However, we are certainly aware of the existence of differences that may occur between each cell model which must be taken into consideration as well.

Cell lines and culture conditions

WSU-FSCCL, WSU-DLCL₂ and WSU-WM were established in our laboratory as

described previously (133-135). WSU-FSCCL is a human B cell follicular small cleaved cell line; WSU-DLCL₂ is a human diffuse large B cell line, WSU-WM is a human Waldenstrom's macroglobulinemia cell line. The human Hodgkin lymphoma cell lines KM-H2, L-540, and L-591 were obtained from DSMZ (Germany). The human diffuse lymphoma cell lines RL and Toledo were purchased from the American Type Culture Collection (Rockville, MD). None of the lymphoma cell lines used was virally transformed. All cell lines and primary cells were cultured in suspension in RPMI 1640 medium supplemented with 10% fetal bovine serum (Denville) and 1% Penicillin Streptomycin (Invitrogen) at 37°C and 5% CO₂ in a humidified incubator. Cells were seeded at a density of 2 x10⁵ cells per mL prior to use in functional assays.

Human Investigation Committee (HIC) approval

Prior to conducting research on patient samples, it was mandatory to meet University and Federal guidelines. Extensive knowledge of protocols for working with human subjects was required for all personnel involved in the research proposal, and instruction on this was completed through the Collaborative Institutional Training Initiatives (CITI) online training module system. Documentation for the proposed research project was submitted by Angela Sosin to the Wayne State University Institutional Review Board (IRB) for expedited review and she designated the Principal Investigator (PI) of the approved study. Patients cells were obtained from the Lymphoma Clinic at the St. John Hospital Van Elslander Cancer Center under the direction of Dr. Ayad Al-Katib in accordance with an IRB approved protocol and all patients had signed informed consent prior to sample procurement. This project was also reviewed and approved by the IRB at St. John Hospital Van Elslander Cancer Center as well as the Human Investigation Committee (HIC) at Wayne State University

School of Medicine (see Appendix A).

Isolation and purification of patient-derived B lymphocytes

Lymphoma tissue was obtained from untreated patients diagnosed with B cell NHL. Peripheral blood was collected from patients with circulating lymphoma cells, (i.e. leukemic phase). In both cases, the samples were the remainder of blood or tumor tissue that have already been drawn or biopsied and had already undergone clinical testing at St. John Van Elslander Cancer Center. Cells from normal, healthy anonymous donors were extracted from discarded apheresis cones and/or filters obtained from the Red Cross and were kindly provided by Dr. Martin Bluth, Associate Director of Detroit Medical Center Transfusion Services.

The methodology described in this section explains a detailed, highly modified protocol for the isolation and purification of primary B lymphocytes that produced consistent results.

Samples collected from the St. John Van Elslander Cancer Center were properly documented using a coded identifier. Patient-derived and normal donor peripheral blood mononuclear cells (PBMCs) were isolated using LymphoPrep (ProGen Biotechnik) density gradient centrifugation (Figure 2.1A). The PBMC fraction contains a mixture of T cells, B cells, NK cells, basophils, macrophages, monocytes and dendritic cells. Tissue was minced using steel mesh in a petri dish and the cells resuspended in RPMI media, and subjected to isolation of mononuclear cells. Peripheral blood drawn from lymphoma patients was diluted with RPMI media in a ratio of 1:4 (Figure 2.1B). Contents of apheresis cones from normal donors (Figure 2.2A) were collected in a 15 mL tube (Figure 2.2B) and diluted 1:9 with RPMI media. Diluted blood was carefully layered in a 1:1 ratio on top of LymphoPrep (Figure 2.1C) to prevent red blood cell (RBC) lysis and

centrifuged at 500 x g for 20 minutes. Four distinct layers are present after centrifugation: the erythrocytes and granulocytes are located at the bottom; the buffy coat or PBMCs are layered thinly on top of the LymphoPrep layer (Figure 2.1D); and the top layer is the media containing plasma and platelets. The PBMCs were carefully collected and transferred to a new 50 mL conical tube (Figure 2.1E), centrifuged at 500 x g for 5 minutes (Figure 2.1E) and, washed with 5 mL of 1X PBS, twice to ensure that the cells are free of any residual, cytotoxic LymphoPrep.

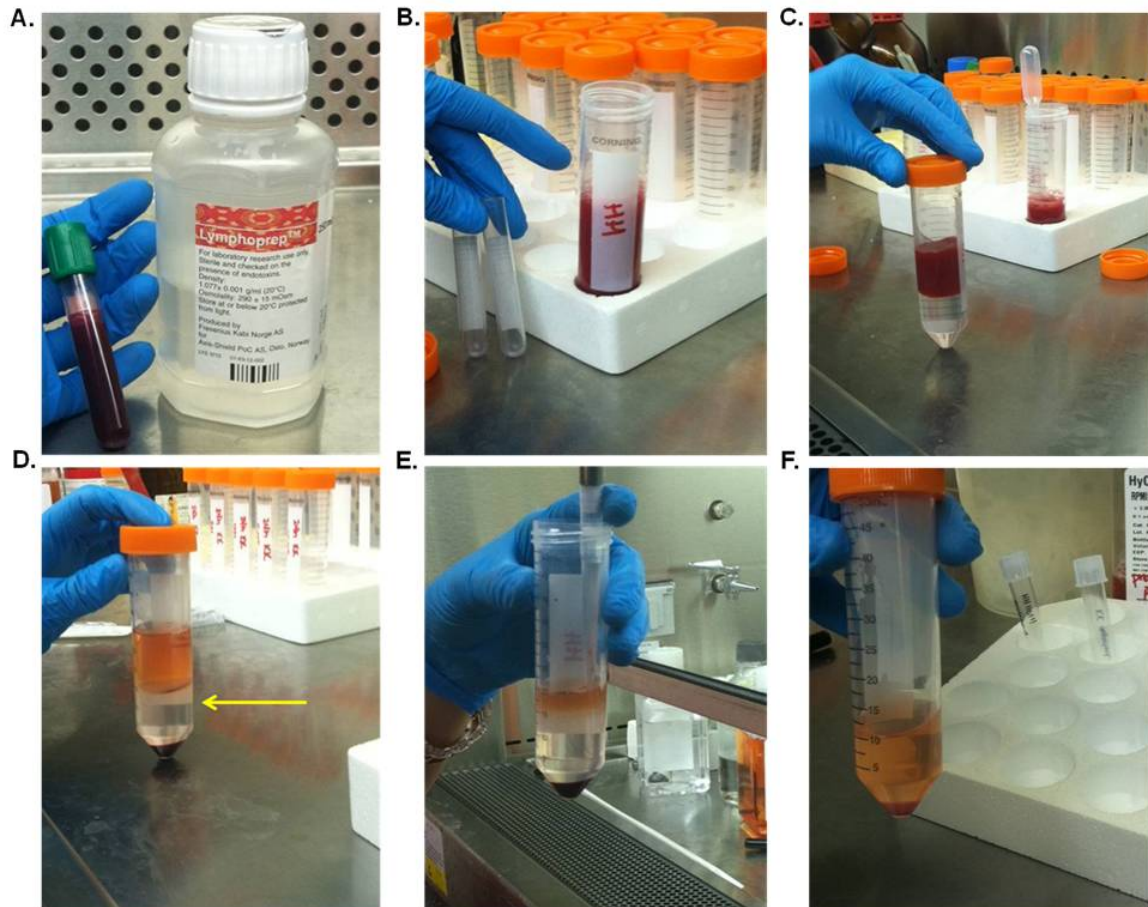


Figure 2.1. Isolation of PBMCs from a lymphoma patient in leukemic phase. **A**, Collection of peripheral blood in a heparin-coated tube. **B**, Peripheral blood transferred to a 50 mL conical tube and diluted with RPMI media without FBS. **C**, Diluted contents were carefully overlaid in a 1:1 ratio onto LymphoPrep. **D**, PBMC buffy coat layer after centrifugation (shown with arrow). **E**, Removal of PBMC layer and transfer to a new 50 mL conical tube. **F**, Resultant cell pellet following centrifugation of PBMC buffy coat.

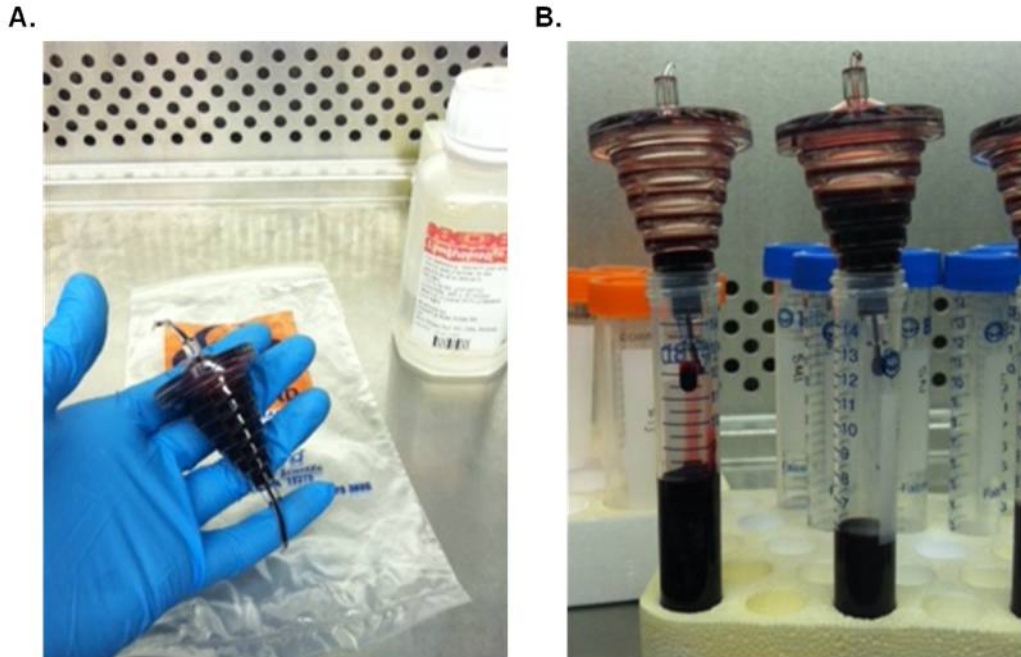


Figure 2.2 Isolation of normal donor B-lymphocytes from post-leukoreduction apheresis cones. **A**, Picture of a discarded apheresis cone. **B**, Contents were eluted by gravity flow through prior to dilution and LymphoPrep separation of PBMC's.

Monocyte Depletion

Cells were resuspended in media and counted on a hemacytometer using Trypan blue exclusion dye to determine cell number and viability. About 40% of the isolated mononuclear cells are monocytes and macrophages and adhere to plastic surfaces, whereas lymphocytes do not. Therefore, resuspended cells were dispensed into T75 flasks and placed in a 37° incubator for approximately 1-2 hours to allow cells to adhere to the plastic surface. Cells devoid of monocytes were then collected and centrifuged at 400 x g for 5 minutes, then resuspended in 1X PBS. An aliquot was analyzed by FACS.

T Cell Depletion

T cells were depleted from the cell suspension lacking monocytes using 100 μ l pan CD2+ Dynabeads (Dyna), which is necessary for negative selection (depletion) for

up to $\sim 5 \times 10^8$ cells. Cells were incubated with prewashed beads for 30 minutes at 4°C while rotating. After the T cells were removed using the DynaMag as a magnetic device, the unbound, negatively selected, highly pure B cell population was removed by aspiration and analyzed using FACS to confirm T cell depletion (Children's Hospital Flow Cytometry Facility, Detroit, MI). The enhanced, purified B lymphocytes were subsequently used for functional assays.

Chemical synthesis, reagents, drug treatment, and competitive binding assay

MI-219 (Ascenta Therapeutics) was synthesized using methods published previously (118, 127). Disulfiram, Nutlin-3 (Sigma Aldrich), its 150-times less active enantiomer (+)-Nutlin-3b (Cayman Chemical), and MI-319 were dissolved in 100% DMSO as 10 mM stock solutions. MG132 (Cayman Chemical) and cycloheximide (Sigma) were dissolved in 100% DMSO as 100 mM stock solutions. Reagents were diluted to working solutions using sterile water. Fluorescence polarization-based competitive binding assays were performed to determine the binding affinity of MI-319 and MI-219 with a recombinant His-tagged HDM2 protein. The assays were carried out as described previously (136).

Cell viability assays

Cells were seeded at a density of 2×10^5 /ml and allowed to adapt overnight before exposure to increasing concentrations of Nutlin-3, MI-319, or MI-219. Control cells were treated with equal volume of DMSO for a final concentration of 0.1%. 3-(4, 5-dimethylthiazol-2-yl)-2, 5-diphenyl-tetrazolium bromide (MTT) reagent (Sigma) was added 24, 48 or 72 hours later to halt reactions. Purple formazan crystals were solubilized in DMSO and absorbance was read in a plate reader at 540 nm. Cell viability was also determined by a Trypan blue dye exclusion assay using 0.4% Trypan blue

(Sigma). IC₅₀ was assessed as 50% inhibitory concentration as compared to vehicle treatment. Data are representative of at least three independent experiments.

Morphology

Cells were exposed to 10 μ M Nutlin-3 and MI-219 for 48 hours. For light microscopic examination, KM-H2 cells were seeded as described above. Briefly, aliquots from untreated cells (control) and treated cells were cytocentrifuged in a Cytospin II centrifuge (Shandon Southern Instruments). Cell smears were air-dried, stained with tetrachrome at full concentration for 5 minutes and then at 50% dilution with distilled water for another 5 minutes. Slides were analyzed under light microscopy (Nikon). Features of apoptosis looked for included nuclear chromatin condensation, formation of membrane blebs, and apoptotic bodies.

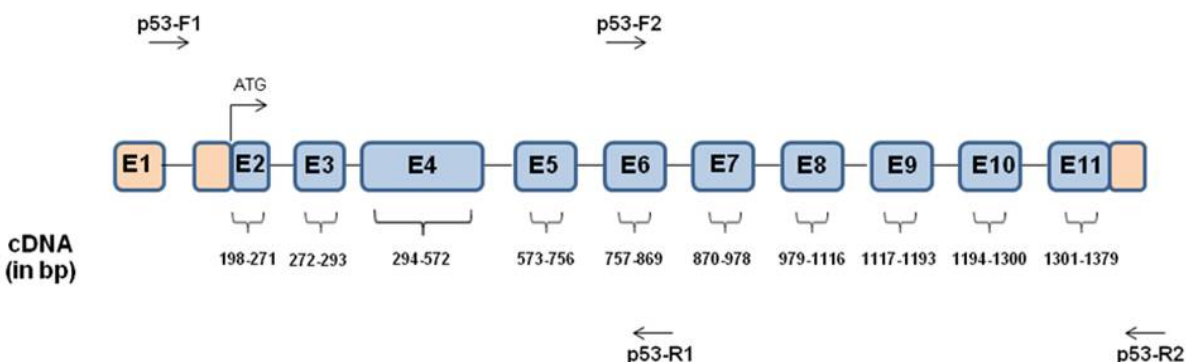
p53 sequencing

To sequence the p53 coding region, RNA was extracted from approximately 1 million cells of each patient sample or cell line using a ZR-*Duet*TM DNA/RNA MiniPrep kit (Zymogen). The amount of RNA was determined by UV absorption at 260 nm. 1 μ g of each sample was reverse-transcribed using the SuperScript[®] VILOTM cDNA synthesis kit per manufacturer's instructions (Invitrogen). 200 ng was used in each reaction of p53 PCR amplification. Two primer sets were designed and used to amplify p53 exons 5-9, which encode the DNA-binding region that contains greater than 90% of all p53 mutations (47). The sequence and characteristics of each primer is listed in Table 2.1 and have been previously published by our lab (137).

Table 2.1. p53 primers used for sequencing.

Primer	Strand	Sequence of Primer (5' to 3')	Start Codon	Stop Codon	Melting Temperature (T _m in °C)	% GC Content
p53-F1	Sense	AAG TCT AGA GCC ACC GTC CA	61	80	54.33	55
p53-R1	Anti-sense	CAT AGG GCA CCA CCA CAC TA	858	839	53.20	55
p53-F2	Sense	GTG GAA GGA AAT TTG CGT GT	786	805	51.49	45
p53-R2	Anti-sense	GTG GGG AAC AAG AAG TGG AG	1403	1384	52.23	55

The location of these primers in relation to the p53 coding sequence is depicted in Figure 2.3 along with the primer sets and PCR conditions used to amplify p53 cDNA in Table 2.2.

**Figure 2.3.** Location of p53 primers on p53 cDNA.**Table 2.2.** p53 primer sets and PCR conditions.

Primer Set	Denaturation (°C)	Annealing (°C)	Extension (°C)	# of Cycles	Product Length (in bp)
p53-F1/p53-R1	94	52	72	35	798
p53-F2/p53-R2	94	52	72	35	618

Amplified PCR products were analyzed by agarose gel electrophoresis. PCR products were then cut and purified using Wizard SV Gel/PCR Cleanup kit (Promega). Two primers, one from each primer set, and 200 ng of PCR product was sequenced by GeneWiz, Inc. Sequencing was performed on the Applied Biosystems ABI Prism 3730xl

DNA Analyzer using fluorescent dye terminator detection (Applied Biosystems, CA). DNA sequences were screened for mutations using BLAST to the p53 coding sequence: NCBI Reference Sequence: NM_000546.4.

RNA extraction, cDNA preparation and real-time quantitative PCR (qRT-PCR)

Total RNA was extracted from treated lymphoma cells using the PureLink™ RNA Mini Kit (Invitrogen). Total RNA was quantified by NanoDrop and 1 µg of each sample was reverse-transcribed using the SuperScript® VILO™ cDNA synthesis kit per manufacturer's instructions (Invitrogen). The resulting cDNA preparations were then cleaned of excess enzyme with Wizard SV Gel/PCR Cleanup kit (Promega). qRT-PCR amplification was conducted in a 10 µl reaction using the Roche LightCycler® 480 SYBR Green I Master (Roche) according to manufacturer's protocol. 100 ng total RNA was used for each reaction and mixed with Quanti Tect Primers (Qiagen) to p53, HDM2, p21, p53AIP1, TIGAR and GAPDH. Reactions were carried out in a 384-well plate using the LightCycler® 480 System (Roche).

Flow cytometric analysis

Apoptosis

For analysis of drug-induced apoptosis, cells were stained with FITC-conjugated Annexin V and propidium iodine using the Annexin V/PI kit according to manufacturer's protocol (BioVision). Apoptosis was also measured using the TUNEL-based ApoDIRECT DNA Fragmentation Assay Kit (BioVision). The percentage of apoptotic cells was quantified using a Coulter EPICS 753 flow cytometer.

Cell cycle

Cell cycle analysis was conducted using flow cytometry of propidium iodide (PI)-stained cells. Following exposure of cells to either Nutlin-3 or MI-219 for the specified

time, cells were harvested, washed and fixed with 75% ice-cold ethanol overnight. Cells were then stained with PI at a final concentration of 50µg/ml and analyzed on Coulter EPICS 753 flow cytometer. All *in vitro* flow cytometric experiments were performed three independent times. The percentage of cells in G0/G1, S, or G2/M was determined using a ModFit 5.2 computer program.

Western blots

Cultured cells were collected by centrifugation, washed twice with 1X PBS, and solubilized in M-PER lysis buffer (ThermoScientific) containing a cocktail of protease and phosphatase inhibitors (ThermoScientific). The concentration of total cell lysate was quantified by BCA protein method. 50 µg of total cell lysate proteins were fractionated onto 14% or 4-20% Tris-Glycine SDS-PAGE gels, transferred onto PVDF membrane, and probed with primary antibody. Secondary antibodies were anti-mouse or anti-rabbit conjugated to HRP (Jackson Immuno). Proteins were visualized using chemiluminescence substrate reagent. A list of the antibodies used in this study is located below in Table 2.3.

Table 2.3 List of antibodies

Antibody	Company	Host	Clonality
p53 (DO-1)	Santa Cruz	Mouse	Monoclonal
HDM2 (AF1244)	R & D Systems	Rabbit	Polyclonal
p21 (2974)	Cell Signaling	Mouse	Monoclonal
Cleaved PARP (5625)	Cell Signaling	Rabbit	Polyclonal
Cleaved Caspase-3 (9664)	Cell Signaling	Rabbit	Polyclonal
Ubiquitin (3936)	Cell Signaling	Mouse	Monoclonal
His-Tag (27E8)	Cell Signaling	Mouse	Monoclonal
GAPDH	Trevigen	Rabbit	Polyclonal
p53 PAb421	Calbiochem	Mouse	Monoclonal
HDM2 (D-12)	Santa Cruz	Mouse	Monoclonal
Caspase-9 (H-170)	Santa Cruz	Rabbit	Polyclonal
HDM2 (SMP-14)	Santa Cruz	Mouse	Monoclonal
CyclinD1 (HD11)	Santa Cruz	Mouse	Monoclonal
LC3A/B (4108)	Cell Signaling	Rabbit	Polyclonal
Caspase-3 (H-60)	Santa Cruz	Rabbit	Polyclonal
Caspase-8 (H-134)	Santa Cruz	Rabbit	Polyclonal
MDR1 (D-11)	Santa Cruz	Mouse	Monoclonal
Rb (C-2)	Santa Cruz	Mouse	Monoclonal

Immunoprecipitation and co-immunoprecipitation

WSU-FSCCL or KM-H2 cells were treated with Nutlin-3 or MI-219 for specified periods of time and collected as described above. 1 mg of total cell lysate was incubated with 5 µg primary antibody overnight (a 1: 1 ratio of HDM2 antibodies SMP-14 and D-12, Santa Cruz) rotating at 4°C. 30 µl Protein G agarose beads (Millipore) were added to each sample and incubated at 4°C for 4 hours. Antibody: antigen complexes were washed 3 times with PBS prior to the addition of 30 µl SDS-PAGE buffer, denatured at 95°C for 5 min, and centrifuged briefly. Immunoprecipitates were then subjected to SDS-PAGE and probed for protein of interest.

HDM2 autoubiquitination assay

Autoubiquitination assays were performed using 200 ng of recombinant His-HDM2 in the presence or absence of E2-conjugating enzyme, UbcH5b, recombinant human E1 (Boston Biochem), and with or without HDM2 SMI. Final concentration of the drug was IC₅₀ or 50 µM for Nutlin-3, MI-219, and MI-319 diluted in 30 µL reaction volume. Disulfiram (10 µM) was used as a control. Samples were incubated for 1.5 hours at 30°C. The reaction was stopped with the addition of 10 µl of 3X SDS loading dye, boiled for 5 minutes, separated on a 4-20% Tris-Glycine gradient gel (Invitrogen), and subjected to immunoblotting.

Gel band quantification

ImageJ densitometry software (Version 1.45, US National Institutes of Health; <http://rsbweb.nih.gov/ij/index.html>) was used for quantification of Western blot bands from treated patient samples. Selected bands were quantified based on their relative integrated intensities, calculated as the product of the selected pixel area and the mean gray value for those pixels normalized to internal control (GAPDH). Fold increase or

decrease was calculated by standardizing each treatment as a ratio to the control.

Data and statistical analyses

Statistical analyses were performed by two-way ANOVA unpaired two-tailed GraphPad Prism v. 4.0 or unpaired two-tailed *t* test using Microsoft Excel. $P < 0.05$ was considered significant. Biostatistical guidance and analyses was performed by Dr. Judith Abrams to verify assumptions, locate outliers, and determine associations.

Relative quantification of mRNA from lymphoma cell lines

Two independent drug treatments per sample were performed in triplicate and each reaction was repeated once to ensure accuracy. The PCR cycle number at threshold (CT) was used for the comparison. Baseline gene expression and that after treatment were quantified by qRT-PCR relative to GAPDH using the $\Delta\Delta C_t$ method and expressed as fold induction of gene expression relative to that in the untreated control (138). Error bars plotted represent mean values \pm SE.

Biostatistical analyses of Western blots from patient samples

Relative density was selected as the endpoint. It is defined as the ratio of the absolute density for a given protein treated with a given drug, at a given concentration, for a specific time, for a specific patient to the absolute density of GAPDH under the same conditions. Evaluation of the shape of the frequency distribution of relative density indicated that a natural log transformation was required to meet the assumptions of the statistical tests. Fixed effects linear models were used with drugs, Nutlin-3 and MI-219 concentrations, proteins, and time as fixed effects and patient as the random effect. Holm's procedure was used to adjust for multiple comparisons.

Biostatistical analyses of tumor cell viability from patient samples

Samples from each patient were treated with Nutlin-3 or MI-219, at 3 different

concentrations (2.5, 5, and 10 μ M) for up to 72 hours. There were a minimum of 2 and a maximum of 6 replications for each patient at each drug, dose, and time point. Cell survival ranged from 0% to 100%. The quantile-quantile plot indicated that the observed data had a longer right tail than would be expected if the data were normally distributed. Nonetheless, a mixed effects analysis of variance was used because the violation was not outrageously extreme and because no better alternative could be found given the experimental design. In the mixed effects model drug, concentration and time were defined as fixed effects; patient and replication were defined as random effects. Holm's procedure was used to adjust for multiple comparisons.

CHAPTER III

BIOLOGICAL EFFECTS OF HDM2 SMIs IN LYMPHOMA CELLS

Introduction

Preclinical assessment of disrupting the p53-HDM2 interaction with Nutlin-3, the proto-typical HDM2 SMI, has shown promise in a variety of cancer types retaining wt-p53 with minimal effects in normal cells. HDM2 SMI inhibition would primarily result in a p53-dependent response and upregulation of its target genes. Previous studies with Nutlin-3 have shown that the anti-tumor response is the result of the upregulation of p53-dependent target genes primarily affecting cell cycle arrest and apoptosis (126). The precise mechanisms of susceptibility to HDM2 SMI induced cancer cell death are not completely understood despite extensive data supporting antitumor activity. Although Nutlins demonstrate ideal characteristics of a nongenotoxic, targeted therapeutic agent, preliminary data from clinical trials are proving to be less fruitful. Thus, research on design of additional SMIs and elucidation of molecular mechanisms has continued. SMIs are believed to penetrate hematological cells such as lymphoma cells with greater ease than solid tumors. This dissertation seeks to expand upon existing observations using the novel spiro-oxindole compounds, MI-319 and MI-219, and lymphoma as a disease model. In particular, lymphomas are an ideal tumor type for HDM2 inhibition considering the high frequency of wt-p53 and HDM2 overexpression found in this disease. Further, p53 signaling and its functional consequences are not fully elucidated in the presence of SMIs in lymphoma cells.

Studies in this chapter were designed to determine the biological effect of MI-319 (initially) and MI-219 on lymphoma cells with wt- and mt-p53 status *in vitro* and isolated primary B-lymphocytes *ex vivo*. These studies also address the involvement of p53-

dependent molecular mechanisms upon HDM2 inhibition with HDM2 SMIs. Since apoptosis and cell cycle arrest are the predominant biological responses of p53 activation, it was important to assess well-known key regulators of these processes upon treatment with HDM2 SMIs, with emphasis on apoptosis. The initial hypotheses for this portion of the study are as follows: 1) HDM2 inhibition in wt-p53 B-lymphoma cells will lead to apoptosis and cell-cycle arrest; 2) MI-319 (MI-219) will induce apoptosis in fresh wt-p53 lymphoma patient samples *ex vivo*; 3) MI-319 (MI-219) mediates its key cellular effects by activating the p53 pathway. Results of preclinical assessment of spiro-oxindoles were compared to Nutlin-3, a *cis*-imidiazole, as a standard and with the rationale that both classes of HDM2 SMI would produce parallel observations. These experiments were designed to delineate p53-dependent responses to HDM2 inhibition in lymphoma cells with the anticipation of translating HDM2 SMIs to the clinic as a potentially new therapeutic intervention strategy.

Results

Spiro-oxindole compounds bind to HDM2 protein with high affinity

MI-319 is a laboratory grade spiro-oxindole HDM2 SMI initially used and the backbone of this study. Some of the growth inhibitory data obtained from this portion of the study were published in *Molecular Cancer* in 2009. In this report, the MDM2 appellation of HDM2 was used. The following was taken from: 'An MDM2 antagonist (MI-319) restores p53 functions and increases the life span of orally treated follicular lymphoma bearing animals.' (Note: this dissertation did not use animals, however, there was an approved animal protocol in place for using these HDM2 SMIs under the supervision of Dr. Ramzi Mohammad, one of the co-authors on the publication). The chemical structure of MI-319 has the same spiro-oxindole structure as MI-219 with the

addition of a Fluoride group, which enhances the solubility and may increase the affinity of the compound (Figure 3.1A). The fluorescence polarization-based competitive binding assay determined that MI-319 binds to recombinant human MDM2 protein with a K_i value of 9.6 ± 3.9 nmol/L, which is lower than the K_i values of 13.3 ± 1.8 nmol/L and 36.0 ± 9.0 nmol/L determined for MI-219 (Figure 3.1B) and Nutlin-3 (139), respectively. Therefore, MI-319 binds to human MDM2 protein with an affinity slightly higher than that of MI-219 and Nutlin-3. It appeared that both MI-319 and MI-219 were more than 500 times more potent than the p53 peptide in binding to MDM2 (Figure 3.1B).

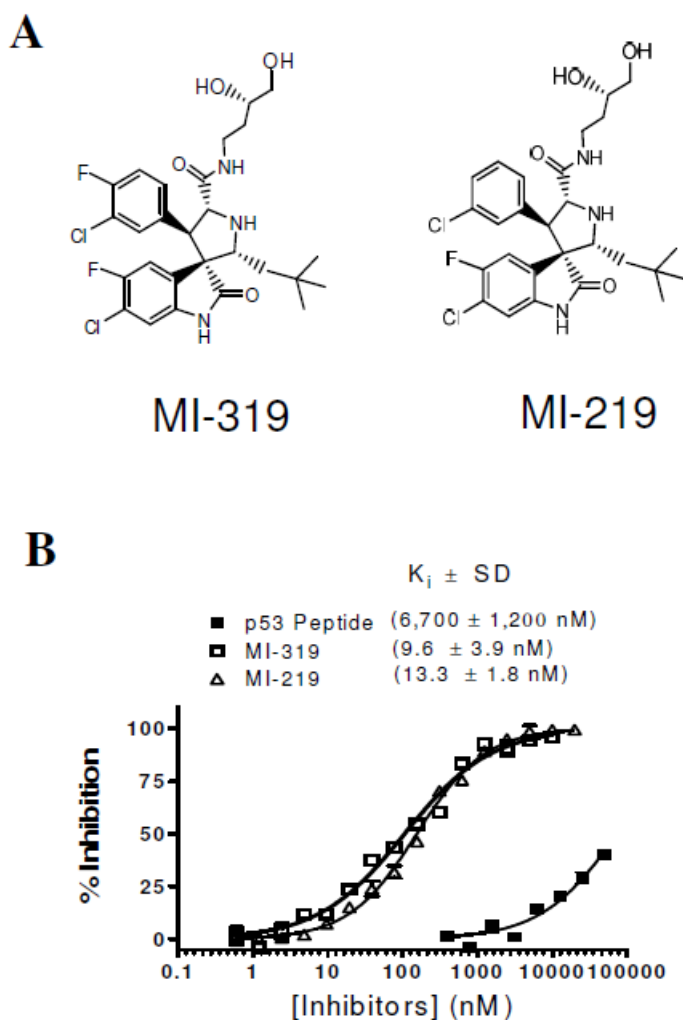


Figure 3.1 Chemical structure of MI-319 and MI-219 and MDM2 protein binding assay. **A**, Chemical structure of MI-319 and MI-219. **B**, MI-319 and MI-219 binding affinities (K_i values) as determined by a competitive fluorescence polarization-based binding assay using recombinant His-tagged MDM2 (amino acids 1-118) and PMDM6-F (5-FAM- β Ala- β Ala-Phe-Met-Aib-pTyr-(6-Cl-LTrp)-Glu-Ac3c-Leu-Asn-NH₂), a fluorescently labeled high-affinity p53-based peptide.

Detection of p53 mutations in lymphoma cell lines

Since wt-p53, but not mt-p53, cells are responsive to HDM2 SMIs, assessment of the mutational status of TP53 was necessary prior to the preclinical screening of these agents. Using the primers listed in Table 2.1, the established lymphoma cell lines WSU-FSCCL, WSU-DLCL₂ and WSU-WM from our lab were first screened for p53 mutations. Since WSU-FSCCL was the only wt-p53 cell line, a literature search was performed in pursuit of wt-p53 NHL and mt-p53 cell lines not immortalized by viral transduction. Toledo and RL were documented to be wt- and mt-p53, respectively; the HL cell lines KM-H2, L-540 and L-591 were purchased subsequently. Figure 3.2A shows the amplification of the p53 coding sequence run on a 1% agarose gel from four of the lymphoma cell lines screened. Primers p53-F1 and p53-R1 produced a PCR product of 798 bps while product size with primers p53-F2 and p53-R2 was 618 bps; the location of each primer is shown in Figure 3.2B. Bands were excised from the gel, purified and sequenced in separate reactions using primers p53-F1 and p53-R2. DNA sequencing and subsequent BLAST to the p53 coding sequence revealed that four lymphoma cell lines contained p53 point mutations: WSU-DLCL₂ had an Arginine (R) to Glutamine (Q) mutation at codon 248; WSU-WM had an Arginine (R) to Glutamine (Q) mutation at codon 213; RL had an Alanine (A) to Proline (P) mutation at codon 138; and Toledo had a mutation at codon 72. What appeared to be a mutation at codon 72 for Toledo, Proline (P) to Arginine (R), ended up being a single nucleotide polymorphism (SNP). Since codon 72 SNPs can vary with the degree of apoptotic induction, as was seen in the growth inhibition assay in the following section, we chose to exclude it for the rest of the project. Table 3 shows a summary of the lymphoma cell lines and their corresponding p53 status.

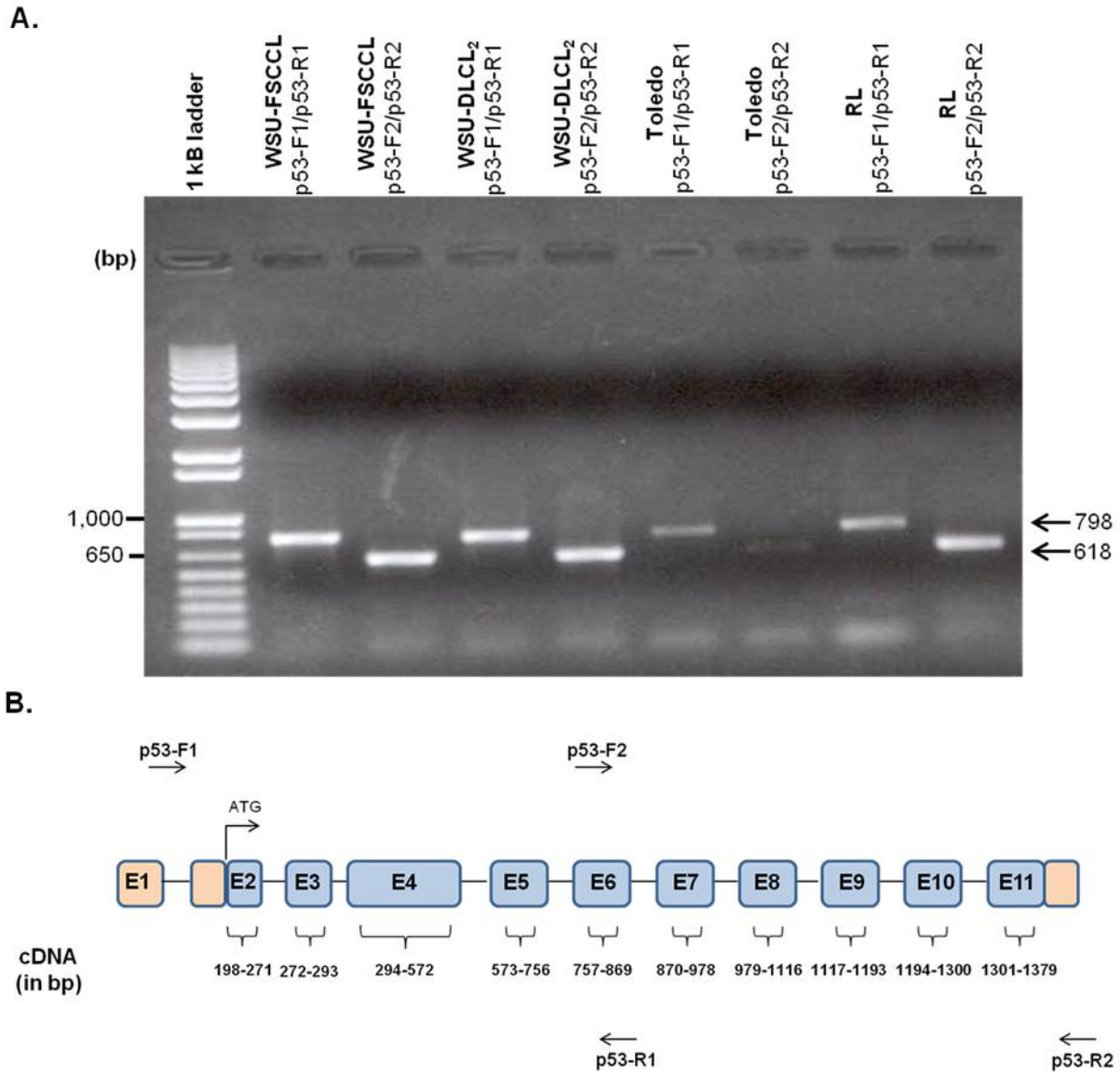


Figure 3.2 Amplification of p53 in four of the lymphoma cell lines used.

A, The entire coding region of p53 was amplified using two different primer sets. Primer set F1-R1 amplified a 798 bp product and set F2-R2 produced a size of 618 bp. B, Location of p53 primers on p53 cDNA.

Table 3.1. *Status of p53 in lymphoma cell lines.*

Cell Line	gDNA Sequenced	cDNA Sequenced	p53 Mutational Status
WSU-FSCCL	exons 5-9	full-length	wild-type
WSU-DLCL2	exons 5-9	full-length	R248Q
WSU-WM	exons 5-9	full-length	R213Q
Toledo	exons 5-9	full-length	P72R
RL	exons 5-9	full-length	A138P
KM-H2	exons 5-9	full-length	wild-type
L-540	exons 5-9	full-length	wild-type
L-591	exons 5-9	full-length	wild-type

Assessment of the growth inhibitory effect of MI-319 on lymphoma cell lines

The following was published in: 'An MDM2 antagonist (MI-319) restores p53 functions and increases the life span of orally treated follicular lymphoma bearing animals.' Four lymphoma cell lines WSU-FSCCL [representing follicular low grade non-Hodgkin's lymphoma type that is wt-p53]; (b) WSU-WM [representing plasmacytoid type that is mt-p53]; (c) RL representing diffuse large B-cell lymphoma, mt-p53; (d) WSU-DLCL₂ [representing diffuse, Intermediate grade non-Hodgkin's lymphoma mt-p53]; were used since they represent a wide spectrum of B-cell lineage tumors. MTT assay was used to monitor cell growth upon exposure to HDM2 SMIs. MI-319, MI-219, and Nutlin-3 inhibited the growth of WSU-FSCCL cells in a dose-dependent manner after 48 hours where the IC₅₀ of each of the SMIs is estimated to be 2.5 μM. The IC₅₀ cannot be determined in each of the three mt-p53 lymphoma cell lines even up to concentrations of 20 μM, and demonstrate approximately a 10-fold greater selectivity in wt- over mt-p53

cells. Interestingly, each of the mt-p53 cell lines responded somewhat differently to HDM2 SMI where WSU-DLCL₂ appeared to exhibit the weakest response (Figure 3.3). (Note: I cannot be certain whether or not the WM treated cells display statistical significance since this was the one cell line that I did not run a MTT assay on and I do not have access to the raw data to perform statistical analyses. This was run by one of the co-authors of the manuscript.)

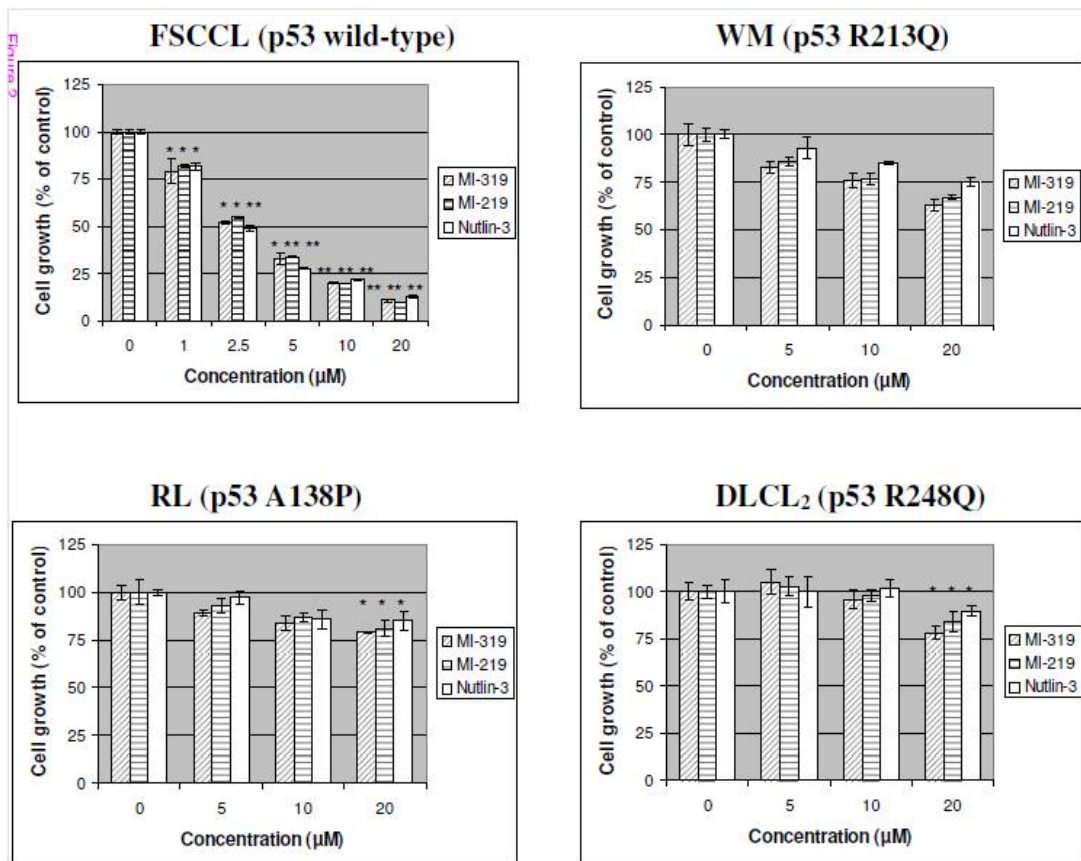


Figure 3.3 Effect of MI-319 on cell viability *in vitro*. Cells were grown for 48 hours. The number of viable cells from established tumor cell lines was determined by MTT assay. Statistical analysis was done using the *t* test (two tailed) with 95% confidence intervals between treated and untreated samples. $P < 0.05$ was used to indicate statistical significance. Bars, \pm SEM.

Additionally, Toledo (p53 P72R) was exposed to increasing concentrations of Nutlin-3 and MI-319 for 24, 48, and 72 hours. Results were not published in the aforementioned manuscript. MTT assay was used to measure the growth inhibitory

effect of HDM2 SMI on this lymphoma cell line. As in the other mt-p53 cell lines, an IC_{50} could not be determined for either Nutlin-3 or MI-319 at doses up to 10 μ M, even though increasing concentrations showed significance compared to control (Figure 3.4). Data are represented as a line graph for each time point (Figure 3.4A) as well as graphed in linear scale for both Nutlin-3 and MI-319 (Figure 3.4B). MI-219 was not assessed in the Toledo cell line because the decision was made to exclude it before MI-219 became available.

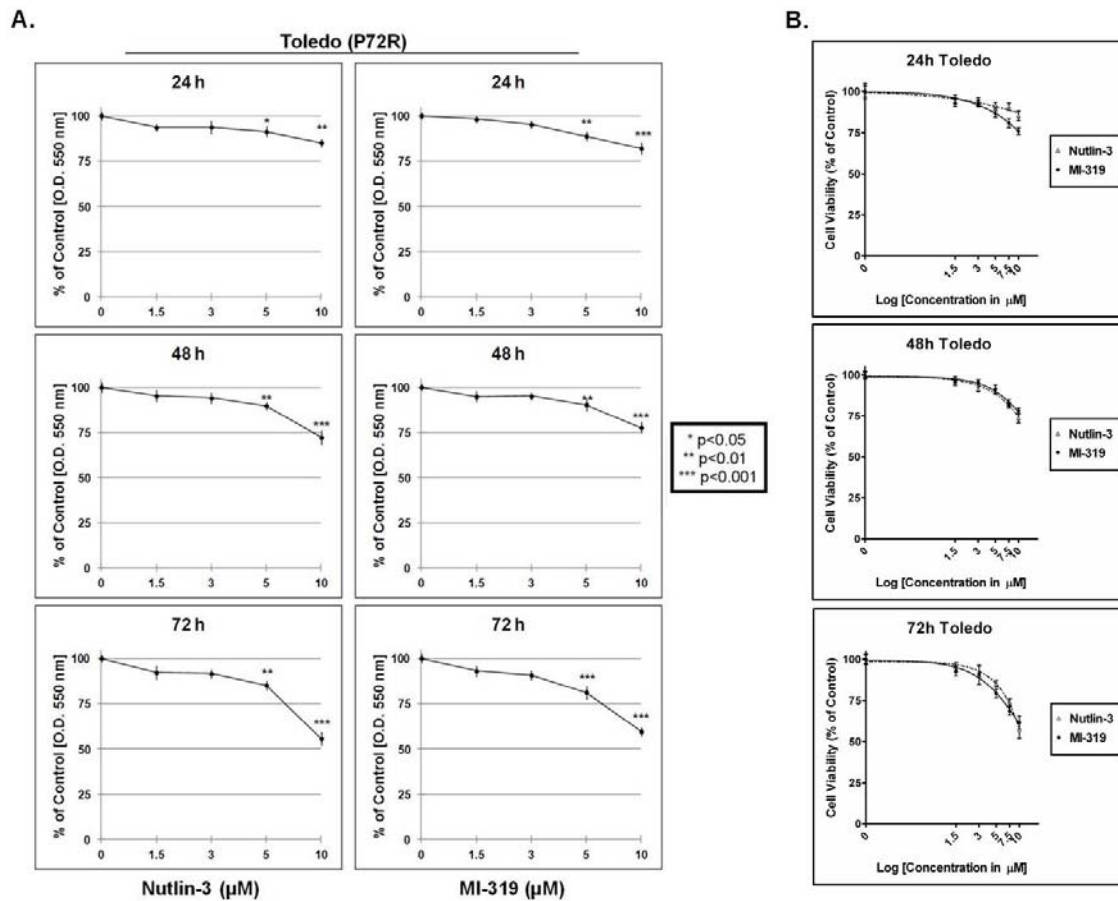


Figure 3.4 Effect of MI-319 on Toledo cell viability does not show a typical wt-p53 response. The number of viable cells from the Toledo cell line was determined by MTT assay after exposure to increasing concentration of Nutlin-3 and MI-319 for 24, 48, and 72 hours. Growth inhibition is expressed as a percentage of the control. Data represent mean \pm SE of three independent experiments, each run in duplicate. $P < 0.05$ was used to indicate statistical significance which was done using a two-tailed Student t-test between treated and untreated sample. **A**, line graphs **B**, Linear scale graphs.

HDM2 inhibition reduces cell numbers in wt-p53 lymphoma cell lines

Shortly after initial preclinical screening of MI-319 and publication of the manuscript, clinical grade MI-219 became readily available. We inferred that the effects seen after treatment with MI-219 would be similar to those seen with MI-319. The rest of this dissertation describes the use of MI-219, with the aim of performing a more comprehensive analysis to elucidate the consequences of p53 reactivation by HDM2 SMIs in lymphoma cells.

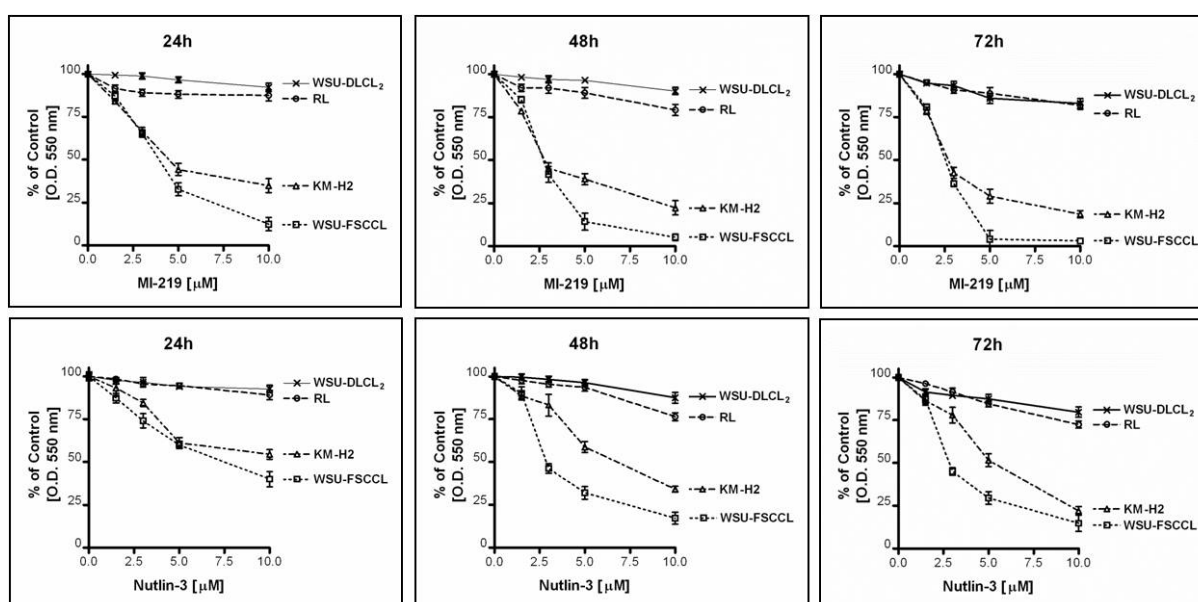


Figure 3.5 HDM2 inhibitors reduce cell viability of wt-p53 lymphoma cells. Wt-p53 (WSU-FSCCL; KM-H2) and mt-p53 (WSU-DLCL₂; RL) lymphoma cells were treated with a range of concentrations of MI-219 (top) or Nutlin-3 (bottom) for 24, 48, and 72 hours. Cell viability was measured by MTT assay as a percentage of controls. Data represent mean \pm SE of three independent experiments, each run in duplicate.

Using the effect of HDM2 SMI on cell count in culture as the endpoint, MI-219 (Figure 3.5, *top*) was more effective in reducing cell numbers compared with Nutlin-3 (Figure 3.5, *bottom*) in the wt-p53 cell lines, WSU-FSCCL and KM-H2. Statistical analysis was performed for each of the cell lines and at each individual time point but is not shown. An example of statistical significance is shown in Figure 3.6 after a 24 hour treatment in WSU-FSCCL (A) and KM-H2 cells (B). Although the IC₅₀ at 48 h was

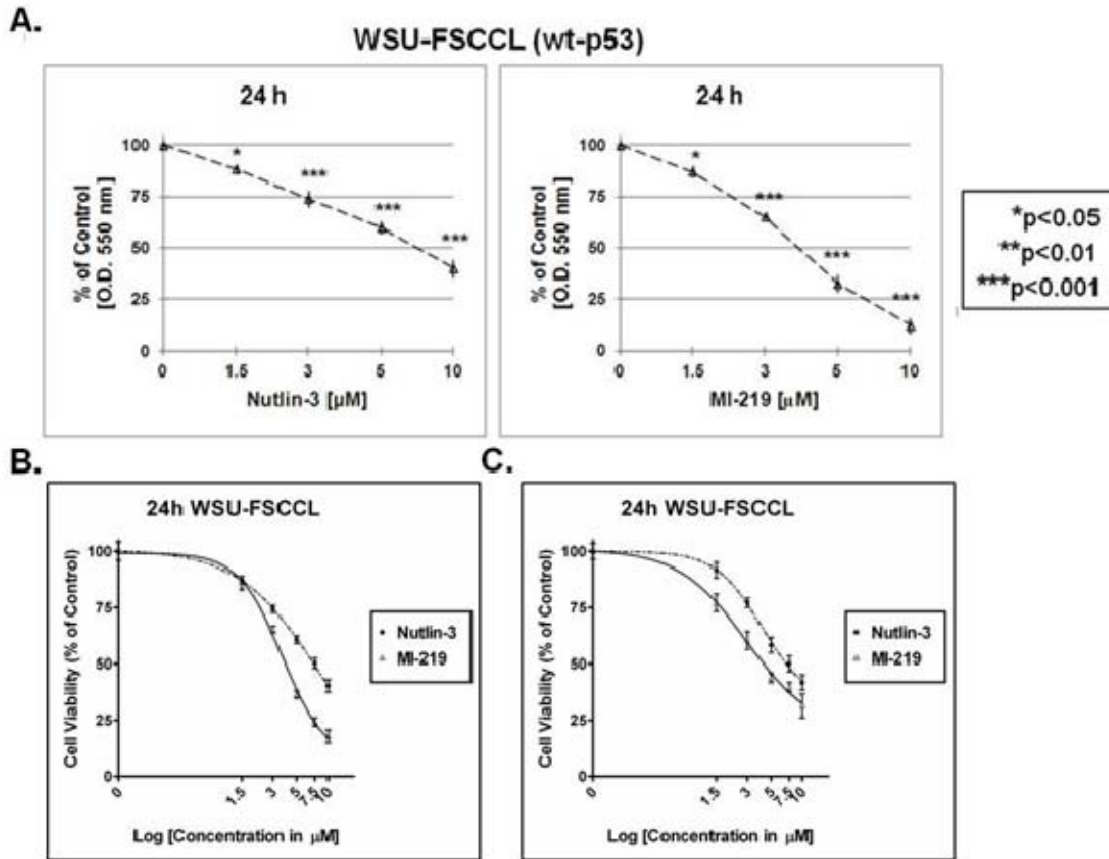


Figure 3.6 Statistical significance of the ability of HDM2 inhibitors to inhibit wt-p53 lymphoma cellular growth. The same wt-p53 data as in Figure 3.5 graphed at a single time point for WSU-FSCCL **A**. Data represented as line graphs. **B**. The same data is represented in a linear graph. **C**. WSU-FSCCL cells were exposed to HDM2 SMI and cell viability was measured by Trypan blue exclusion assay. $p < 0.05$ was used to indicate statistical significance which was done using a two-tailed Student t-test between treated and untreated sample. Bars, \pm SEM.

similar for both agents in wt-p53 WSU-FSCCL cells (2.5 and 3 μM , respectively), unlike Nutlin-3 MI-219 treatment led to complete cell elimination by 72 hours at the 5 μM and 10 μM . The IC_{50} was significantly different in wt-p53 KM-H2 cells (8 μM for Nutlin-3 vs. 3 μM for MI-219) suggesting that Hodgkin lymphoma may be less sensitive to this treatment modality. There was no significant effect for either agent, however, in the mt-p53 cell lines, WSU-DLCL₂ and RL, at the concentrations used. Similar results were obtained using Trypan blue dye exclusion assays and representative graphs are shown

in Figure 3.6C. Additionally, we were able to conclude that the IC_{50} 's at 48h were comparable in each of these two assays to monitor cellular growth inhibition. The inactive enantiomer Nutlin-3b did not exhibit comparable reduction in cell growth, even at 20 μ M, as detected by MTT assay (Figure 3.7). This demonstrates the selectivity of active HDM2 SMIs in contrast to the inactive Nutlin-3b.

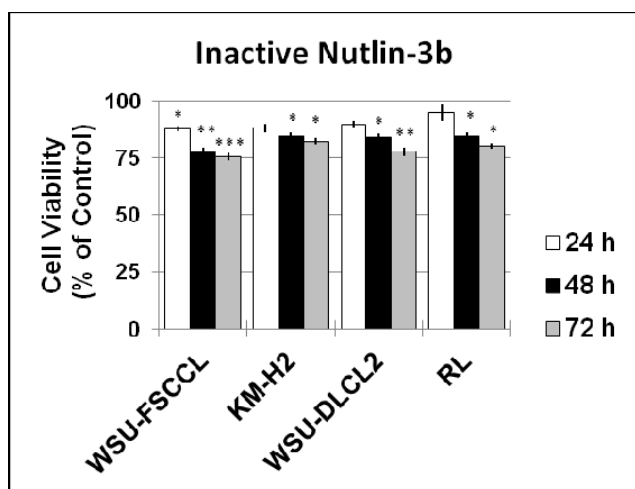


Figure 3.7 Inactive enantiomer of HDM2 inhibitor on lymphoma cell viability. Treatment with 20 μ M of inactive Nutlin-3b has no growth inhibitory effects, demonstrating the selectivity of active HDM2 SMIs binding to the p53 binding pocket of HDM2. Bars, \pm SEM.

Characteristics of lymphoma patient samples

To extend the findings in lymphoma cell lines, the effects of HDM2 inhibition in a number of lymphoma patient samples *ex vivo* was studied. Analyzable tumor samples obtained from peripheral blood of 13 patients with B-cell lymphoma in leukemic phase were enriched for peripheral B lymphocytes and exposed to MI-219 or Nutlin-3. Cells were then analyzed for cell viability, p53 status and selected protein expression. Patient characteristics are shown in Table 3.2. Eight patients had small lymphocytic lymphoma (SLL)/chronic lymphocytic leukemia (CLL), 3 had marginal zone lymphoma (MZL), 1 had Follicular lymphoma, and 1 had diffuse large B cell lymphoma (DLBCL). Male: female ratio was 5: 8; median age was 69 years (range 62-86). Of the 8 SLL/CLL patients, 6 had 13q- and the remaining 2 had trisomy 12. All patients, except one

(patient #9) exhibited wt- p53. Patient # 9, with 17p- chromosomal abnormality detected in 9% of cells also contained a p53 mutation (Lys132Arg). None of the patients were on active therapy at the time of study although several patients had been previously treated.

Table 3.2 Comprehensive list of lymphoma patients.

Patient #	AGE	SEX	RACE	TYPE OF LYMPHOMA	CYTOGENETICS/ KARYOTYPE	p53 status Exons 5-9 (cDNA)	IgH STATUS
1 (JP100909)	61	F	Caucasian	DLBCL	Normal/46, XX [20]	wt	wt
2 (RC102609)	49	F	Caucasian	FL	23%- t(14;18)(q32;q21.3)	wt	IgH-BCL2 fusion
3 (FH032310)	62	M	Caucasian	MZL	Normal/46,XY [20]	wt	wt
4 (CS052010)	76	M	Caucasian	CLL/SLL	84.5%-trisomy 12 15.5%- deletion of 17p 11%-loss of IgH locus	wt	11%-loss of IgH locus
5 (AN052510)	86	M	Caucasian	MZL	Normal/46, XY [20]	wt	wt
6 (VFO11311)	71	F	Caucasian	CLL/SLL	67.5%-trisomy 12	wt	wt
7 (MS020111)	64	F	African-American	CLL/SLL	86.5%-deleted 13q	wt	wt
8 (JL020811)	72	M	Caucasian	MZL	45%-t(2;7)(p12;q21-22)	wt	wt
9 (KK060211)	64	F	Caucasian	CLL/SLL	54.5%-deleted 13q	wt	wt
10 (HH110111)	81	F	Caucasian	CLL/SLL	58.5%-deleted 13q	wt	wt
11 (KM111511)	69	F	Caucasian	CLL/SLL	51%- deleted 13q 9%- deleted 17p	mt (Lys132Arg)	wt
12 (EM111711)	62	M	Caucasian	CLL/SLL	23.5%-deleted 13q 26%-3 IgH copies	wt	26%-3 IgH copies
13 (PH122211)	69	F	Caucasian	CLL/SLL	72%- deleted 13q	wt	wt

Optimization of patient-derived B lymphocytes

As a starting point *ex vivo*, the IC₂₅, IC₅₀ and IC₁₀₀ of each HDM2 SMI determined in the cell lines was used for the first two patient samples; doses were optimized further in subsequent samples. Primary lymphoma cells from patient #2, RC102609, show a time- and concentration-dependent decrease in cell viability (Figure 3.8A) upon exposure to HDM2 SMIs. Annexin V/PI assay was performed on the remaining primary

cells from patient #2 to monitor apoptotic cell death and show only a slight increase in Annexin V positively stained cells compared to untreated cells after a 24 hour treatment with Nutlin-3 and MI-219. This did not correspond to the growth inhibitory data as we had expected since there was not a great difference in treated versus untreated cells (Figure 3.8B). An unusual number of untreated cells stained positively for Annexin V whereas Trypan blue did not show similar results for apoptotic cells (data not shown). Drug concentrations were standardized (2.5, 5, and 10 μM) shortly thereafter for the rest of the B cells isolated from lymphoma patients.

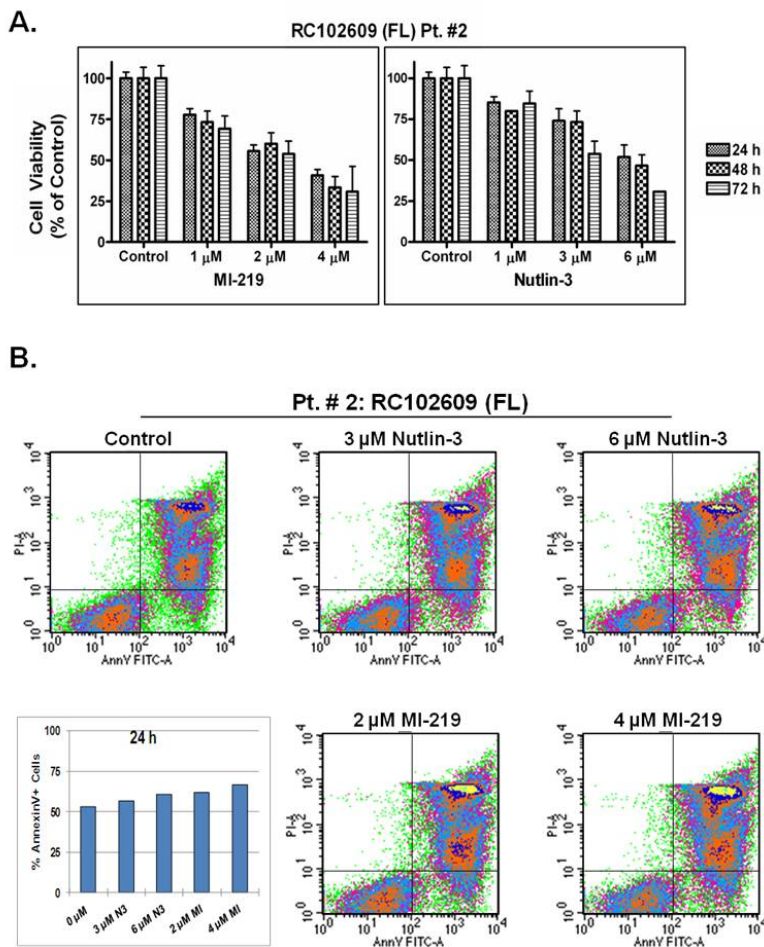


Figure 3.8 Optimization of HDM2 inhibitors in primary lymphoma cells. **A**, B-lymphocytes from patient RC102609 were treated with increasing concentrations of Nutlin-3 or MI-219 for 24, 48, or 72 hours. Cell counts were performed in triplicate and cell viability was determined by the Trypan blue exclusion assay as a percentage of the controls. **B**, Annexin V/PI assay was performed on the remaining cells to test for apoptosis after 24 h of treatment. There are no error bars or statistical analysis as only one independent experiment is illustrated. Bars, Mean \pm SE.

The high number of Annexin V positive cells in the control in patient #2, RC102609, seemed unusual, so the assay was used once again in B lymphocytes

isolated from patient #3, FH032310 after exposure to HDM2 SMI for 48 hours (Figure 3.9A). Again, total number of Annexin V positively stained cells was quite high in the untreated control and dose-dependent increases in the number of apoptotic cells was more difficult to assess. The percentage of early (Figure 3.9D) and late (Figure 3.9C) apoptotic cells were graphed separately and indicate that MI-219 treated cells appear to have completed or have just about completed apoptosis at this particular time point. Only PI-stained cells, indicative of dead cells, were seen after 10 μ M MI-219 treatment, which may explain the reduction of total cells staining positively for Annexin V at the higher concentrations.

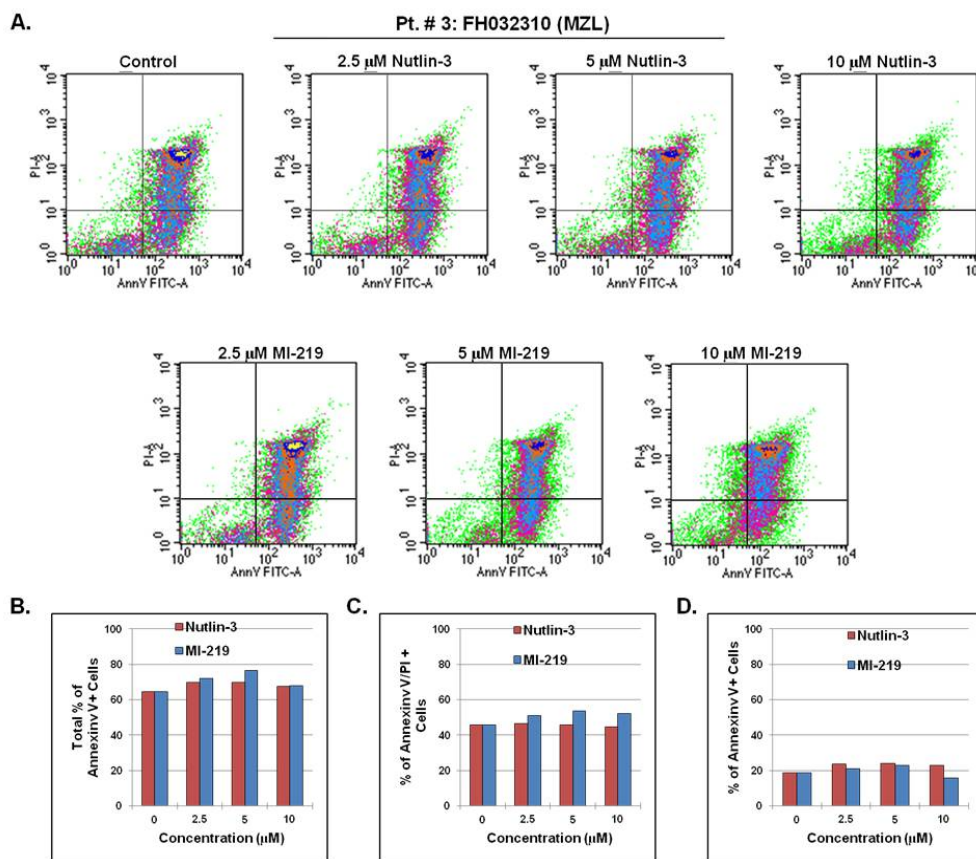


Figure 3.9 Annexin V/PI is not an appropriate assay to represent apoptosis after exposure of primary lymphoma cells to HDM2 inhibitors. **A**, B-lymphocytes from patient FH032310 were treated with increasing standardized concentrations of Nutlin-3 or MI-219 for 48 h. **B**, Total percentage of Annexin V/PI positive cells, including early (**D**) and late apoptotic (**C**) cells detected in the lower right and upper right quadrants of the flow cytometric results. Data are representative of one independent experiment.

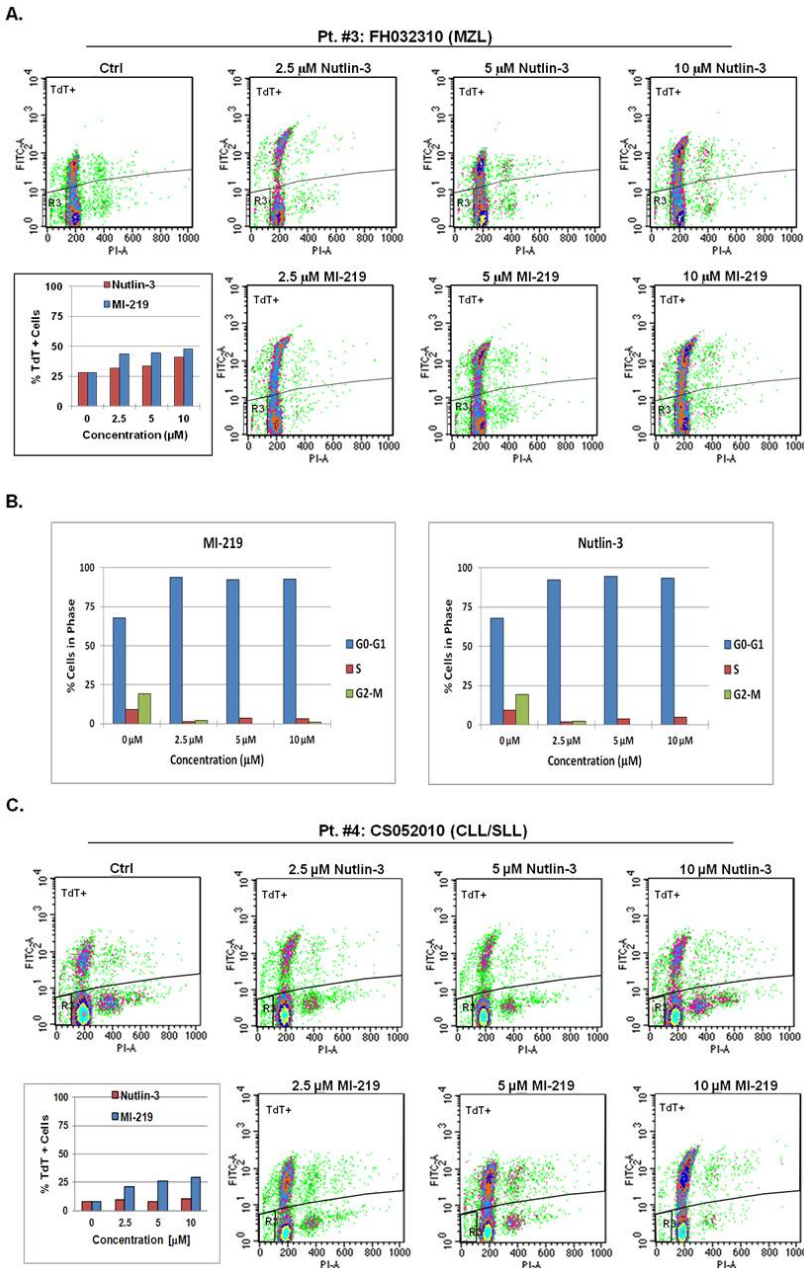


Figure 3.10 TUNEL/PI positive cells after exposure of primary lymphoma cells to HDM2 SMI. **A**, TdT+ B lymphocytes from patient #3, FH032310 (MZL), were treated with increasing concentrations of Nutlin-3 or MI-219 for 48 h. **B**, Cell cycle analysis extrapolated from the TUNEL/PI data for patient #3, FH032310. **C**, TdT+ B lymphocytes from patient #4, CS052010 (CLL/SLL), were treated with increasing concentrations of Nutlin-3 or MI-219 for 24 h. Data are representative of one independent experiment.

Primary lymphoma cells from patient #3, FH032310 (MZL), show a concentration-dependent increase in TdT positive cells (Figure 3.10A) upon exposure to HDM2 SMIs for 48 hours. Apoptosis results, in terms of number of cells differ between the Annexin V/PI assay and the TUNEL/PI assay. Primary B lymphoma cells show very little differences in cell cycle arrest between cells treated with HDM2 SMIs and control (Figure 3.10B), due to the lack of active cell proliferation. Primary lymphoma cells

isolated from patient #4, CS052010 (CLL/SLL), also show a dose-dependent increase in TdT positive cells (Figure 3.10A) after treatment with HDM2 SMIs for 24 hours (Figure 3.10C). TUNEL/PI may be a more appropriate assay to use when assessing apoptosis in patient samples.

FACS analysis in patient-derived B lymphoma cells

In a normal human being, B lymphocytes typically comprise up to 25% and T-cells upwards of 75% of the PBMC cell population. Patient-derived B lymphocytes levels may be extremely elevated due to the clonal expansion of B-cells driving the disease. Considering the high percentage of T-cells typical in an individual without lymphoma, it was postulated that the biological response of primary lymphoma cells may occur from T, rather than B lymphocytes. At the very least, residual T cells could affect the results or interpretation of the data. To eliminate this possibility, a T-cell depletion step was implemented to ascertain that the patient-derived B lymphocyte population is truly as enriched as it can be. The enhancement of B lymphocytes from two different patient samples was tested by flow cytometry. Patient #6, VF011311 (SLL/CLL), went from 87.7% CD19+, CD2- B lymphocytes (Figure 3.11A, *right*) in the non-depleted PBL (peripheral blood lymphocyte) cellular fraction to 98.7% after T-cell depletion (Figure 3.11A, *left*). Patient #10, HH110111 (SLL/CLL), went from coexpressing CD19+ CD5+ (CD5+ is abnormally found on SLL/CLL) on 96.3% of non-depleted PBL cells (Figure 3.11B, *left*) to 99.8% CD19+ CD5+ post T-cell depletion (Figure 3.11B, *right*). The use of two different T-cell markers, CD2+ and CD5+, was used to confirm that the depletion was not specific to a particular T-cell subset fraction.

A.

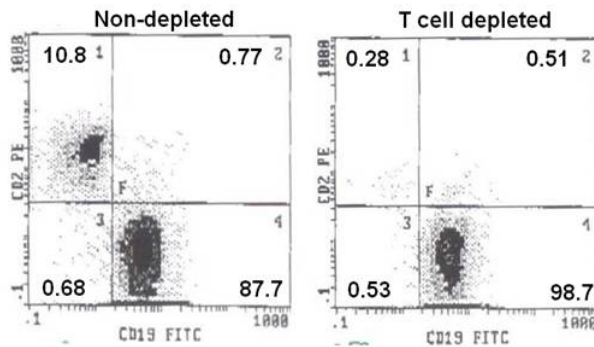
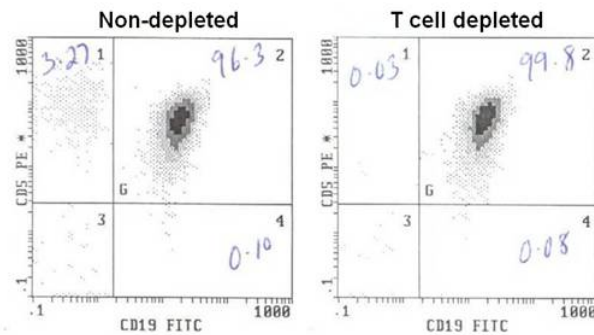
pt: VF011311

Figure 3.11 Flow cytometric assessment of the purity of patient-derived B lymphocytes. **A**, CD19+ primary B lymphoma cells isolated from patient #6, VF011311, were enhanced from 87.7% to 98.7%. **B**, Pan CD2+ depletion enhanced CD19+CD5+ coexpressing cells from 96.3% to 99.8% in patient #10, HH110111.

B.

pt: HH110111

FACS analysis in B lymphocytes from normal donors

Consistent T-cell depletion was achieved in normal donors using the optimized protocol described Chapter II (Figure 3.12). The enhancement of B lymphocytes from three different normal donors was confirmed by flow cytometric analysis. T cell depletion in the donors was detected by overall reductions in T cell subsets CD4 and CD8 (Figure 3.12, 1st and 3rd columns). In each of these three normal donors, CD19+ B lymphocytes were enhanced a minimum of 4 to 6-fold (Figure 3.12, 2nd and 4th columns).

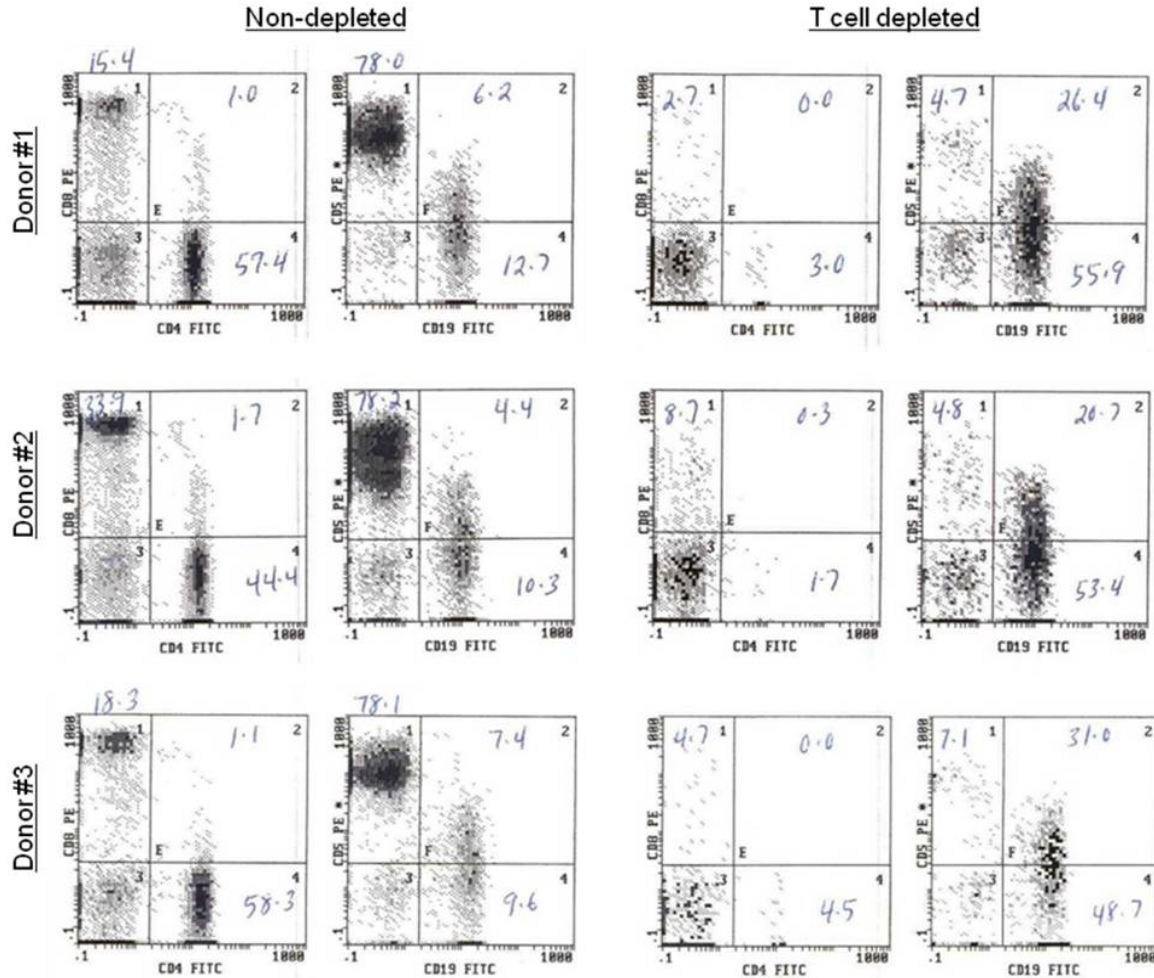


Figure 3.12 FACS analysis of B lymphocyte purity after pan CD2+ T cell depletion in normal blood donors. CD19+ primary B lymphocytes isolated from donor #1 were enhanced more than 4-fold; donors #2 and #3 were enhanced more than 5-fold.

Growth inhibition in primary lymphoma cells

Enriched primary B lymphocytes were analyzed for cell viability and selected protein expression. To show individual responses to HDM2 SMIs, three patient samples representing two different types of lymphomas: AN052510 and FH032510 (mantle zone lymphomas (MZL)) and VF011211 (small lymphocytic lymphoma/chronic lymphocytic leukemia (SLL/CLL)) were used. Treatment of each patient sample with Nutlin-3 or MI-219 caused a time- and dose-dependent growth inhibition as determined by Trypan blue exclusion (Figure 3.13A). Trypan blue was also used to determine the percentage of

apoptosis. Apoptosis in patient samples showed time- and dose-dependent increases in Trypan blue positively stained cells (Figure 3.13B). MI-219 appeared to have a slightly greater potency in the induction of apoptosis in primary lymphoma cells compared to Nutlin-3.

Overall, HDM2 SMIs reduce the cell viability of patient lymphoma cells. Cumulative cell viability results from $n=11$ patients for each drug, concentration, and time point is shown in Figure 3.14. Since there were so many variables involved, a comprehensive biostatistical analysis was performed by Dr. Judith Abrams on 10 of the 11 patient samples to determine whether there were differences between Nutlin-3 and MI-219 and their effect on cell viability. The mean cell survival along with standard errors, for each combination of drug, concentration and time is shown in Figure 3.15 and Table 3.3 demonstrating that MI-219 is significantly more effective ($p<0.001$) at reducing the cell viability of primary lymphoma cells than Nutlin-3. Of note, the statistics performed did not allow the control to fit into each of the combinations (below) resulting in percent survival of less than 100%.

MI-219 versus Control

The percent survival of patient cells treated with MI-219 is significantly lower at each concentration used compared to untreated control ($p<0.001$ for 2.5, 5 and 10 μM). Cell survival averaged 16% lower at 2.5 μM than for control, 32% at 5 μM , and 49% at 10 μM .

Nutlin-3 versus Control

The percent survival of patient cells treated with Nutlin-3 is significantly lower at each concentration used compared to untreated control ($p<0.001$ for 2.5, 5 and 10 μM). Cell survival averaged 10% lower at 2.5 μM than for control, 21% at 5 μM , and 36% at

10 μM .

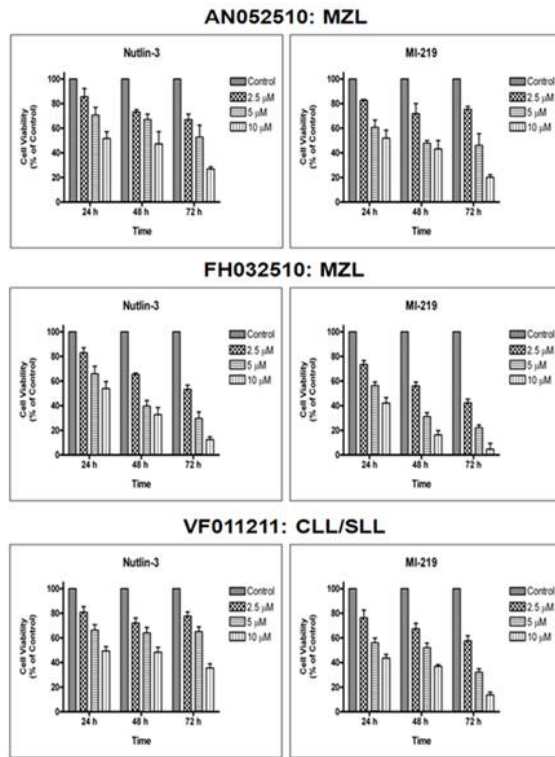
MI-219 versus Nutlin-3: Simple Mode

In this type of analysis, the main effects are only of drug and concentration. This model fits time as a continuous factor and drug and concentration as nominal factors. It shows that there is a significant difference between each of the drugs ($p < 0.001$) and that the percent survival of patient cells averaged 10% lower with MI-219 than with Nutlin-3. During each 24 hour interval, the survival decreases significantly ($p < 0.001$) by 14%.

MI-219 versus Nutlin-3: Complex Mode

In this type of analysis, the main effects are of each drug by concentration tested against each of the other drug by concentration. During each 24 hour interval, the survival decreases significantly ($p < 0.001$) by 14%, similar to the simple mode. Compared to a concentration of MI-219 of 2.5 μM , cell survival at a concentration of 5 μM averages 16% lower and at a concentration of 10 μM averages 33% (both $p < 0.001$). Cell survival at a concentration of 10 μM is significantly lower ($p < 0.001$) than at a concentration of 5 μM . Survival with Nutlin-3 averages 12% lower at a concentration of 5 μM and 26% lower at concentration of 10 μM compared to survival at a concentration of 2.5 μM (both $p < 0.001$). The difference in cell survival between concentrations of 5 μM and 10 μM is significant ($p < 0.001$). Regardless of concentration, survival is significantly lower with MI-219 than with Nutlin-3 ($p < 0.001$ for 2.5, 5 and 10 μM).

A.



B.

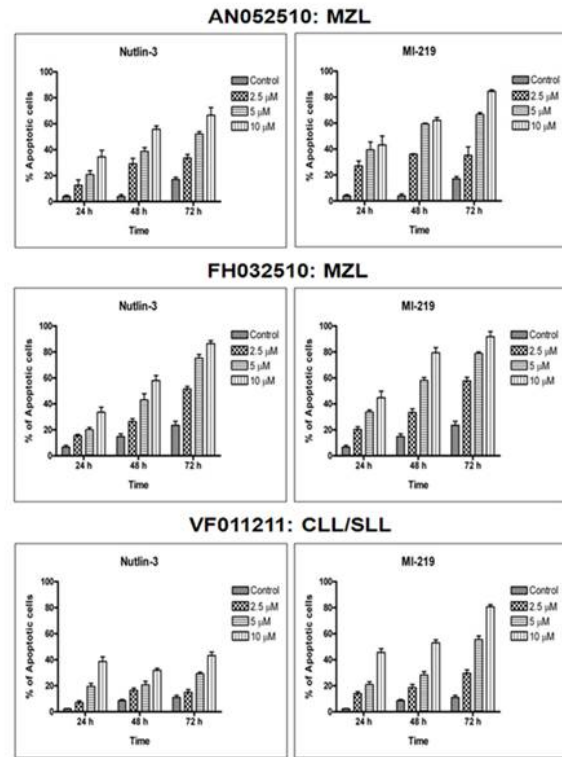


Figure 13.13 HDM2 inhibition dose-dependently reduced cell viability and increased apoptosis in wt-p53 lymphoma patient cells. **A, B.** B-lymphocytes from patient samples AN052510, FH032510, and VF011211 were treated with increasing concentrations of Nutlin-3 or MI-219 for 24, 48, or 72 hours. Cell viability and apoptosis was determined by the Trypan blue exclusion assay as a percentage of the controls. Cell counts were performed at minimum in triplicate.

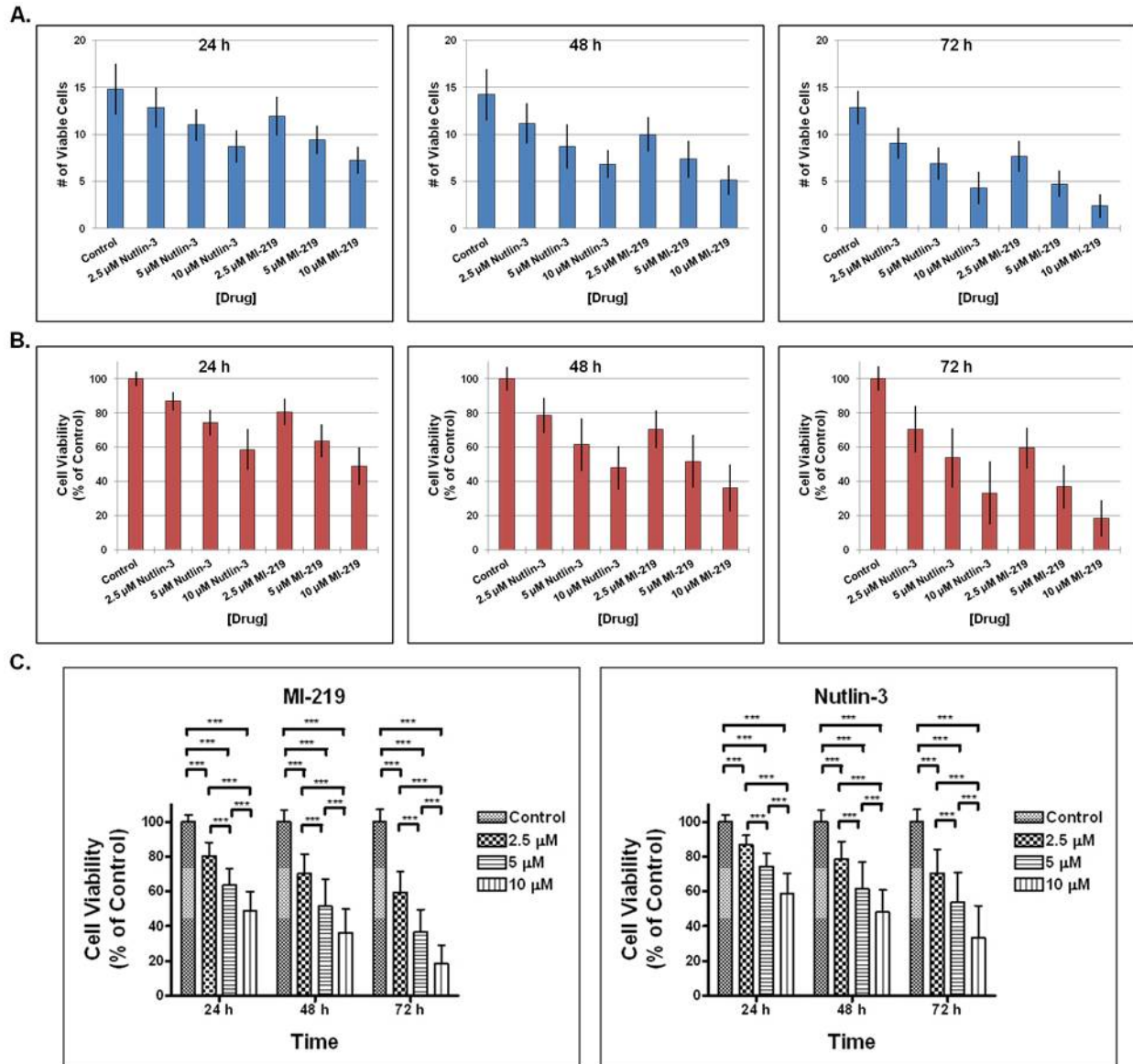


Figure 3.14 Cumulative time- and dose-dependent reduction of cell viability of primary B lymphoma cells after HDM2 inhibition. Pooled data from ($n=11$) patient samples after 24, 48, and 72 hr treatment ($n=37$ replicates per time point) with increasing concentrations of MI-219 and Nutlin-3. **A**, Mean (cumulative) of the raw number of viable cells. **B**, Cell viability was measured as a percentage of untreated controls at each time point. **C**, Statistical analysis was performed using two-way ANOVA, followed by Bonferroni and the differences were considered significant when $p < 0.05$. All results are expressed as the mean \pm S.D.

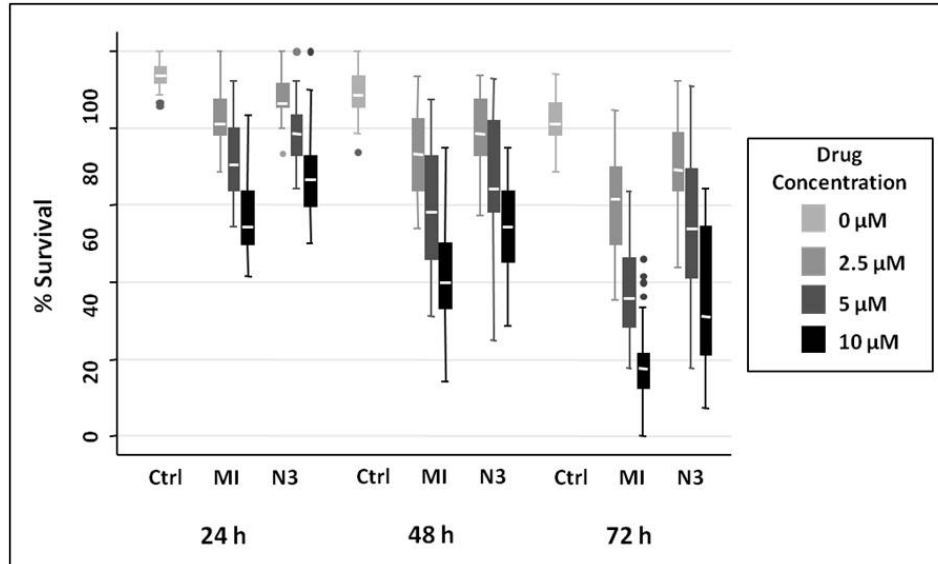


Figure 3.15 HDM2 inhibition reduces cell survival in patient-derived lymphoma cells. Box plots show the percent survival found in primary lymphoma cells isolated from lymphoma patients ($n=11$) after increasing concentrations of MI-219 and Nutlin-3 treatment compared to control at the indicated time point as detected by Trypan blue exclusion assay. There were replicates ($n=37$) for each patient using each drug, dose, and time point. Survival is expressed as a percentage of live cells relative to the total number of cells detected. The horizontal white line in the box represents the median while the upper and lower lines of the box endorse the 25th and 75th interquartile range (IQR). The upper- and lower-most lines extend to cover points within 1.5 times the IQR and circles outside of the lines indicate outliers. A mixed effects analysis of variance was used where drug, concentration and time were defined as fixed effects; patient and replication were defined as random effects. Holm's procedure was used to adjust for multiple comparisons. MI-219 is statistically more effective at reducing primary lymphoma cell viability than Nutlin-3 ($p<0.001$).

Table 3.3 Biostatistical analyses of lymphoma patient samples.

Concentration	Time	N	Percent Cell Survival		
			Control	MI-219	Nutlin-3
			Mean (SEM)	Mean (SEM)	Mean (SEM)
0	24	37	94 (0.7)		
	48	37	89 (1.1)		
	72	37	82 (1.2)		
2.5	24	37		83 (1.2)	88 (0.9)
	48	37		74 (1.9)	79 (1.6)
	72	37		61 (2.0)	70 (2.2)
5	24	37		72 (1.6)	79 (1.2)
	48	37		59 (2.6)	68 (2.5)
	72	37		38 (2.1)	55 (2.8)
10	24	37		59 (1.9)	68 (1.8)
	48	37		41 (2.3)	55 (2.0)
	72	37		18 (1.8)	35 (2.9)

A dose dependent increase in p53 was seen in patient lymphoma cells after HDM2 inhibition. Both Nutlin-3 and MI-219 activated p53 resulting in the upregulation of p53, selected p53 target proteins, and apoptosis markers as visualized by Western blot (Figure 3.16). Additional proteins were probed for such as Cyclin D1, Rb, and Mdr1 and these preliminary results will be discussed and further interpreted in Chapter V. Later time points (48 hours) showed decreased expression presumably due to degradation, which will be further discussed in Chapter IV (Figure 3.16 A, B). Effects were best captured after 24 hour exposure of cells to the agents (Figure 3.16 C-F). Exposure to MI-219 treatment resulted in enhanced expression of p53 protein compared to that observed with Nutlin-3 at equivalent concentrations in all wt-p53 cells.

ImageJ was used for densitometry and quantification of patient sample Western blot bands. Relative density was selected as the endpoint for biostatistical analyses that was performed by Dr. Judith Abrams (Figure 3.17). It is defined as the ratio of the absolute density, a unitless measure, for a given protein treated with a given drug, at a given concentration, for a specific time, for a specific patient to the absolute density of GAPDH under the same conditions. Evaluation of the shape of the frequency distribution of relative density indicated that a natural log transformation was required to meet the assumptions of the statistical tests. When cumulative data for HDM2, p53, and p21 were pooled together from the each of the patient samples, the relative density of proteins in MI-219-exposed cells was significantly greater than that of Nutlin-3 ($p=0.001$) (Figure 3.17A). Differences in relative density between each of the proteins HDM2, p21 and p53 at both time points were statistically significant at $p<0.001$ with both p21 and p53 having lower density than HDM2, and p21 having significantly lower density than p53 (Figure 3.17C). For p53 protein expression at 24 hours (Figure 3.17C), relative

density of cells treated with MI-219 is marginally higher than that of cells treated with Nutlin-3 at a concentration of 2.5 μM ($p=0.05$), significantly higher at a concentration of 5 μM ($p=0.02$) and significantly higher at a concentration of 10 μM ($p=0.03$). Of special interest is the observation that MI-219, but not Nutlin-3 induced both higher and lower HDM2 species which were of greater intensity than that observed in wt-p53 cell lines (discussed below) at the same time period and equal drug concentration

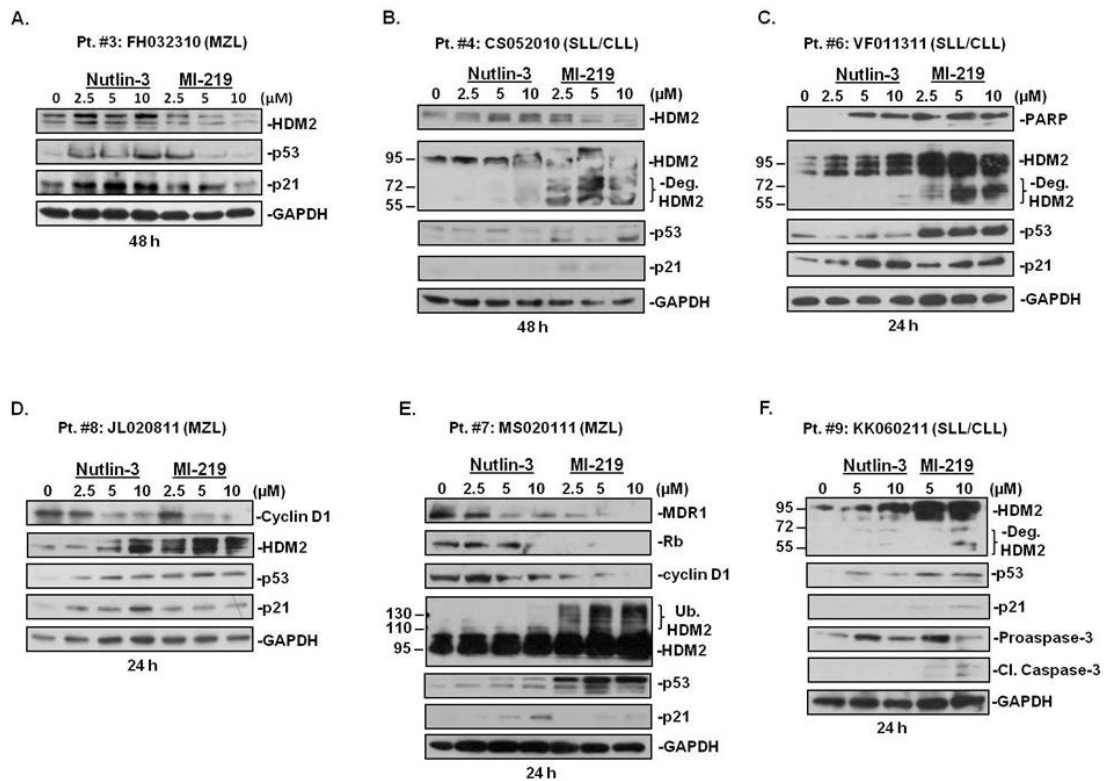


Figure 3.16 HDM2 antagonists activate the p53 pathway and MI-219, but not Nutlin-3, stimulates HDM2 self-ubiquitination and degradation in primary B lymphocytes. Shown are Western blots from six out of ten representative patients that had enough cells for this type of analysis. B lymphocytes were isolated from whole blood, purified, and treated with increasing concentrations of HDM2 SMIs for 24 or 48 hours. Purified B lymphocytes isolated from patients #3 (**A**) and #4 (**B**) were exposed to HDM2 SMIs for 48 hours. p53 target proteins showed an unexpected reduction in protein expressive levels at this time point. **C-F**, Treatment for 24 hours (patients #3-13; #5 did not have enough cells for protein analysis) was found to be the optimal exposure time to HDM2 SMIs for patient samples.

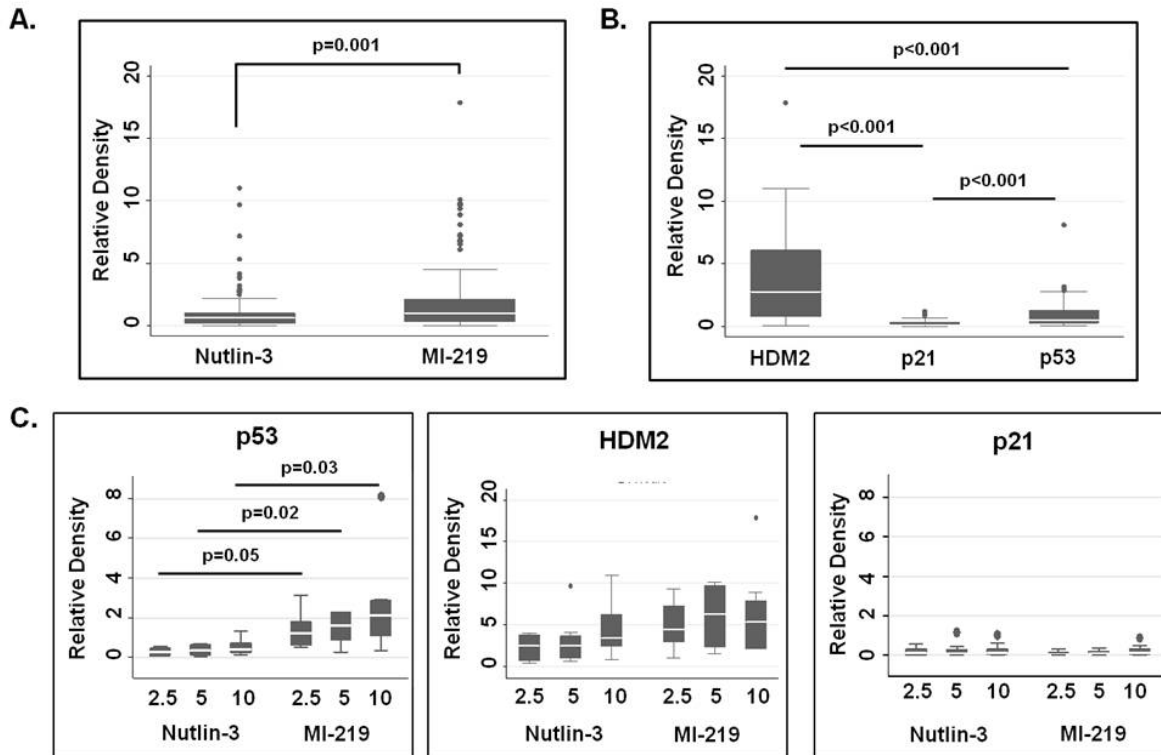


Figure 3.17 Upregulation of p53 protein predicts efficacy and biological response to MI-219 in primary lymphoma cells. Box plots show the cumulative biostatistical analyses of p53 target protein expression levels to estimate response predictors to HDM2 antagonists in primary B lymphocytes isolated from lymphoma patients ($n=10$). Western blots for each patient ($n=10$) for each drug, dose, and time point for each protein detected. Quantification of Western blot bands (relative density) was calculated using ImageJ and normalized to internal control (GAPDH). **A**, MI-219 is statistically more effective than Nutlin-3 ($p=0.001$) overall regardless of p53 target protein or time point. **B**, Differences in the upregulation of protein expression as a function of relative density between each of the proteins HDM2, p21 and p53 at both time points combined. HDM2 protein expression is significantly higher than both p21 ($p<0.001$) and p53 ($p<0.001$). p53 protein expression is significantly higher than p21 ($p<0.001$). **C**, For p53 protein expression at 24 hours, relative density of cells treated with MI-219 is marginally higher than that of cells treated with Nutlin-3 at a concentration of 2.5 μM ($p=0.05$), significantly higher at a concentration of 5 μM ($p=0.02$) and significantly higher at a concentration of 10 μM ($p=0.03$). The differences between drugs under all other combinations of experimental conditions are not statistically significant (all $p>0.50$). The horizontal white line in the box represents the median while the upper and lower lines of the box endorse the 25th and 75th interquartile range (IQR). The upper- and lower-most lines extend to cover points within 1.5 times the IQR and circles outside of the lines indicate outliers. Fixed effects linear models were used to monitor relative density as an endpoint where HDM2 SMIs, concentrations, proteins, and time were defined as fixed effects; patient was defined as the random effect. Holm's procedure was used to adjust for multiple comparisons.

Similarly, there was also no significant effect on normal peripheral blood lymphocytes (PBL) isolated from healthy donors (Figure 3.18A). Furthermore, Western blot analysis showed that HDM2 SMI have little effect on p53 protein and its targets in normal B lymphocytes after 24 hours of treatment (Figure 3.18B). Induction of apoptosis was detected only upon exposure to 500 nM of Doxorubicin. The biological responses observed post-drug treatment can be attributed to B lymphocytes as flow cytometry confirmed the enhancement of the CD19+ B lymphocyte population, minimizing the chance of response occurring from the T cells.

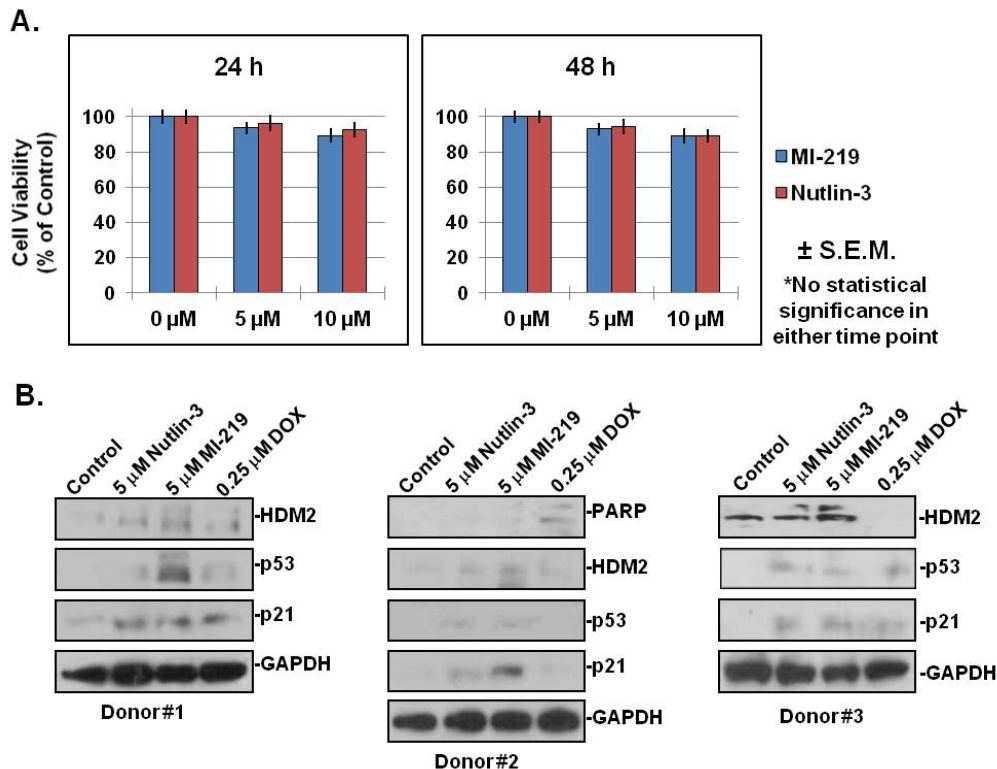


Figure 3.18 Lack of effect of HDM2 SMI on the cell viability of peripheral B lymphocytes from normal blood donors. **A**, Normal B lymphocytes derived from three (n=3) different donors were exposed to increasing concentrations of Nutlin-3 or MI-219 for 24 and 48 hours. Cell viability was measured by Trypan Blue exclusion assay as a percentage of controls. Data represent three independent treatments with duplicate readings. No detection of significance as determined by unpaired Student t-test. **B**, Primary B lymphocytes from two of the normal donors were exposed to HDM2 SMI for 24 hours. Western blot was used to detect p53 target proteins. *Bars*, Mean \pm SE.

Evaluation of the induction of p53-dependent apoptosis and cell cycle arrest

To clarify the mechanisms of growth inhibition upon HDM2 antagonism, a series of experiments examining key apoptotic and cell cycle regulators was performed. Annexin V/PI and TUNEL/PI staining were used to assess drug-induced apoptosis in each cell line. Wt-p53 WSU-FSCCL cells demonstrated a dose-dependent increase in Annexin V positively stained cells (Figure 3.19A). Apoptosis primarily occurred after the first 24h of treatment, as the percentage of Annexin V positive cells did not drastically increase over time. Interestingly, however, the percentage of Annexin V stained cells varied dramatically between Nutlin-3 and MI-219 at the same dose, where Nutlin-3 induced far less apoptosis than MI-219. Wt-p53 KM-H2 cells showed a similar pattern of dose-dependent increases in Annexin V positive cells, although to a lesser extent than WSU-FSCCL. Mt-p53 WSU-DLCL₂ cells did not demonstrate an increase in Annexin V positively stained cells at any time point with either Nutlin-3 or MI-219, even at the highest concentration (Figure 3.19B). Due to technical difficulties, we were not able to analyze Annexin V/PI in RL cells but apoptotic TdT+ cells were detected by the TUNEL/PI assay.

Cell cycle analysis after 24 h treatment demonstrates that Nutlin-3 treatment arrests wt-p53 WSU-FSCCL and KM-H2 cells at G₀/G₁ and G₂/M (Figure 3.19C, top). There is a greater proportion of G₀/G₁ cells with MI-219 treatment, but this is likely due to apoptotic cells falling off into G₀ and indicates that MI-219 induces cell cycle arrest as well as apoptosis. Cell cycle arrest is not affected in mt-p53 WSU-DLCL₂ or RL cells (Figure 3.19C, bottom). Taken together, these results demonstrate that both Nutlin-3 and MI-219 induce a cell cycle arrest, but Nutlin-3 to a lesser extent than MI-219, and the accumulation of G₀/G₁ arrest is most likely apoptotic cells. TdT+ cells would be the

best way to help distinguish between true cell cycle arrest and accumulation of cells in this phase due to apoptosis.

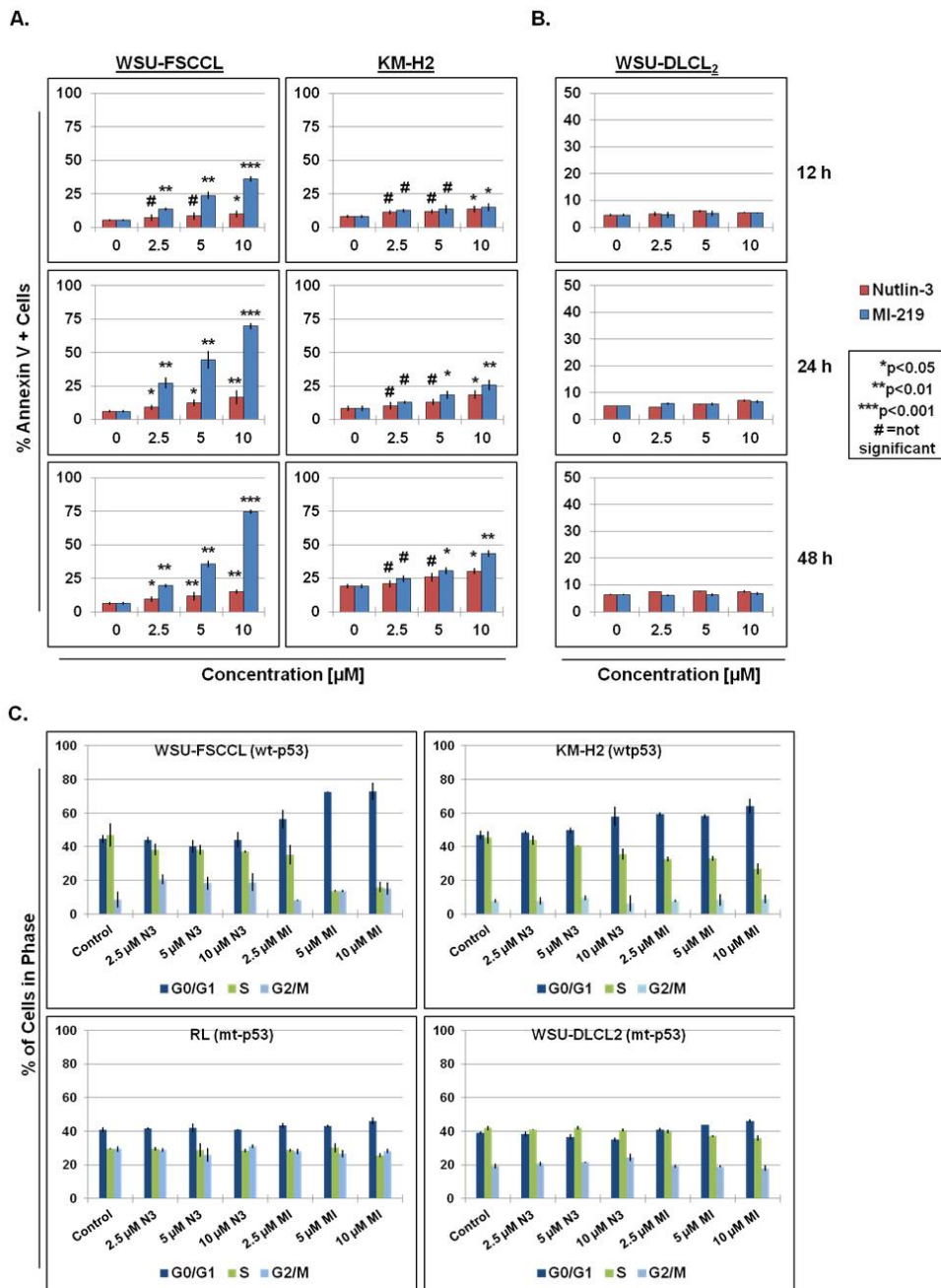


Figure 3.19 Biological response of lymphoma cell lines to HDM2 SMIs. The percentage of Annexin V positive cells is measured upon exposure to HDM2 SMIs after 12, 24, and 48 hours in wt-p53 (**A.**) and mt-p53 (**B.**) lymphoma cell lines. **C.** Cell-cycle analysis in wt- and mt-p53 lymphoma cells after 24 hours of HDM2 inhibition. Results are the mean of at least three independent experiments. Statistical analysis for Annexin V/PI was performed using two-tailed Student t-test between treated and untreated sample per time point and the differences were considered significant when $p < 0.05$. Bars, SEM.

Table 3.4 Cell cycle arrest p values.

24h WSU-FSCCL						
	G0/G1		G2/M		S	
c v 2.5N	0.709272	NS	0.011299	*	0.084812	NS
c v 5N	0.712645	NS	0.010813	*	0.029148	*
c v 10N	0.269605	NS	0.019871	*	0.022637	*
c v 2.5MI	0.024805	*	0.990714	NS	0.009969	**
c v 5MI	0.000277	***	0.132902	NS	0.000948	***
c v 10MI	0.000144	***	0.129975	NS	0.000598	***

24h KM-H2						
	G0/G1		G2/M		S	
c v 2.5N	0.212508	NS	0.846443	NS	0.537633	NS
c v 5N	0.102345	NS	0.310741	NS	0.035021	*
c v 10N	0.029496	*	0.625015	NS	0.015599	*
c v 2.5MI	0.005114	**	0.914694	NS	0.027521	*
c v 5MI	0.002775	**	0.635546	NS	0.001774	**
c v 10MI	0.003047	**	0.530712	NS	0.001613	**

TUNEL/PI was also used to as another experimental method to confirm the Annexin V/PI results after a 24 hour treatment. Weak TdT positive staining was detected at all concentrations of Nutlin-3 in wt-p53 WSU-FSCCL cells (Figure 3.20). In contrast, dose dependent TdT positive cells were seen upon treatment with MI-219, indicative of cells undergoing drug-induced apoptosis, Nutlin-3 to a lesser extent. The levels of apoptotic cells appeared to vary between each of the assays although the difference between each of the two HDM2 SMIs was still apparent. Mt-p53 WSU-DLCL₂ and RL cells did not display TdT positive staining with either SMI at any concentration.

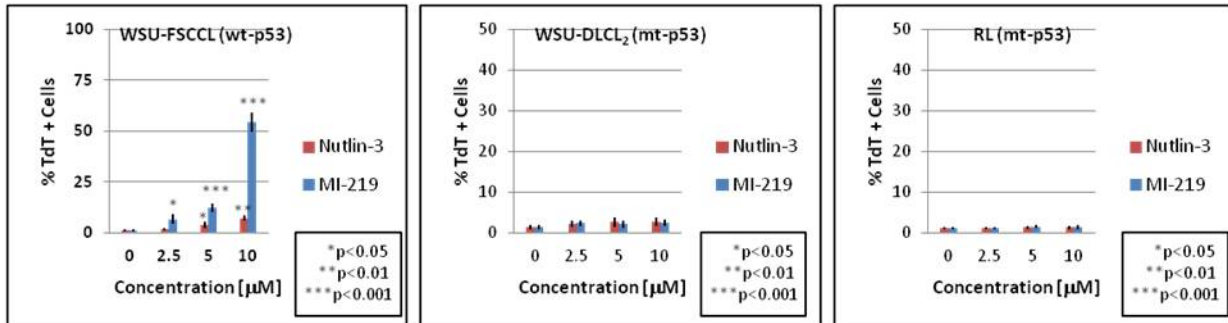


Figure 3.20 Assessment of apoptosis after HDM2 inhibition in lymphoma cell lines. HDM2 inhibitors activate the apoptotic pathway in WSU-FSCCL, but not WSU-DLCL₂ or RL cells. The percentage of TdT+ positive cells is measured upon exposure to HDM2 SMIs after 24 hours. No statistical significance in mt-p53 lymphoma cell lines WSU-DLCL₂ and RL. Results are the mean of three independent experiments. Bars, SEM.

To clarify the discordance between apoptosis assays, levels of caspase-3 and PARP cleavage, indicators of apoptosis, were further tested. Cleavage of caspase-3 and PARP was detected in a dose-dependent manner at each of the time points in wt-p53 WSU-FSCCL with evidence of greater induction of apoptosis with MI-219 treatment than with Nutlin-3 (Figure 3.21). Moreover, caspase-3 and PARP cleavage corresponds with the results obtained from TdT positive staining more than results from Annexin V/PI staining. The requirement for functional p53 activity is further confirmed by the lack of activity seen in mt-p53 lymphoma cells. Overall, these data indicate that HDM2 antagonists promote the reactivity of wt-, but not mt-, p53 in lymphoma cells.

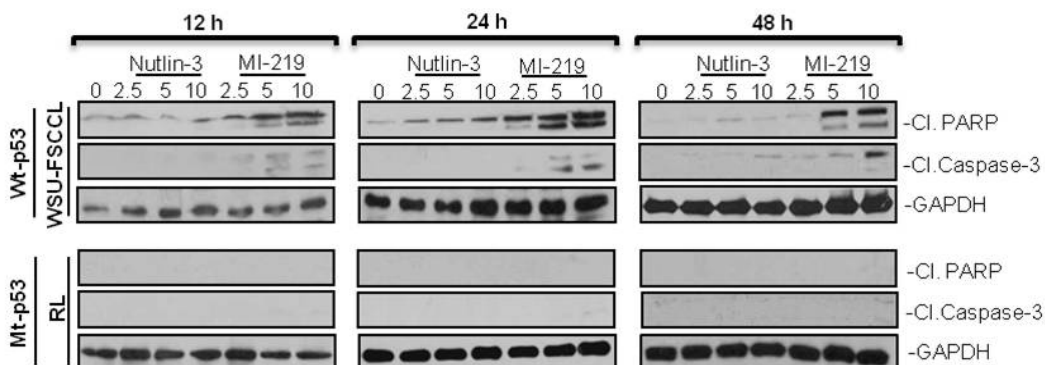


Figure 3.21 MI-219 induces greater apoptosis than Nutlin-3 in wt-p53 WSU-FSCCL cells. Cleavage of PARP and caspase-3, two indicators of apoptosis, was detected by Western blot analysis after 12, 24, and 48 hours of exposure to HDM2 SMIs. GAPDH was used as a loading control.

Evaluation of p53 protein and p53 target proteins

Activation of the p53 pathway results in upregulation of p53-target proteins and genes. In order to characterize p53 activation, p53 protein levels and its selected targets were analyzed. Wt-p53 WSU-FSCCL and KM-H2 cells (Figure 3.22, top half) showed dose-dependent increases in p53 as well as its targets HDM2 and p21 in treated cells compared to vehicle control treated cells. Differences in the kinetics of protein expression between Nutlin-3 and MI-219 were observed. Effects were evident 12 to 48 hours after exposure to HDM2 SMIs. Upregulation of protein expression was greatest with MI-219 treatment, compared to Nutlin-3 treated cells. Interestingly, HDM2 expression in WSU-FSCCL at 48 hours appeared to Mt-p53 RL and WSU-DLCL₂ cells (Figure 3.22, bottom half) showed slightly elevated levels in HDM2 and p53 protein levels upon HDM2 inhibition. However, levels of p21 protein were barely detectable upon HDM2 inhibition. This suggests that the slight increase is likely p53-independent. These data indicate that wt-p53 lymphoma cells, but not mt-p53, are sensitive to HDM2 SMIs.

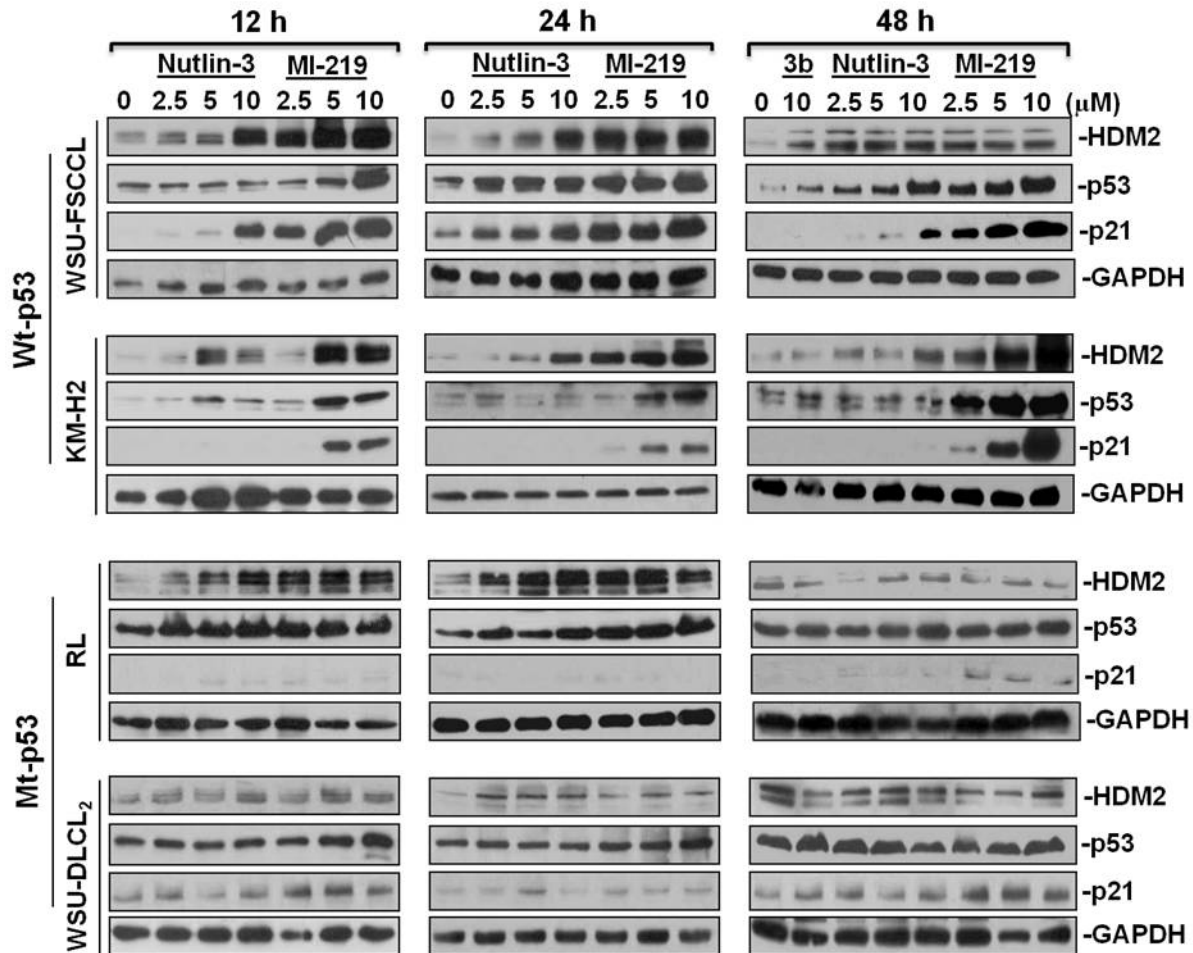


Figure 3.22 Kinetics of p53 reactivation upregulates p53 and its targets upon HDM2 inhibition in lymphoma cell lines. Wt- and mt-p53 lymphoma cell lines were treated with increasing concentrations of Nutlin-3 or MI-219 for 12, 24, and 48 hours and the levels of p53-target proteins were assessed by Western blot analysis.

HDM2 inhibition upregulates p53-dependent genes in wt-p53 lymphoma cell lines

To investigate the effects of HDM2 inhibition on p53 transcriptional regulation, we assessed the effect of SMI-mediated reactivity of p53 to enhance target gene expression levels (Figure 3.23). Wt-p53 WSU-FSCCL cells exhibited increases in p53-target genes HDM2, p21, p53AIP1 and TIGAR (TP53-induced glycolysis and apoptosis regulator) upon HDM2 inhibition compared to control cells albeit with variable kinetics (Figure 3.23). Overall, MI-219 treatment demonstrated a surprisingly greater induction of p53-target genes compared to Nutlin-3. There was much higher and more sustained

induction of HDM2 mRNA by MI-219 compared with Nutlin-3. Effect on HDM2 transcript peaked at 12 hours but was still remarkable at 24 hour in MI-219-treated cells. Both agents induced upregulation of p21 mRNA in WSU-FSCCL cells with overall higher induction by Nutlin-3 compared with MI-219. However, MI-219 effect was more evident at the earlier time points (12 and 24 hours) and at lower concentrations (2.5 and 5 μ M) compared with Nutlin-3. The later induced a delayed induction (48 hours) of p21mRNA. MI-219 was more effective than Nutlin-3 in inducing p53AIP1 mRNA. Induction of TIGAR was relatively unaffected by MI-219, except transiently by high concentration (10 μ M) at 12 hour, whereas Nutlin-3 induced delayed (48 hour) but significant increase in TIGAR. Taken together, these findings indicate MI-219 is more effective in inducing apoptosis than Nutlin-3 and Nutlin-3 treated cells may cause cells to go into senescence with the upregulation of TIGAR. There were no significant changes induced by either agent on any of the genes tested in the mt-p53 RL cells. The data are comparable with the upregulation in p53-dependent target protein levels in Figure 3.22, with the exception of p21, which may be degraded by HDM2, but was not tested in this study.

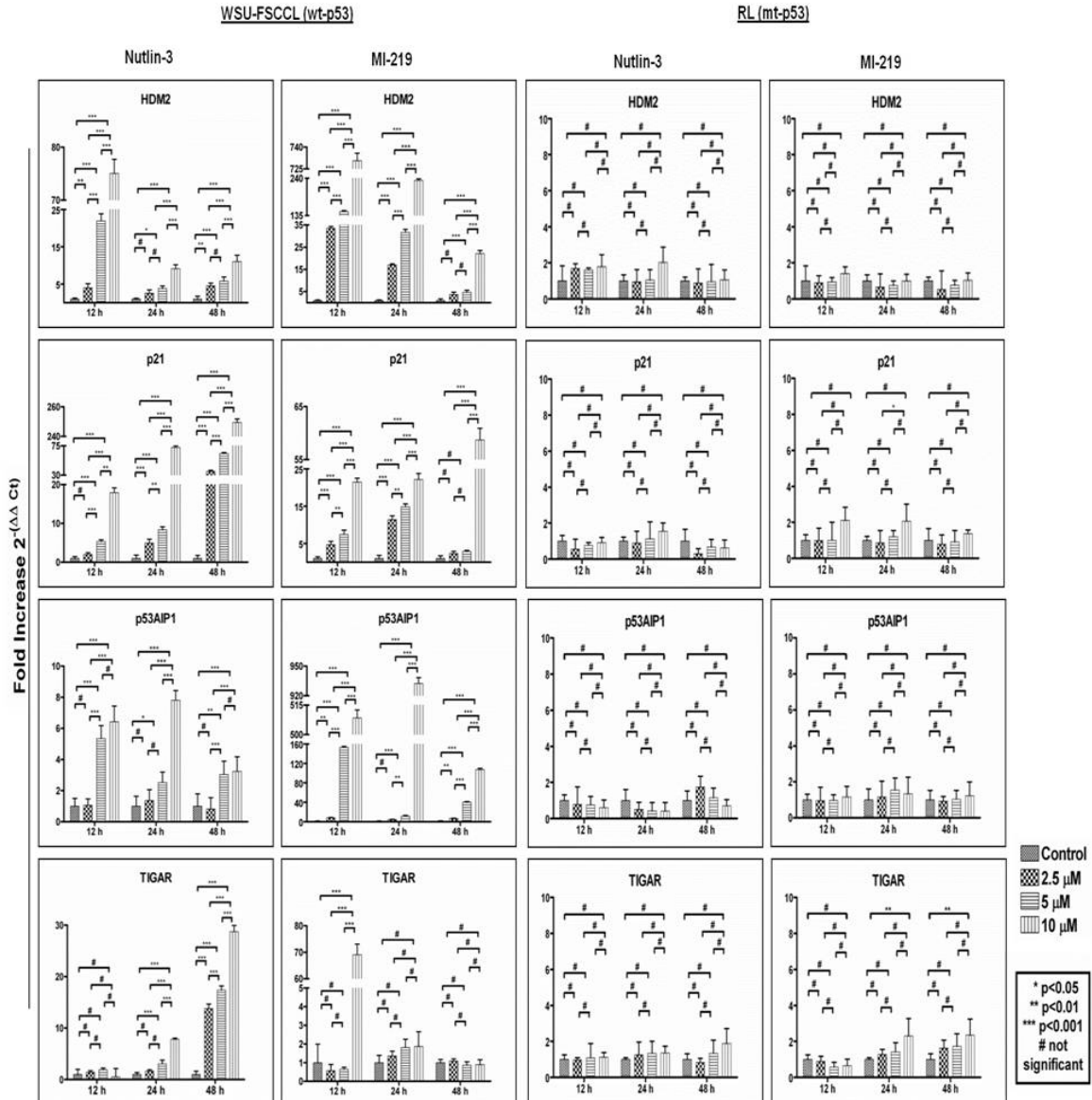


Figure 3.23 Effect of HDM2 inhibition on p53-dependent gene expression. mRNA expression levels upon exposure to HDM2 SMI in WSU-FSCCL and RL cells for the times indicated. Baseline gene expression and that after treatment were quantified by qRT-PCR relative to GAPDH using the $\Delta\Delta C_t$ method and expressed as fold induction of gene expression relative to that in the untreated control. Error bars plotted represent mean values \pm SE performed in triplicate from two independently treated experiments.

HDM2 inhibition enhances p53 stability at the posttranslational level

HDM2 inhibition is hypothesized to increase p53 stability by reducing HDM2-mediated degradation. However, p53 stability could also be the result of enhanced p53 protein translation. To demonstrate that upregulation of p53 protein expression shown in the Western blots were the result of HDM2 inhibition by SMIs, the half-life of p53 was monitored. The inhibition of protein synthesis by treatment with 50 μ M cycloheximide alone led to a marked decrease of p53 protein expression over time (Figure 3.24A). Furthermore, addition of 10 μ M of the proteasome inhibitor MG132 alone (Figure 3.24B) ameliorates the degradation of p53, thereby enhancing its stabilization. Whether p53 stability is related to HDM2 inhibition was evaluated by pre-incubation of 10 μ M Nutlin-3 or MI-219 for 24 hours in wt-p53 WSU-FSCCL cells followed by treatment with 50 μ M CHX at the indicated time points. Blocking protein synthesis while concurrently treating with HDM2 SMI led to an overall increase in p53 protein expression (Figure 3.24C, D). Intriguingly, MI-219 treatment was more effective in enhancing p53 stability than that of Nutlin-3. Furthermore, these results indicate that the increase of p53 protein is not due to an upregulation of p53 mRNA (Figure 3.24E) at earlier time points. Although we did not test for a drug washout, it appears that the HDM2 SMIs, particularly MI-219, may be bound to HDM2 for somewhere between 24-48 hours. p53 mRNA after 48h of treatment appears to begin transcription of itself suggesting that the HDM2-p53 feedback loop has normalized.

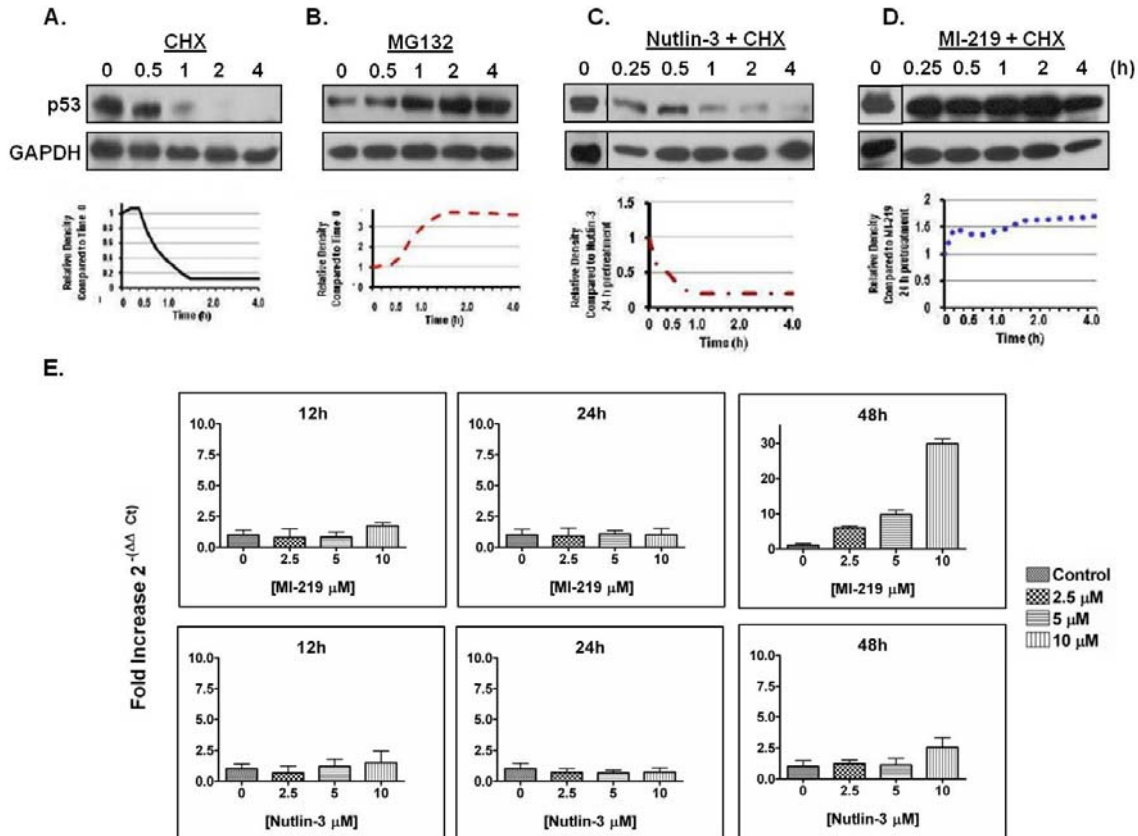


Figure 3.24 MI-219 enhances the stability of p53 to a greater extent than Nutlin-3. **A, B.** Treatment of wt-p53 WSU-FSCCL cells with 50 μ M cycloheximide decreases the half-life of endogenous p53 over time. Similarly, blocking the proteasome by treatment with 10 μ M MG132 increased p53 protein stability. Relative density of each band was measured and normalized to GAPDH. **C, D.** WSU-FSCCL cells were treated with 10 μ M of Nutlin-3 or MI-219 for 24 hours prior to the addition of 50 μ M cycloheximide for the indicated time points. p53 protein levels were detected by Western blot. **E,** p53 protein stability is not a result of mRNA translation into protein at early time points.

Next, we studied the direct effect of HDM2 inhibition on the disruption of the endogenous HDM2-p53 interaction in WSU-FSCCL cells, since this may be important to our understanding of the biological outcome. In WSU-FSCCL cells treated for 4 h, the amount of HDM2 associated with p53 is reduced with increasing drug concentration. However, it is interesting to note that MI-219 appeared to prevent the association of HDM2-p53 greater than Nutlin-3. 10 μ M MG132 was used as a positive control, as it does not prevent dissociation, and normal mouse IgG used as a negative control. Furthermore, whole cell lysate (WCL) input indicates that the presence of p53 is

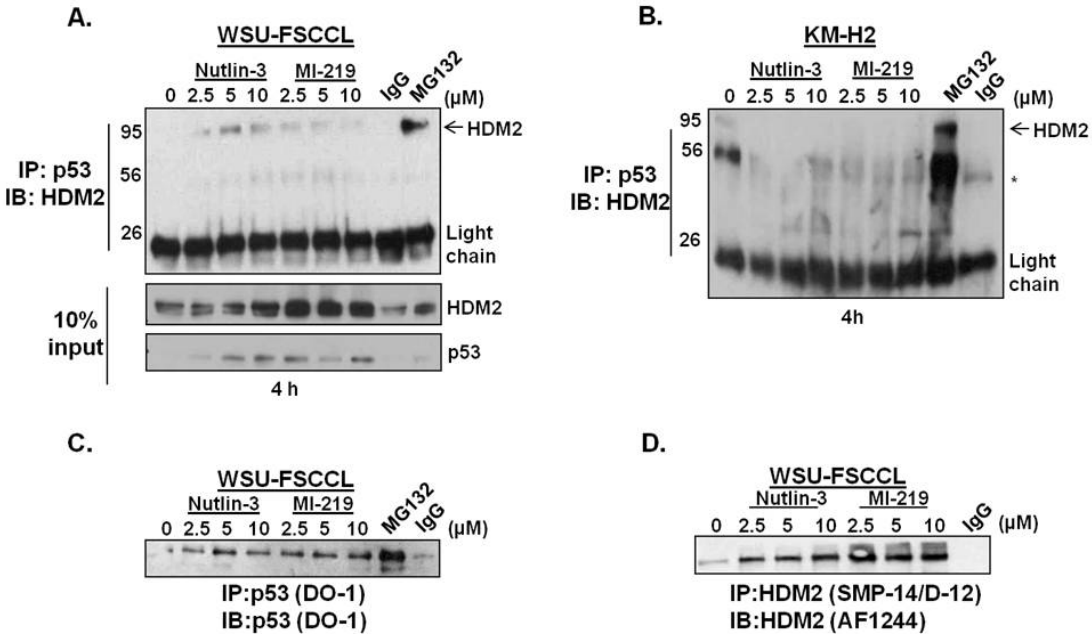


Figure 3.25 HDM2 inhibition results in disruption of the HDM2-p53 protein-protein interaction. **A, B** WSU-FSCCL and KM-H2 cells were treated for 4 hours with increasing concentrations of Nutlin-3 or MI-219. Addition of 10 μ M MG132 to cells was used as a positive control. Cell lysates were immunoprecipitated with anti-p53 (DO-1 for WSU-FSCCL), anti-p53 (pAb421 for KM-H2), or normal mouse serum (IgG). The immunoprecipitates were analyzed by immunoblotting against antibodies to HDM2 (AF1244). 10% of WSU-FSCCL total cell lysate was used for input. **C, D** WSU-FSCCL cells were treated for 12 hours with increasing concentrations of Nutlin-3 and MI-219. The blots were probed for the protein that was immunoprecipitated.

detectable in the control. Increasing levels of both HDM2 and p53 are seen, indicative of enhanced p53 stabilization in the presence of HDM2 SMI. The WSU-FSCCL co-IP caused a few issues because of the antibody used. p53 DO-1 binds to the N-terminus where HDM2 also binds and making it difficult to pulldown endogenous p53, let alone bound to HDM2 as shown in Figure 3.25C. The KM-H2 co-IP uses a different p53 antibody that recognizes the C-terminus of p53 and this blot demonstrates clearly that p53 and HDM2 are physically interacting in control and MG132 treated cells as indicated by the proteins located at the molecular weights of HDM2 and p53, but are absent in the Nutlin-3 and MI-219 treated cells (Figure 3.25B).

HDM2 SMI_s demonstrate differential effects on wt-p53 lymphoma cells

A comprehensive profile of the kinetics of wt-p53 lymphoma cells over the course of 72 h treatment with HDM2 SMI_s shows that both agents arrest wt-p53 WSU-FSCCL and KM-H2 cells at G0/G1 in a time- and dose-dependent manner (Figure 3.26). However, KM-H2 appears to arrest some cells in G2/M as well, albeit to a lesser extent.

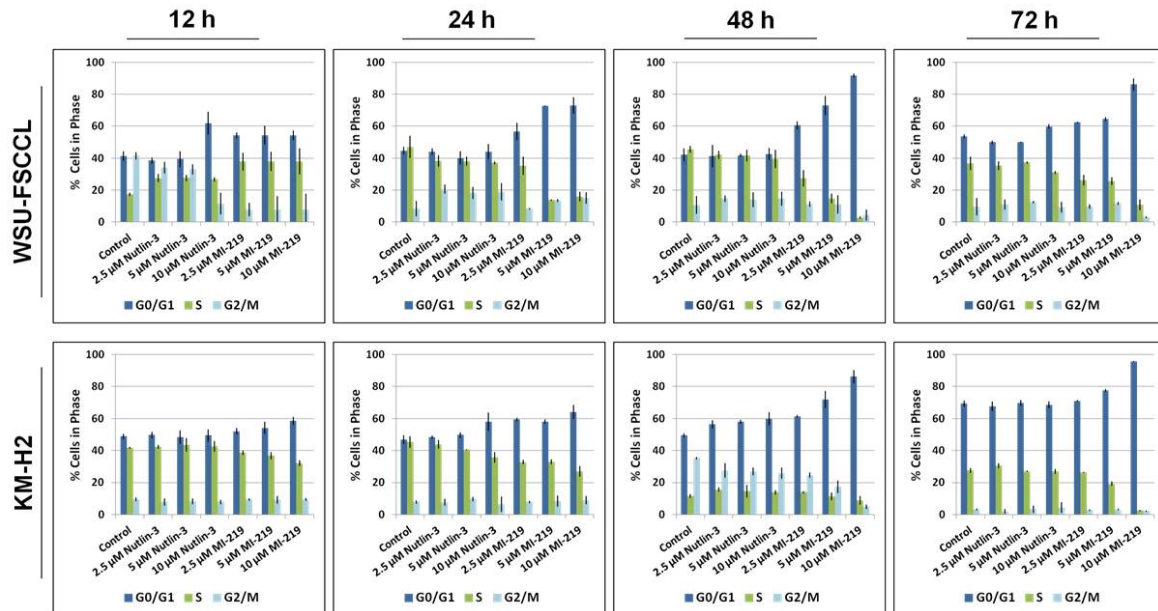


Figure 3.26 HDM2 inhibition causes cell cycle arrest in wt-p53 lymphoma cell lines. WSU-FSCCL and KM-H2 demonstrate time- and dose-dependent cell cycle arrest in G0/G1, and to a lesser extent, in G2/M. Error bars represent SEM of three independent experiments.

Considering the growth of both wt-p53 cell lines was inhibited and showed cell cycle arrest, it was surprising to detect apoptosis in WSU-FSCCL, but not in KM-H2. Particularly when the Annexin V/PI data indicate increases in Annexin V+ cells in a time- and dose-dependent manner (Figure 3.27A). When the TUNEL/PI assay was implemented, KM-H2 cells did not demonstrate time- or dose-dependent increases in TdT+ cells (Figure 3.27B), suggesting a lack of apoptosis. p53-dependent target genes were assessed after exposure to 10 μM MI-219 and Nutlin-3 for 12, 24, and 48 hours

(Figure 3.27C). Interestingly, the kinetics of upregulation varied between WSU-FSCCL and KM-H2, but more importantly, HDM2 SMIs did not upregulate p53AIP1 mRNA, also indicating that KM-H2 cells were not undergoing cell death upon treatment.

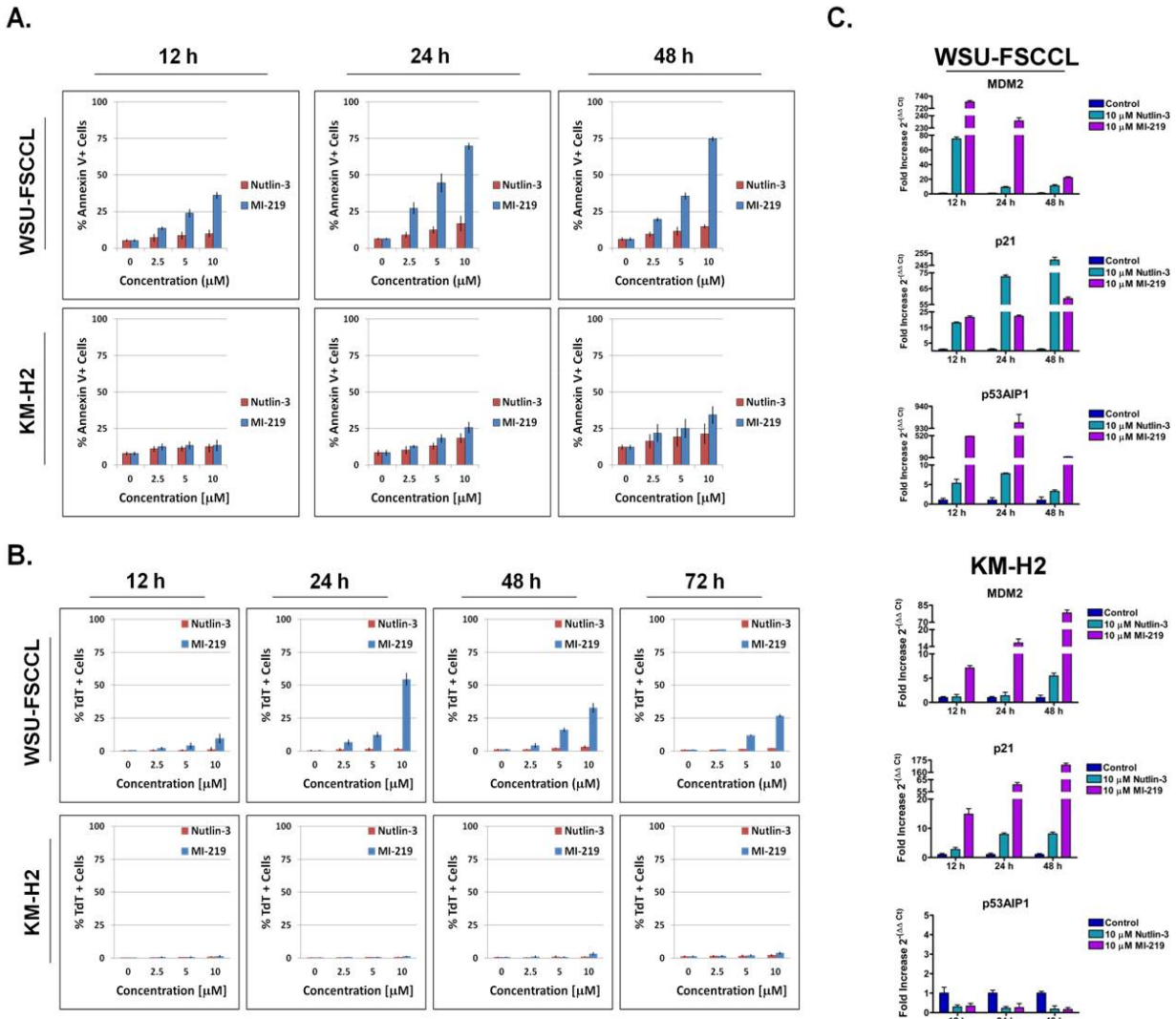


Figure 3.27 HDM2 inhibition induces apoptosis in WSU-FSCCL, but not KM-H2 lymphoma cells. **A., B.** The percentage of Annexin V and TdT positive cells is measured upon exposure to MDM2 SMIs over time. Results are the mean of at least two independent experiments. *Bars*, SEM. **C.** mRNA expression levels in response to HDM2 SMIs in WSU-FSCCL and KM-H2 cells for the times indicated. Baseline gene expression and that after treatment were quantified by qRT-PCR relative to GAPDH using the $\Delta\Delta C_t$ method and expressed as fold induction of gene expression relative to that in the untreated control. Error bars plotted represent mean values \pm SE performed in triplicate from two independently treated experiments.

When KM-H2 cells were immunoblot for apoptosis proteins, there was no PARP, caspase-3, or even caspase-9 cleavage after 24 hours of exposure to HDM2 SMIs compared to WSU-FSCCL wt-p53 lymphoma cells (Figure 3.28A, B). Tetrachrome staining of KM-H2 cells after 48 hours after treatment with 10 μ M Nutlin-3 and MI-219 showed indicators of apoptosis such as membrane blebbing, but no chromatin fragmentation or breakdown of nuclear membrane (Figure 3.28C). Visually, KM-H2 cells are not apoptotic and the membrane blebbing indicates that the Annexin V/PI assay detected false positive apoptotic cells and that Annexin V bound to phosphatidylserine of the membrane simply because the membrane was compromised.

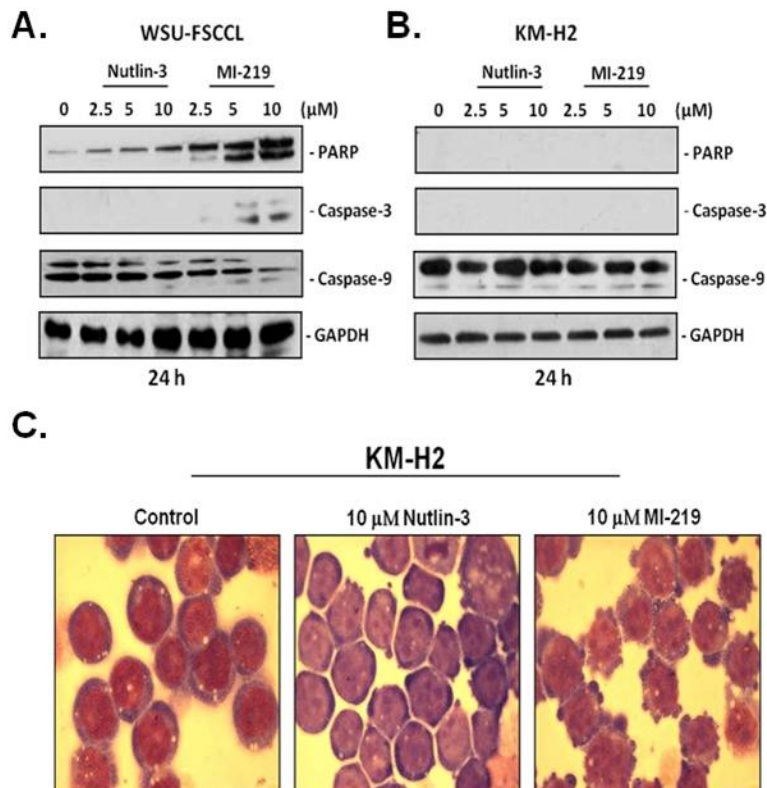


Figure 3.28 KM-H2 does not undergo apoptosis upon exposure to HDM2 SMIs. **A.**, **B.** Cleavage of PARP, caspase-3, and caspase-9, three indicators of apoptosis, were evaluated by Western blot analysis after 24 hours of exposure to HDM2 SMIs. GAPDH was used as a loading control. **C.** Tetrachrome staining of KM-H2 cells as visualized by light microscopy after a 48 hour treatment.

It is not clear from these data whether lack of apoptosis in KM-H2 is cell line specific or applicable to all Hodgkin lymphomas. The discrepancy that was noted between the wt-p53 lymphoma cell lines prompted screening of Nutlin-3 and MI-219 in additional HL cell lines, L-540 and L-591. Such analyses would allow for distinguishing whether or not our observations is specific to the KM-H2 cell line or whether this is disease specific.

HDM2 SMIs reduce the growth of wt-p53 HL cell lines, albeit at higher concentrations

HL cell lines L-540 and L-591 (both wt-p53) were exposed to increasing concentrations of Nutlin-3 and MI-319 for 24, 48, and 72 hours as previously discussed. Trypan blue exclusion assay was used to measure the growth inhibitory effect of HDM2 SMIs. Similar to the other wt-p53 cell lines, L-540 and L-591 were responsive to HDM2 inhibition and IC_{50} for Nutlin-3 and MI-219. However, whereas each HDM2 inhibitor showed different IC_{50} 's in KM-H2, they show similar IC_{50} 's in L-540 and L-591 after 48 hours (Figure 3.29, middle pannels). Data are represented as a line graph for each time point (Figure 3.4A) as well as graphed in linear scale for both Nutlin-3 and MI-319 (Figure 3.4B). The IC_{50} 's in each of the three wt-p53 HL cell lines is much higher than the IC_{50} in WSU-FSCCL, suggesting that HL cells may be inherently more resistant to HDM2 inhibition than NHL cells.

The biological effects of HL cells were investigated upon exposure to HDM2 SMIs. Similar to WSU-FSCCL wt-p53 cells, both L-540 and L-591 showed increases in Annexin V+ and TdT+ cells upon exposure to MI-219 (Figure 3.30). Nutlin-3 also showed dose-dependent increases in apoptotic cells, except it was much less compared to MI-219.

To ensure that HL cells, particularly KM-H2, were capable of undergoing

conventional apoptosis, they were exposed to proteasome inhibitor and doxorubicin, a DNA-damaging agent along with HDM2 SMIs and probed for apoptosis markers. MI-219 showed higher molecular weight forms of HDM2 similar to that seen in WSU-FSCCL and in patient samples. Also, HL cell lines appeared to be more resistant to HDM2 inhibition compared to wt-p53 cell line WSU-FSCCL. KM-H2 was able to undergo conventional apoptosis with exposure to doxorubicin and MG132, as detected by PARP cleavage (Figure 3.31).

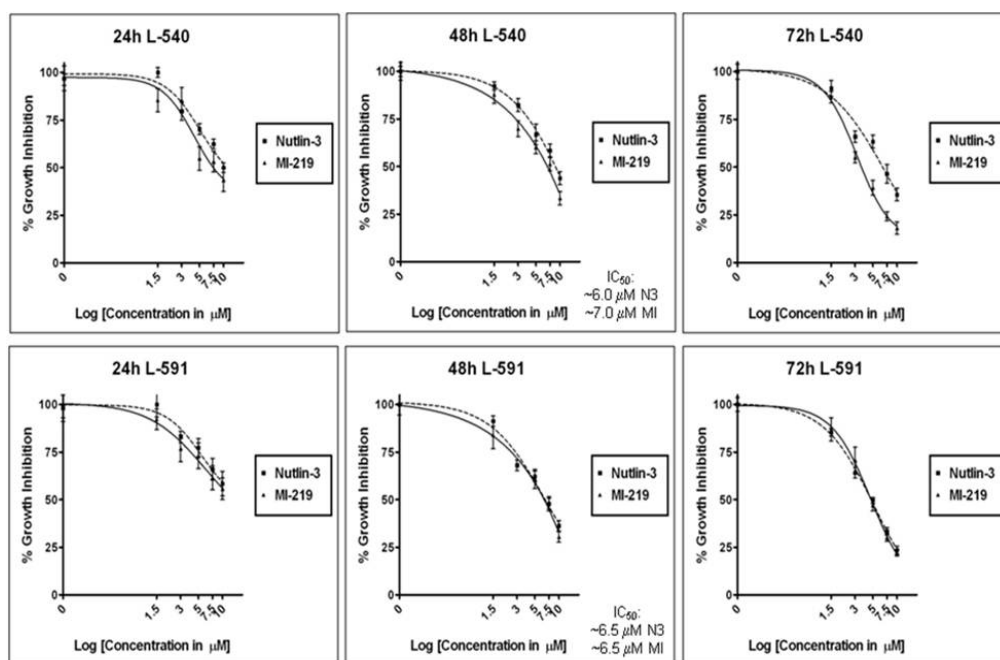


Figure 3.29 HDM2 SMIs reduce cell growth of wt-p53 HL cells. Wt-p53 (L-540, top; L-591, bottom) HL cells were treated with a range of concentrations of MI-219 and Nutlin-3 for 24, 48, and 72 hours. Cell viability was measured by Trypan blue exclusion assay as a percentage of controls. Data represent three independent experiments, with quadruplicate readings. Bars, \pm SEM.

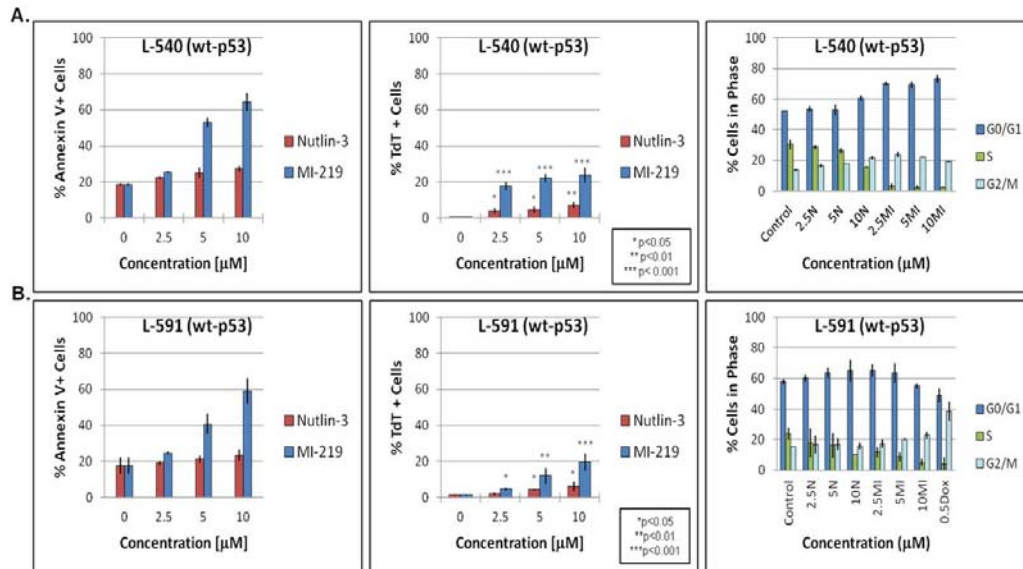


Figure 3.30 Biological effects of HL cell lines to HDM2 SMIs after a 24 hour treatment. The percentage of Annexin V positive cells is measured upon exposure to HDM2 SMIs after 12, 24, and 48 hours in wt-p53 (**A.**) and mt-p53 (**B.**) lymphoma cell lines. **C.** Cell-cycle analysis in wt- and mt-p53 lymphoma cells after 24 hours of HDM2 inhibition. Results are the mean of at least three independent experiments. Statistical analysis for Annexin V/PI was performed using two-tailed Student t-test between treated and untreated sample per time point and the differences were considered significant when $p < 0.05$. Bars, SEM.

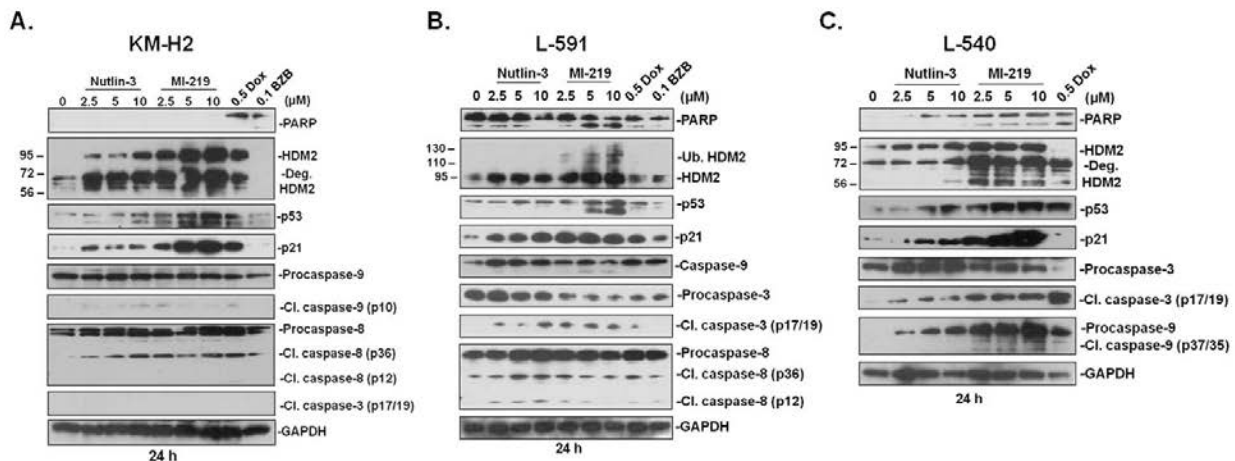


Figure 3.31 HDM2 antagonism in HL cell lines reactivates wt-p53, but are resistant to p53-induced apoptosis. p53, p53-dependent targets, and apoptosis mediators were detected by Western blot analysis after 24 hours of exposure to HDM2 SMIs in wt-p53 KM-H2 (**A.**), L-591 (**B.**), and L-540 (**C.**) HL cells. GAPDH was used as a loading control.

Summary

The following data in Chapter III demonstrates that exposure of lymphoma cells to HDM2 SMIs results in the restoration of wt-p53 tumor suppressor activity by disrupting the HDM2-p53 interaction. By means of an *in vitro* and *ex vivo* approach, HDM2 inhibition was shown to reduce cell growth and result primarily in biological responses of cell cycle arrest and apoptosis. Both agents disrupted the HDM2-p53 protein-protein interaction and stabilized p53 protein by minimizing HDM2-mediated degradation. Furthermore, the data unexpectedly reveals that MI-219 elicits a statistically significant difference in potency compared to the well-studied Nutlin-3. The results from the primary lymphoma cells are consistent with the results from the wt-p53 lymphoma cell lines. This suggests that Nutlin-3 primarily induces a cell cycle arrest, whereas MI-219 induces apoptosis, as the primary growth inhibitory effect in lymphoma cells. The surprising existence of significant quantitative and qualitative differences between effects of two different classes of HDM2 SMIs: Nutlin-3 and MI-219 indicates that the p53-HDM2 interaction and methods of its disruption are more complex than is currently realized.

HDM2 antagonism produces distinct biological responses in wt-p53 lymphoma cells, adding to the complexity of the expected outcome from a wt-p53 response. Although HDM2 SMIs demonstrate activity in wt-p53 Hodgkin lymphoma (HL) cells, p53 activation alone does not appear to be sufficient for the induction of apoptosis. These results demonstrate that HL cells may be inherently more resistant to apoptosis compared to NHL cells. Differences in sensitivity between HL and NHL are not currently known. The data prompts speculation that the mechanisms underlying drug-induced apoptosis involve additional molecular determinants which need to be further studied.

More in-depth understanding of the consequences of HDM2-p53 disruption by SMIs will aid in maximizing their therapeutic exploitation.

CHAPTER IV

NOVEL MECHANISM OF ACTION FOR MI-219

Introduction

Ubiquitination is one process that can impact the functional activity of wt-p53 once it is released from HDM2, and the blocking of the p53-HDM2 interaction is thought to be the mechanism of action of Nutlin-3. Although HDM2 inhibition demonstrates efficacy in tumor cells in a p53-dependent manner, the regulatory mechanisms mediating this effect are still relatively uncertain. The mechanism of action of Nutlins is thought to block the p53-HDM2 interaction but may not interfere with other functions of HDM2, such as its ubiquitin ligase activity (140). Studies using HDM2 SMIs have generated sufficient data to demonstrate that these inhibitors can effectively be used to elicit antitumor response. However, the precise mechanisms of susceptibility to HDM2 SMI induced cancer cell death are not completely understood. The extent that HDM2 SMIs influence p53-independent functions of HDM2 remains to be determined.

For example, it was initially thought that HDM2 inhibition completely abrogated all functionality of the protein after release of p53. Studies using Nutlins show that HDM2 is capable of retaining its p53-independent functions, even when p53-dependent activity is the primary effect seen. Of importance is the E3 ubiquitin ligase activity of HDM2. The regulation of HDM2 auto-ubiquitination and ubiquitination of p53 in the presence of an HDM2 inhibitor to the p53 binding domain are currently unknown. The precise mechanisms regulating the balance of ubiquitination and de-ubiquitination on protein-protein interactions such as p53 and HDM2 are not entirely well-defined. Elucidating some of these mechanisms can enhance our understanding of the therapeutic potential and limitations HDM2 inhibitors in B-cell lymphoma. Results from this chapter were in

part to investigate additional molecular effects of MI-319 (MI-219) on HDM2 upon physical disruption of HDM2-p53. In addition, they aid in the development of a retrospective hypothesis when parts of data from Chapter 3 were re-analyzed.

Results

The functionality of HDM2 E3 ubiquitin ligase activity in the presence of HDM2 SMIs

One of the pitfalls to HDM2 SMIs is the upregulation of HDM2 since it is a direct target of p53 due to the negative feedback loop. Our data shows a tremendous amount of HDM2 mRNA being produced, especially in the presence of MI-219 (Figure 3.23). One of the caveats to using HDM2 SMIs is that the high HDM2 levels can negate effects of newly released p53. This can happen in one of two ways: if HDM2 SMIs hinder the E3 ligase activity of HDM2, the protein product remains high and stabilized. On the other hand, if HDM2 retains its HDM2 E3 ligase activity, degradation of itself is possible, although it may also be possible that HDM2 still ubiquitinates p53 (or additional proteins) even in the presence of HDM2 SMIs, reducing the stability of reactivated p53.

To determine if HDM2 retains its autoubiquitination in the presence of HDM2 SMIs, a cell free autoubiquitination assay was performed using recombinant proteins. Neither class of agents inhibits the E3 ligase function of HDM2 (Figure 4.1A). Autoubiquitination of recombinant His-tagged HDM2 was not inhibited by the addition of Nutlin-3, MI-319 or MI-219 at IC_{50} or even much higher (50 μ M) concentrations after 1.5 hours incubation and subsequent separation onto a 4-20% SDS-PAGE gel. Disulfiram, on the other hand, completely abrogated autoubiquitination at 10 μ M, and was included as a control.

The importance of this assay was not realized right away. It was not until some

unusual observations were re-analyzed and interpreted that allowed for the development of a retrospective hypothesis: that HDM2 inhibition by MI-219 alters the functional activity of HDM2 and that it may correspond to biological activity. A key piece of data that aided in such interpretation is shown in Figure 4.2. D24 treatment at 10 μ M showed autoubiquitination and degradation of recombinant HDM2 when immunoblot with His-tagged antibody. The 60 kDa degradatory fragment of HDM2 is clearly shown on the blot. Since this was a cell free autoubiquitination assay, there were no indicators that additional proteins could have enhanced HDM2 autoubiquitination and degradation. Results supporting this hypothesis may help to explain the unexpected differences that were noted in between each class of HDM2 SMI in Chapter 3.

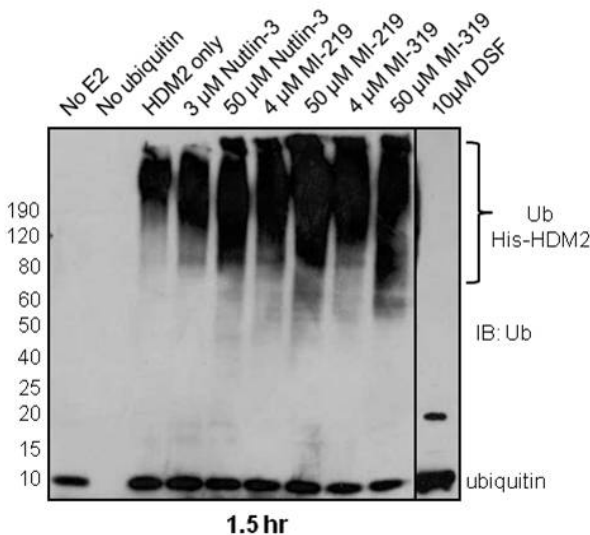


Figure 4.1 HDM2 SMIs do not inhibit E3 ligase function of HDM2. Recombinant His-tagged HDM2 was used in a cell free autoubiquitination reaction. IC₅₀ or 50 μ M of Nutlin-3, MI-219, or another spirooxindole compound, MI-319 was added to the reaction for 1.5 hours. Lack of E2 enzyme, ubiquitin alone, disulfiram (DSF), and DMSO vehicle were all included as controls. Immunoblot using anti-ubiquitin antibody was used to assess HDM2 autoubiquitination.

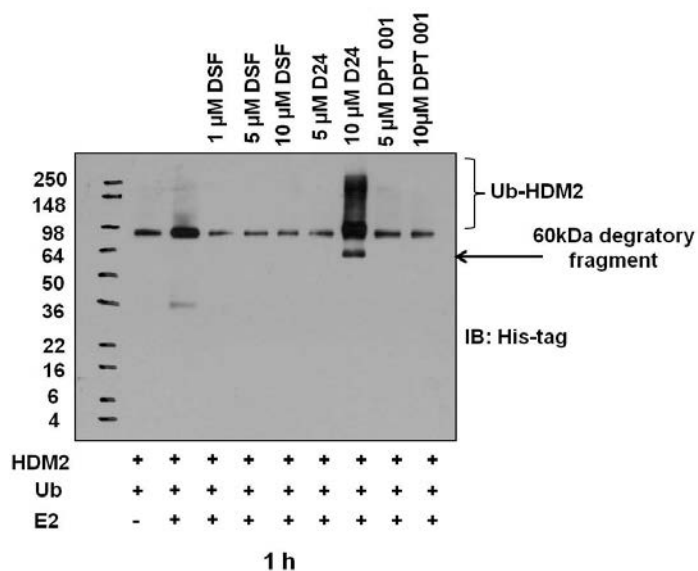


Figure 4.2 A higher concentration of zinc ejector D24 induces autoubiquitination and degradation HDM2. His-tagged HDM2 was incubated in the presence or absence of increasing concentrations of zinc ejectors for 1.5 h in a cell free autoubiquitination assay. Immunoblot was probed for using anti-His tag antibody and clearly detects the 60 kDa degradable fragment of HDM2. Removal of zinc from E3 ligases is supposed to render them nonfunctional.

Based on this finding we hypothesized that these agents should induce HDM2 ubiquitination and degradation in cell based assays. We, therefore, re-examined the effects of HDM2 SMIs on HDM2 protein expression in the WSU-FSCCL cells. Initial experiments used 14% SDS-PAGE gels to separate whole cell lysates which are not optimal for detecting posttranslationally modified proteins which prompted us to switch to the 4-20% SDS-PAGE gels for further examination and confirmation of HDM2 modification upon HDM2 inhibition. Both full length and smaller size bands consistent with degraded HDM2 were evident in MI-219-treated cells as early as 12 hours and peaked at 24 hours (Figure 4.3A, B). Higher exposure also detected larger size band consistent with autoubiquitinated HDM2 which occurred at the early time point (12 hours). HDM2 expression pattern in Nutlin-3-treated cells was similar to control with the exception of a faint degraded band detected at 48 hours in the highest concentration (10 μM). Similar effects were also observed in the wt-p53 KM-H2 and the L-591 Hodgkin lymphoma cell lines (Figure 4.3B, C). Interestingly, the higher molecular weight species appeared to correspond to biological activity, as increased apoptotic cells were apparent in the MI-219, but not the Nutlin-3, treated HL cells for 24 hours (Figure 4.3C).

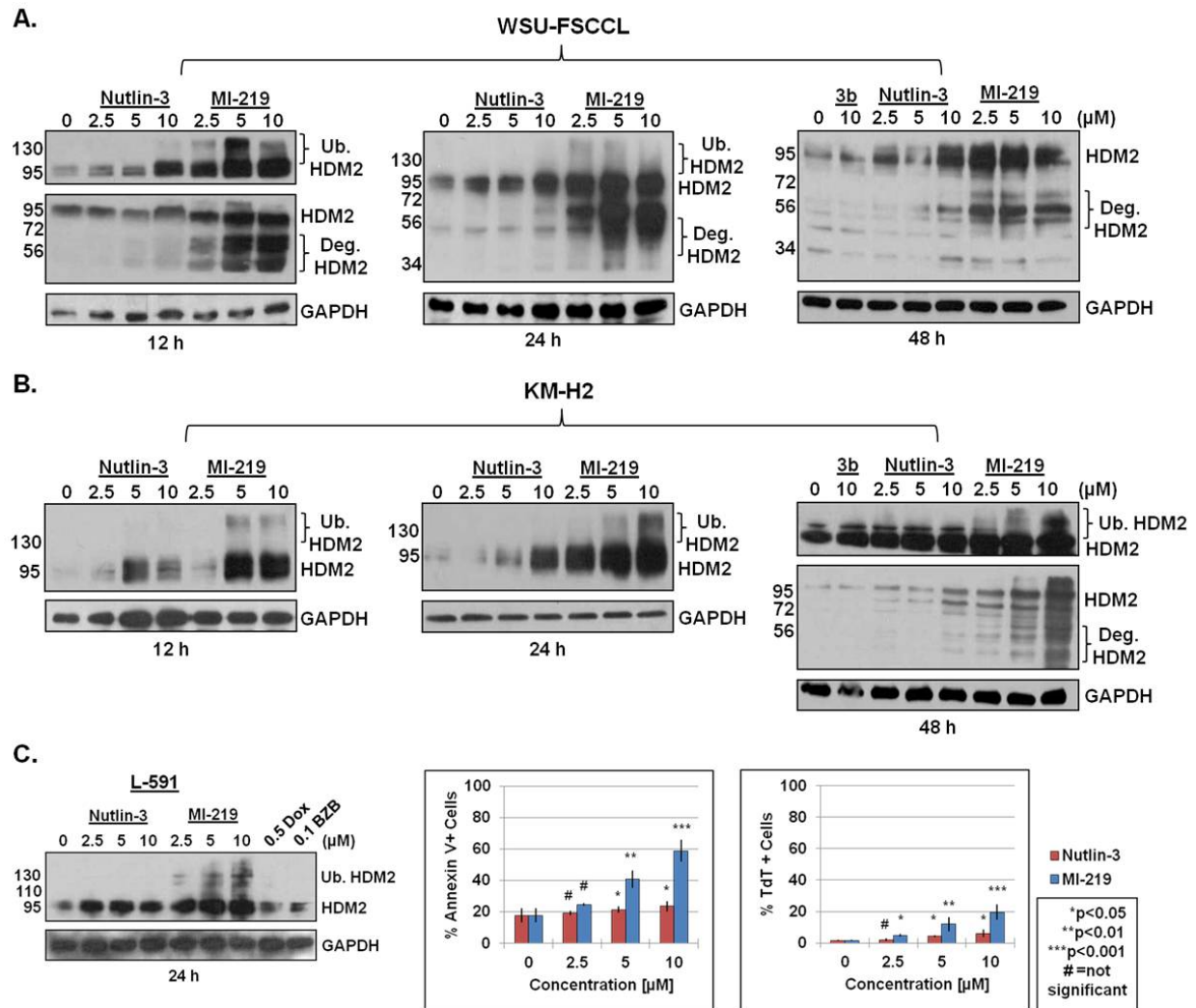


Figure 4.3 HDM2 autoubiquitination and degradation is detected in whole cell lysates from treated wt-p53 WSU-FSCCL (**A**) and KM-H2 cells (**B**). Autoubiquitination appears to occur at earlier time points, which then degrades full-length HDM2. **C**, HL cell line L-591 also demonstrates higher molecular weight bands indicative of HDM2 autoubiquitination after a 24 hour exposure to HDM2 SMIs. This also appears to correspond with increased apoptotic cells at the same time point.

To confirm the nature of the smaller molecular weight bands, we conducted an immunoprecipitation (IP) experiment using WSU-FSCCL. After exposure to MI-219 or Nutlin-3 for 12 hours, HDM2 protein was immunoprecipitated using 1:1 ratio of SMP-14: D-12 antibodies (the former is known to detect degraded HDM2). Immunoblotting (IB) with HDM2 polyclonal antibody (AF1244) revealed the full length HDM2 in addition to

higher molecular weight species (likely autoubiquitinated HDM2) and ~60kDa band, the major degraded species of HDM2 (Figure 4.4A). The intensity of this band was concentration-dependent in MI-219-treated cells but was not seen in Nutlin-3-treated cells. These findings suggest that MI-219 but not Nutlin-3 posttranslationally regulates HDM2 protein by inducing autoubiquitination and degradation of itself as a way of compensating for the high levels of HDM2 mRNA produced.

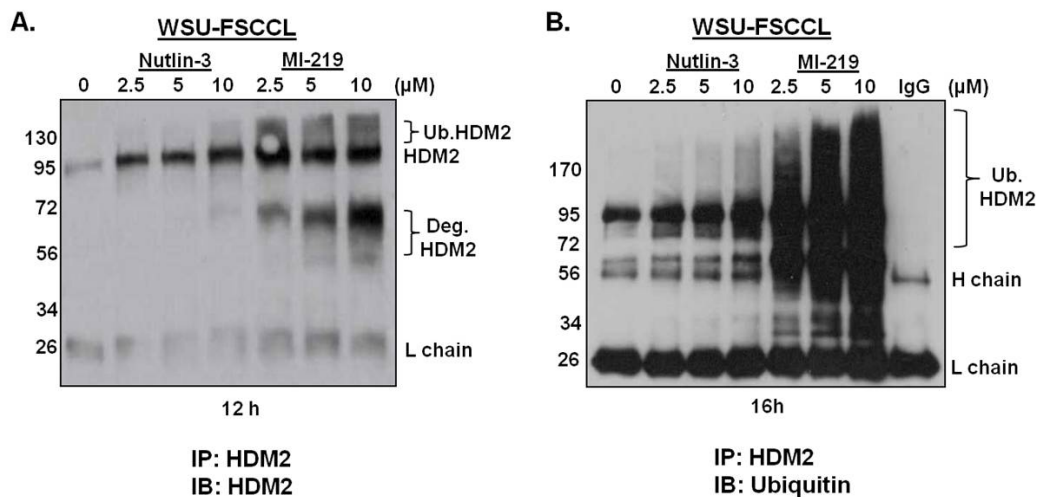


Figure 4.4 MI-219 enhances endogenous HDM2 self-ubiquitination and degradation. **A**, WSU-FSCCL cells were treated with increasing concentration of HDM2 SMI for 12h. Cells were collected and subject to immunoprecipitation with a 1:1 ratio of mouse monoclonal HDM2 antibodies (SMP-14: D-12) and blot using rabbit polyclonal HDM2 antibody AF1244. SMP-14 is known to detect the 60 kDa degraded fragment of HDM2. **B**, WSU-FSCCL cells were treated with increasing concentration of HDM2 SMI for 16h. Prior to cell collection, cells were exposed to 10 μM of MG132 for 15 minutes to preserve ubiquitinated proteins and were subject to immunoprecipitation as in **B**, but blot with anti-ubiquitin monoclonal antibody.

Summary

The results from Chapter 4 strongly imply that MI-219, but not Nutlin-3, regulates HDM2 destruction via autoubiquitination. Later time points (48 h) results in a reduction of HDM2 protein, suggesting that enhancement of HDM2 E3 ligase activity occurs at earlier time points to reduce the high levels of mRNA and protein produced from the

p53-HDM2 autoregulatory loop. Therefore, p53 may be contributing to regulate its own activity since this was not seen in mt-p53 lymphoma cells. Furthermore, it may also correspond with biological activity since there appeared to be an association between HDM2 destabilization and p53-dependent apoptotic response. The results show that HDM2 retains its E3 ligase activity in the presence of Nutlin-3 and both MI compounds. Various higher and lower molecular weight species were detected endogenously in various lymphoma cell lines and primary lymphoma patient samples when treated with increasing concentrations of MI-219, but not Nutlin-3. This supports our proposed mechanism of action for MI-219 that posttranslationally regulates or modifies HDM2 by autoubiquitination and degrades itself as a way of compensating for the high levels of HDM2 produced.

CHAPTER V

CONCLUSIONS, SIGNIFICANCE AND FUTURE DIRECTIONS

Although the vast majority of lymphomas have high rates of remission induction and survival with the current chemotherapy regimens, many patients still do not respond well to therapy. Failure to respond to initial treatment or relapse following a brief remission is typically the case. A majority of lymphomas retain wt-p53 status and have developed mechanisms to compromise p53 signaling, such as HDM2 overexpression, deletions in p14ARF, and viral oncogenes (141-143). It is clear that HDM2 plays an important role in lymphoma tumorigenesis. HDM2 inhibitors R7112 (Nutlin-3 analog) and JNJ-26854165 (a tryptamine derivative) are currently under clinical evaluation in Phase I studies (NCT00623870, NCT00559533, NCT00676910) and the first results have recently been published (129, 144). We previously investigated MI-319 in FL (137), and have gained access to MI-219, the clinical grade spiro-oxindole and selective activator of the p53 pathway in tumor cells, not in normal cells (139). Therefore, we further examined the effects of targeting HDM2 in lymphoma cells in order to understand the molecular mechanisms required to translate lab findings into clinically relevant outcomes.

Limitations of primary lymphoma cells

Results produced from the cell lines were expected to be similar to those obtained in the patient samples. Unfortunately this may not have entirely been the case due to heterogeneity of the primary cell population. Although the protocol that was performed for the majority of the lymphoma patient samples was optimized immensely to enhance a purified B lymphocyte cell population, we cannot rule out potential carryover of other cell types that may not have been excluded entirely in the process.

However, we are confident that the biological responses observed post drug treatment are predominantly due to B lymphocytes as flow cytometry confirmed the enhancement of the CD19+ B lymphocyte population (Figure 3.7).

Whereas cell lines are relatively homogenous cell populations and have distinct growth rates, primary derived B lymphocytes do not actively grow once they are resuspended in media. Therefore, isolation, purification and drug treatment must be performed right away otherwise cells will die off naturally, making it difficult to collect enough cells for experimental analyses such as immunoblotting. A major limitation when using patient derived B lymphocytes is the number of cells obtained. First, they do not actively grow in RPMI media. The cells remain dormant or die off. Second, blood draws vary in white blood cell count numbers from patient to patient and also depends on the diagnosis and extent of disease. Third, cells are lost during the isolation and purification process from multiple washes and from the monocyte and CD2+ T cell depletion steps. Approximately 20-30 million B lymphocytes are lost from the initial extraction of PBMCs to the resuspension of the final pellet of purified B cells. Yet another limiting factor is the duplicity of experimental procedures. More often than not, there is only one opportunity to process, set up, and analyze primary lymphoma patient samples. Therefore, it is of utmost importance to use extra caution at each and every step up to and including data analyses in order to make the most of the data obtained. There may be no chance to redo an experiment if something goes awry due to that particular patient undergoing chemotherapy, regression of disease with a possible reduction in that individual patient's cell counts the subsequent doctor visit, and progression may lead to a change from the initial diagnosis (FL transforming into DLBCL).

The number of Annexin V positive cells in the untreated control was surprisingly

high. Also, retrospectively looking back at this data, if one were to use flow cytometry to monitor apoptosis for future patient samples, the TUNEL/PI kit may be the more suitable choice, since both PI and FITC-labeled TdT enzyme must enter the nucleus after fixation and do not rely on the integrity of the plasma membrane. Primary B lymphocytes are much smaller and less robust than that of their cell line counterparts. Consequently, this renders the plasma membrane much more susceptible to Annexin V binding. Additionally, non-specific Annexin V binding causing issues (i.e. megakaryocytes, platelets, some myeloid lineage cells) as well as Annexin V binding buffers being proapoptotic (Ca^{2++}) which sensitizes the delicate B lymphocytes and may create false positives by exposing phosphatidylserine (145). PI can create false positive by binding to cytosolic RNA, but these effects were minimized by treating each sample with 1ug/ul of RNase prior to the addition of PI.

The molecular events upon HDM2 antagonism elicit stress responses through nongenotoxic activation of p53. A number of lymphoma cell lines were used along with a panel of primary B-cell lymphoma patient samples. The results indicate that HDM2 inhibition restored functional activity to wt-p53, but not mt-p53 lymphoma cells. We performed a time-course analysis to achieve a better understanding of the consequences of HDM2 inhibition on lymphoma cells. We showed that HDM2 SMIs demonstrate growth inhibitory effects in a time- and dose-dependent manner with increased sensitivity in wt-p53 lymphoma cells. Furthermore, molecular changes were induced in the p53 pathway resulting in cell cycle arrest and apoptosis as the primary consequences of growth inhibition.

The p53 regulated target genes p21, HDM2 and p53AIP1 were activated following treatment in wt-p53 WSU-FSCCL cells, although the degree of activation

varied depending on time point, dose, and HDM2 SMI selected for treatment. Mt-p53 RL did not show significant activation of p53-target genes, confirming that HDM2 SMIs primarily require wt-p53 in order to mediate its antitumor response (146). We noted that the degree of induction of p53 and its transcriptional targets following treatment corresponded to a concurrent upregulation in p53-target protein expression. One perplexing finding was that of the significantly high levels of HDM2 mRNA associated with upregulated HDM2 protein that was induced upon MI-219, but far less with Nutlin-3, treatment (Figures 3.22 and 3.23). This was surprising to us since restoration of the p53-HDM2 autoregulatory loop is known to decrease p53 protein levels and activity (76). How then, does p53 remain activated in the presence of such high levels of HDM2? HDM2 destabilization has previously been reported to correlate with p53 transcriptional activity and has been suggested to play an important role in determining p53 response (96, 97). Additionally, we observed that HDM2 inhibitors do not inhibit the ubiquitin E3 ligase activity of HDM2 (Figure 4.1). Interference with HDM2 self-degradation could negate effects seen from p53 reactivation and potentially be detrimental for the advancement of HDM2 SMIs into the clinic. Therefore, we postulate that HDM2 may undergo rapid turnover due to forced autoubiquitination and degradation in the presence of MI-219. Further studies are necessary to determine if this is important in shaping p53 responses to HDM2 SMIs.

The results suggest that the molecular mechanism of p53 reactivation involves disruption of the HDM2-p53 interaction which occurs posttranslationally. Treatment of lymphoma cells with HDM2 SMIs caused p53 stabilization due to increased half-life and decreased proteasomal degradation by HDM2. Therefore, accumulation of p53 protein levels is due to release of p53 from HDM2 and not because of *de novo* protein

synthesis or due to a reduction in proteasome activity. The results indicate that the transcriptional activity could be attributed to HDM2-p53 disruption by HDM2 SMIs.

Here, we provide experimental evidence that MI-219 effectively reactivates functional activity of wt-p53 in lymphoma cells by inducing apoptosis as the primary growth inhibitory effect. The marked difference in biological response is more pronounced when exposed to MI-219 than Nutlin-3. This was unexpected considering the low frequency of p53 mutations and the amount of previous studies reporting on the relative sensitivity of hematological malignancies to Nutlin-3 induced cell death. Instead, Nutlin-3 seemed to elicit a strong cell cycle arrest as the primary growth inhibitory effect. This was not an artifact of cell culture conditions as similar results were found in lymphoma cells isolated from patient samples (Figure 3.16). However, considerable variability has been demonstrated to affect cellular response upon Nutlin-3 treatment in wt-p53 cancer cells as well. Certain cancer cell lines have been reported to possess Nutlin-sensitivity over others (147-151). Whereas cancer cells typically undergo cell cycle arrest and apoptosis, senescence, differentiation, and endoreduplication have also been described (152). Furthermore, cell lines with MDM4 overexpression have been shown to confer enhanced sensitivity to Nutlin-3 treatment (149, 153). Whether or not MDM4 overexpression is the cause of increased potency in our model system remains to be determined.

It would be interesting to compare gene expression profiles to assess the genome-wide involvement of Nutlin-3 and MI-219 treatment on lymphoma cells. By comparing each individual treatment to control and each individual treatment to each other, such data would provide insight as to what may be causing the different biological responses. Additionally, proteomic analysis may also help to identify crucial cofactors

that may be necessary for the induction of growth arrest compared to apoptosis.

Our data indicate that restoration of p53 activity is clearly diverse between each class of HDM2 SMI in the context of human lymphoma cells. This difference was particularly evident in the transcriptional activity of p53 target genes as well as the degree of apoptosis seen in WSU-FSCCL cells. A recent study also noted a more pronounced biological effect induced upon RITA treatment than after Nutlin-3A treatment (154). They postulated that RITA enhanced p53 transcriptional activity for numerous proapoptotic genes as the key difference in response. Although this could also be true of MI-219, p53AIP1 was the only p53-dependent target gene tested in this study. It would be interesting to monitor the consequences of p53 reactivation between MI-219 and RITA in our cell lines, considering the distinct modes of p53 activation of each. The dynamics of tight p53 regulation can be greatly attributed to the numerous upstream and downstream molecules known to interact with and posttranscriptionally modify p53 activity.

Additional functions of HDM2 exist besides downregulation of p53. For example, HDM2 has been shown to interact with and regulate other proteins such as E2F1, p73, Rb, etc. Although this study did not investigate these proteins, it is highly likely that one explanation to the difference in drug susceptibility is due to modulation of HDM2 interacting proteins upon HDM2 inhibition. Previous studies observed disruption between some of these proteins and HDM2 in the presence of Nutlin-3 in mt-p53 cells. This may explain the p53-independent effects seen at higher concentrations in WSU-DLCL₂ and RL that were observed. Recent studies have suggested that specific p53-interacting proteins can regulate the selectivity of p53 target gene activation (155). The dynamics of tight p53 regulation can be greatly attributed to the numerous upstream

and downstream molecules known to interact with and posttranscriptionally modify p53 activity.

It is plausible that each class of HDM2 SMI induced a conformational change in HDM2 that may also explain the different biological effects seen. Accumulated experimental evidence suggests that changes in the N-terminus can affect HDM2 folding. The Selivanova group (154) hypothesized that RITA binds to the N-terminal region of p53 with fast kinetics, and then undergoes a slow conformational change that prevents HDM2 binding. Krajewski et al (156) reported that RITA may not block the p53-HDM2 interaction *in vitro* (using NMR) and that these changes propagate to the p53 core domain. More recently, HDM2 was found to bind to the C-terminal domain of p53 at its acid domain. This supports the co-immunoprecipitation results and indicates that HDM2 can bind to p53 in the newly changed conformation upon treatment with MI-219. However, these results remain puzzling considering that increasing concentrations of MI-219 led to an increase in interaction. Further investigation is necessary to determine whether scaffolding proteins or HDM2 isoforms are the cause of enhanced p53-HDM2 interaction. Since additional proteins interact with HDM2 at the region besides p53, it is unclear how SMIs affect the interaction of these molecules and whether or not they may play a role in antitumor response upon treatment.

Therefore, further investigation is necessary to understand the precise mechanisms regulating modifications of reactivated p53 in the presence of HDM2 SMIs and how to utilize such agents for combinational therapy. Moreover, future studies will offer solutions to the therapeutic potential and shortcomings of HDM2 SMIs in not only lymphoma, but in other cancer types as well. Altogether, these results provide experimental evidence that p53 reactivation, particularly by MI-219, may prove to be

therapeutically beneficial in lymphoma patients that retain wt-p53 status.

MI-219 is a selective activator of the p53 pathway. We compared four cell lines: two wt-p53 and two mt-p53. Our results, which were consistent with those obtained for other types of cancer, show that HDM2 inhibition restored functional activity to p53 in WSU-FSCCL and KM-H2 lymphoma cells. We performed a time-course analysis to achieve a better understanding of the consequences of HDM2 inhibition on lymphoma cells. We show that HDM2 SMI demonstrate growth inhibitory effects in a time- and dose-dependent manner with increased sensitivity in wt-p53 lymphoma cells.

The p53 regulated target genes p21, HDM2 and p53AIP1 were activated following treatment, although the degree of activation varied from case to case. We noted that the degree of induction of p53 and its transcriptional targets following treatment correlated with the level of its protein product at designated time point.

Here, we provide conclusive experimental evidence that MI-219 effectively reactivates functional activity of wt-p53 in lymphoma cells. The marked difference in biological response is more pronounced upon MI-219 treatment than Nutlin-3 treatment. This was unexpected considering the low frequency of p53 mutations and the amount of previous studies reporting on the relative sensitivity of hematological malignancies to Nutlin-3 induced cell death (157, 158). However, considerable variability has been demonstrated to affect cellular response upon Nutlin-3 treatment in wt-p53 cancer cells as well. Certain cancer cell lines have been reported to possess Nutlin-sensitivity over others (159, 160).

Despite the promise of restoring wt-p53 activity by HDM2 SMIs, the successful translation into the clinical has proven rather modest results. Clearly, researchers are only scratching the surface in terms of the overall complexity of p53, HDM2 and their

independent functions from each other. The question now becomes: how is it possible to fully harness p53 reactivation to eliminate cancer cells?

APPENDIX A

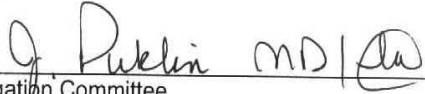
**WAYNE STATE
UNIVERSITY**

HUMAN INVESTIGATION COMMITTEE
101 East Alexandrine Building
Detroit, Michigan 48201
Phone: (313) 577-1628
FAX: (313) 993-7122
<http://hic.wayne.edu>



NOTICE OF EXPEDITED APPROVAL

To: Angela Sosin
Cancer Biology
550 E. Canfield

From: James E. Puklin, M.D. 
Chairman, Human Investigation Committee

Date: July 31, 2009

RE: HIC #: 071009MP2E
Protocol Title: Targeting MDM2 for Therapeutic Intervention in B-Cell Lymphoma
Sponsor: ° Internal Medicine
Protocol #: 0906007271

Expiration Date: July 30, 2010

Risk Level / Category: Research not involving greater than minimal risk

The above-referenced protocol and items listed below (if applicable) were **APPROVED** following *Expedited Review* (Category 5*) by the Chairperson/designee for the Wayne State University Behavioral Institutional Review Board (MP2) for the period of 07/31/2009 through 07/30/2010. This approval does not replace any departmental or other approvals that may be required.

- DMC Research Review Authorization, dated 07-20-09.
- Protocol Summary Form, revised 07-27-09.
- Protocol, revised 07-27-09.

- ° Federal regulations require that all research be reviewed at least annually. You may receive a "Continuation Renewal Reminder" approximately two months prior to the expiration date; however, it is the Principal Investigator's responsibility to obtain review and continued approval **before** the expiration date. Data collected during a period of lapsed approval is unapproved research and can **never** be reported or published as research data.
- ° All changes or amendments to the above-referenced protocol require review and approval by the HIC **BEFORE** implementation.
- ° Adverse Reactions/Unexpected Events (AR/UE) must be submitted on the appropriate form within the timeframe specified in the HIC Policy (<http://www.hic.wayne.edu/hicpol.html>).

NOTE:

1. Upon notification of an impending regulatory site visit, hold notification, and/or external audit the HIC office must be contacted immediately.
2. Forms should be downloaded from the HIC website at **each** use.

*Based on the Expedited Review List, revised November 1998

REFERENCES

1. Siegel R, Naishadham D, Jemal A. Cancer statistics, 2012. *CA Cancer J Clin.* 2012;62:10-29.
2. Howlader N NA, Krapcho M, Neyman N, Aminou R, Waldron W, Altekruse SF, Kosary CL, Ruhl J, Tatalovich Z, Cho H, Mariotto A, Eisner MP, Lewis DR, Chen HS, Feuer EJ, Cronin KA, Edwards BK (eds). SEER Cancer Statistics Review, 1975-2008, National Cancer Institute. Bethesda, MD, http://seer.cancer.gov/csr/1975_2008/, based on November 2010 SEER data submission, posted to the SEER web site, 2011.
3. Hicks EB, Rappaport H, Winter WJ. Follicular lymphoma; a re-evaluation of its position in the scheme of malignant lymphoma, based on a survey of 253 cases. *Cancer.* 1956;9:792-821.
4. Rappaport H, Wright DH, Dorfman RF. Suggested criteria for the diagnosis of Burkitt's tumor. *Cancer Res.* 1967;27:2632.
5. Harris NL, Jaffe ES, Diebold J, Flandrin G, Muller-Hermelink HK, Vardiman J, et al. The World Health Organization classification of neoplastic diseases of the hematopoietic and lymphoid tissues. Report of the Clinical Advisory Committee meeting, Airlie House, Virginia, November, 1997. *Ann Oncol.* 1999;10:1419-32.
6. Rosenberg SA, Kaplan HS. Evidence for an orderly progression in the spread of Hodgkin's disease. *Cancer Res.* 1966;26:1225-31.
7. Lister TA, Crowther D, Sutcliffe SB, Glatstein E, Canellos GP, Young RC, et al. Report of a committee convened to discuss the evaluation and staging of patients with Hodgkin's disease: Cotswolds meeting. *J Clin Oncol.* 1989;7:1630-6.

8. Carbone PP, Kaplan HS, Musshoff K, Smithers DW, Tubiana M. Report of the Committee on Hodgkin's Disease Staging Classification. *Cancer Res.* 1971;31:1860-1.
9. Jakic-Razumovic J, Aurer I. The World Health Organization classification of lymphomas. *Croat Med J.* 2002;43:527-34.
10. Armitage JO. Staging non-Hodgkin lymphoma. *CA Cancer J Clin.* 2005;55:368-76.
11. Shipp MA. Prognostic factors in aggressive non-Hodgkin's lymphoma: who has "high-risk" disease? *Blood.* 1994;83:1165-73.
12. Armitage JO, Weisenburger DD. New approach to classifying non-Hodgkin's lymphomas: clinical features of the major histologic subtypes. Non-Hodgkin's Lymphoma Classification Project. *J Clin Oncol.* 1998;16:2780-95.
13. Pileri SA, Falini B. Mantle cell lymphoma. *Haematologica.* 2009;94:1488-92.
14. Vitolo U, Ferreri AJ, Montoto S. Follicular lymphomas. *Crit Rev Oncol Hematol.* 2008;66:248-61.
15. Buske C, Hoster E, Dreyling M, Hasford J, Unterhalt M, Hiddemann W. The Follicular Lymphoma International Prognostic Index (FLIPI) separates high-risk from intermediate- or low-risk patients with advanced-stage follicular lymphoma treated front-line with rituximab and the combination of cyclophosphamide, doxorubicin, vincristine, and prednisone (R-CHOP) with respect to treatment outcome. *Blood.* 2006;108:1504-8.
16. Hjalgrim H, Askling J, Pukkala E, Hansen S, Munksgaard L, Frisch M. Incidence of Hodgkin's disease in Nordic countries. *Lancet.* 2001;358:297-8.
17. Hodgkin. On some Morbid Appearances of the Absorbent Glands and Spleen.

- Med Chir Trans. 1832;17:68-114.
18. Poppema S DG, Pileri S. . Nodular lymphocyte predominant Hodgkin lymphoma. In: Swerdlow S CE, Harris NL, editor. WHO Classification of Tumors of the Hematopoietic and Lymphoid Tissue. Lyon, France: IARC; 2008. p. 323-5.
 19. Fisher RI, Gaynor ER, Dahlberg S, Oken MM, Grogan TM, Mize EM, et al. Comparison of a standard regimen (CHOP) with three intensive chemotherapy regimens for advanced non-Hodgkin's lymphoma. N Engl J Med. 1993;328:1002-6.
 20. Duggan DB, Petroni GR, Johnson JL, Glick JH, Fisher RI, Connors JM, et al. Randomized comparison of ABVD and MOPP/ABV hybrid for the treatment of advanced Hodgkin's disease: report of an intergroup trial. J Clin Oncol. 2003;21:607-14.
 21. Bonadonna G, Zucali R, Monfardini S, De Lena M, Uslenghi C. Combination chemotherapy of Hodgkin's disease with adriamycin, bleomycin, vinblastine, and imidazole carboxamide versus MOPP. Cancer. 1975;36:252-9.
 22. Canellos GP, Anderson JR, Propert KJ, Nissen N, Cooper MR, Henderson ES, et al. Chemotherapy of advanced Hodgkin's disease with MOPP, ABVD, or MOPP alternating with ABVD. N Engl J Med. 1992;327:1478-84.
 23. Bonfante V, Santoro A, Viviani S, Devizzi L, Balzarotti M, Soncini F, et al. Outcome of patients with Hodgkin's disease failing after primary MOPP-ABVD. J Clin Oncol. 1997;15:528-34.
 24. Longo DL, Duffey PL, Young RC, Hubbard SM, Ihde DC, Glatstein E, et al. Conventional-dose salvage combination chemotherapy in patients relapsing with Hodgkin's disease after combination chemotherapy: the low probability for cure. J

- Clin Oncol. 1992;10:210-8.
25. Coiffier B, Lepage E, Briere J, Herbrecht R, Tilly H, Bouabdallah R, et al. CHOP chemotherapy plus rituximab compared with CHOP alone in elderly patients with diffuse large-B-cell lymphoma. *N Engl J Med*. 2002;346:235-42.
 26. Marcus R, Imrie K, Belch A, Cunningham D, Flores E, Catalano J, et al. CVP chemotherapy plus rituximab compared with CVP as first-line treatment for advanced follicular lymphoma. *Blood*. 2005;105:1417-23.
 27. Czuczman MS, Weaver R, Alkuzweny B, Berlfein J, Grillo-Lopez AJ. Prolonged clinical and molecular remission in patients with low-grade or follicular non-Hodgkin's lymphoma treated with rituximab plus CHOP chemotherapy: 9-year follow-up. *J Clin Oncol*. 2004;22:4711-6.
 28. Gaidano G, Pastore C, Capello D, Cilli V, Saglio G. Molecular pathways in low grade B-cell lymphoma. *Leuk Lymphoma*. 1997;26 Suppl 1:107-13.
 29. Seto M. Molecular mechanisms of lymphomagenesis through transcriptional dysregulation by chromosome translocation. *Int J Hematol*. 2002;76 Suppl 1:323-6.
 30. Rock KL, Goldberg AL. Degradation of cell proteins and the generation of MHC class I-presented peptides. *Annu Rev Immunol*. 1999;17:739-79.
 31. Glickman MH, Ciechanover A. The ubiquitin-proteasome proteolytic pathway: destruction for the sake of construction. *Physiol Rev*. 2002;82:373-428.
 32. Grune T, Merker K, Sandig G, Davies KJ. Selective degradation of oxidatively modified protein substrates by the proteasome. *Biochem Biophys Res Commun*. 2003;305:709-18.
 33. Welchman RL, Gordon C, Mayer RJ. Ubiquitin and ubiquitin-like proteins as

- multifunctional signals. *Nat Rev Mol Cell Biol.* 2005;6:599-609.
34. Pickart CM. Mechanisms underlying ubiquitination. *Annu Rev Biochem.* 2001;70:503-33.
 35. Kress M, May E, Cassingena R, May P. Simian virus 40-transformed cells express new species of proteins precipitable by anti-simian virus 40 tumor serum. *J Virol.* 1979;31:472-83.
 36. Linzer DI, Levine AJ. Characterization of a 54K dalton cellular SV40 tumor antigen present in SV40-transformed cells and uninfected embryonal carcinoma cells. *Cell.* 1979;17:43-52.
 37. Finlay CA, Hinds PW, Levine AJ. The p53 proto-oncogene can act as a suppressor of transformation. *Cell.* 1989;57:1083-93.
 38. Baker SJ, Fearon ER, Nigro JM, Hamilton SR, Preisinger AC, Jessup JM, et al. Chromosome 17 deletions and p53 gene mutations in colorectal carcinomas. *Science.* 1989;244:217-21.
 39. Takahashi T, Nau MM, Chiba I, Birrer MJ, Rosenberg RK, Vinocour M, et al. p53: a frequent target for genetic abnormalities in lung cancer. *Science.* 1989;246:491-4.
 40. Harvey M, McArthur MJ, Montgomery CA, Jr., Butel JS, Bradley A, Donehower LA. Spontaneous and carcinogen-induced tumorigenesis in p53-deficient mice. *Nat Genet.* 1993;5:225-9.
 41. Soussi T, Wiman KG. Shaping genetic alterations in human cancer: the p53 mutation paradigm. *Cancer Cell.* 2007;12:303-12.
 42. Hollstein M, Sidransky D, Vogelstein B, Harris CC. p53 mutations in human cancers. *Science.* 1991;253:49-53.

43. McBride OW, Merry D, Givol D. The gene for human p53 cellular tumor antigen is located on chromosome 17 short arm (17p13). *Proc Natl Acad Sci U S A*. 1986;83:130-4.
44. Malkin D. The role of p53 in human cancer. *J Neurooncol*. 2001;51:231-43.
45. Baptiste N, Friedlander P, Chen X, Prives C. The proline-rich domain of p53 is required for cooperation with anti-neoplastic agents to promote apoptosis of tumor cells. *Oncogene*. 2002;21:9-21.
46. Prokocimer M, Unger R, Rennert HS, Rotter V, Rennert G. Pooled analysis of p53 mutations in hematological malignancies. *Hum Mutat*. 1998;12:4-18.
47. Hainaut P, Hollstein M. p53 and human cancer: the first ten thousand mutations. *Adv Cancer Res*. 2000;77:81-137.
48. Rivlin N, Brosh R, Oren M, Rotter V. Mutations in the p53 Tumor Suppressor Gene: Important Milestones at the Various Steps of Tumorigenesis. *Genes Cancer*. 2011;2:466-74.
49. Kato S, Han SY, Liu W, Otsuka K, Shibata H, Kanamaru R, et al. Understanding the function-structure and function-mutation relationships of p53 tumor suppressor protein by high-resolution missense mutation analysis. *Proc Natl Acad Sci U S A*. 2003;100:8424-9.
50. Moller MB, Ino Y, Gerdes AM, Skjodt K, Louis DN, Pedersen NT. Aberrations of the p53 pathway components p53, MDM2 and CDKN2A appear independent in diffuse large B cell lymphoma. *Leukemia*. 1999;13:453-9.
51. Murray-Zmijewski F, Lane DP, Bourdon JC. p53/p63/p73 isoforms: an orchestra of isoforms to harmonise cell differentiation and response to stress. *Cell Death Differ*. 2006;13:962-72.

52. Oren M. Regulation of the p53 tumor suppressor protein. *J Biol Chem.* 1999;274:36031-4.
53. Kortlever RM, Higgins PJ, Bernards R. Plasminogen activator inhibitor-1 is a critical downstream target of p53 in the induction of replicative senescence. *Nat Cell Biol.* 2006;8:877-84.
54. Gatz SA, Wiesmuller L. p53 in recombination and repair. *Cell Death Differ.* 2006;13:1003-16.
55. Crichton D, Wilkinson S, O'Prey J, Syed N, Smith P, Harrison PR, et al. DRAM, a p53-induced modulator of autophagy, is critical for apoptosis. *Cell.* 2006;126:121-34.
56. Green DR, Chipuk JE. p53 and metabolism: Inside the TIGAR. *Cell.* 2006;126:30-2.
57. Teodoro JG, Parker AE, Zhu X, Green MR. p53-mediated inhibition of angiogenesis through up-regulation of a collagen prolyl hydroxylase. *Science.* 2006;313:968-71.
58. Brooks CL, Li M, Hu M, Shi Y, Gu W. The p53--Mdm2--HAUSP complex is involved in p53 stabilization by HAUSP. *Oncogene.* 2007;26:7262-6.
59. Zhang Y, Xiong Y, Yarbrough WG. ARF promotes MDM2 degradation and stabilizes p53: ARF-INK4a locus deletion impairs both the Rb and p53 tumor suppression pathways. *Cell.* 1998;92:725-34.
60. Pomerantz J, Schreiber-Agus N, Liegeois NJ, Silverman A, Alland L, Chin L, et al. The Ink4a tumor suppressor gene product, p19Arf, interacts with MDM2 and neutralizes MDM2's inhibition of p53. *Cell.* 1998;92:713-23.
61. Giaccia AJ, Kastan MB. The complexity of p53 modulation: emerging patterns

- from divergent signals. *Genes Dev.* 1998;12:2973-83.
62. Levine AJ, Oren M. The first 30 years of p53: growing ever more complex. *Nat Rev Cancer.* 2009;9:749-58.
63. de Toledo SM, Azzam EI, Dahlberg WK, Gooding TB, Little JB. ATM complexes with HDM2 and promotes its rapid phosphorylation in a p53-independent manner in normal and tumor human cells exposed to ionizing radiation. *Oncogene.* 2000;19:6185-93.
64. Perry ME, Piette J, Zawadzki JA, Harvey D, Levine AJ. The mdm-2 gene is induced in response to UV light in a p53-dependent manner. *Proc Natl Acad Sci U S A.* 1993;90:11623-7.
65. Peller S, Rotter V. TP53 in hematological cancer: low incidence of mutations with significant clinical relevance. *Hum Mutat.* 2003;21:277-84.
66. Gudkov AV, Komarova EA. The role of p53 in determining sensitivity to radiotherapy. *Nat Rev Cancer.* 2003;3:117-29.
67. Slatter TL, Ganesan P, Holzhauer C, Mehta R, Rubio C, Williams G, et al. p53-mediated apoptosis prevents the accumulation of progenitor B cells and B-cell tumors. *Cell Death Differ.* 2010;17:540-50.
68. Mitani N, Niwa Y, Okamoto Y. Surveyor nuclease-based detection of p53 gene mutations in haematological malignancy. *Ann Clin Biochem.* 2007;44:557-9.
69. Evan GI, Vousden KH. Proliferation, cell cycle and apoptosis in cancer. *Nature.* 2001;411:342-8.
70. Stilgenbauer S, Bullinger L, Lichter P, Dohner H. Genetics of chronic lymphocytic leukemia: genomic aberrations and V(H) gene mutation status in pathogenesis and clinical course. *Leukemia.* 2002;16:993-1007.

71. Sablina AA, Budanov AV, Ilyinskaya GV, Agapova LS, Kravchenko JE, Chumakov PM. The antioxidant function of the p53 tumor suppressor. *Nat Med.* 2005;11:1306-13.
72. Post SM, Quintas-Cardama A, Terzian T, Smith C, Eischen CM, Lozano G. p53-dependent senescence delays Emu-myc-induced B-cell lymphomagenesis. *Oncogene.* 2010;29:1260-9.
73. Bristol ML, Di X, Beckman MJ, Wilson EN, Henderson SC, Maiti A, et al. Dual functions of autophagy in the response of breast tumor cells to radiation: Cytoprotective autophagy with radiation alone and cytotoxic autophagy in radiosensitization by vitamin D 3. *Autophagy.* 2012;8.
74. Amrein L, Soulieres D, Johnston JB, Aloyz R. p53 and autophagy contribute to dasatinib resistance in primary CLL lymphocytes. *Leuk Res.* 2011;35:99-102.
75. Levine AJ. p53, the cellular gatekeeper for growth and division. *Cell.* 1997;88:323-31.
76. Wu X, Bayle JH, Olson D, Levine AJ. The p53-mdm-2 autoregulatory feedback loop. *Genes Dev.* 1993;7:1126-32.
77. Lee DH, Goldberg AL. Proteasome inhibitors: valuable new tools for cell biologists. *Trends Cell Biol.* 1998;8:397-403.
78. Hershko A, Ciechanover A. The ubiquitin system. *Annu Rev Biochem.* 1998;67:425-79.
79. Haas AL, Warms JV, Hershko A, Rose IA. Ubiquitin-activating enzyme. Mechanism and role in protein-ubiquitin conjugation. *J Biol Chem.* 1982;257:2543-8.
80. de Bie P, Ciechanover A. Ubiquitination of E3 ligases: self-regulation of the

- ubiquitin system via proteolytic and non-proteolytic mechanisms. *Cell Death Differ.* 2011;18:1393-402.
81. Haglund K, Di Fiore PP, Dikic I. Distinct monoubiquitin signals in receptor endocytosis. *Trends Biochem Sci.* 2003;28:598-603.
 82. Coux O, Tanaka K, Goldberg AL. Structure and functions of the 20S and 26S proteasomes. *Annu Rev Biochem.* 1996;65:801-47.
 83. Wilkinson KD. Ubiquitination and deubiquitination: targeting of proteins for degradation by the proteasome. *Semin Cell Dev Biol.* 2000;11:141-8.
 84. Song MS, Salmena L, Carracedo A, Egia A, Lo-Coco F, Teruya-Feldstein J, et al. The deubiquitylation and localization of PTEN are regulated by a HAUSP-PML network. *Nature.* 2008;455:813-7.
 85. Meulmeester E, Maurice MM, Boutell C, Teunisse AF, Ovaa H, Abraham TE, et al. Loss of HAUSP-mediated deubiquitination contributes to DNA damage-induced destabilization of Hdmx and Hdm2. *Mol Cell.* 2005;18:565-76.
 86. Zauberman A, Flusberg D, Haupt Y, Barak Y, Oren M. A functional p53-responsive intronic promoter is contained within the human mdm2 gene. *Nucleic Acids Res.* 1995;23:2584-92.
 87. Momand J, Wu HH, Dasgupta G. MDM2--master regulator of the p53 tumor suppressor protein. *Gene.* 2000;242:15-29.
 88. Brown CY, Mize GJ, Pineda M, George DL, Morris DR. Role of two upstream open reading frames in the translational control of oncogene mdm2. *Oncogene.* 1999;18:5631-7.
 89. Cheng TH, Cohen SN. Human MDM2 isoforms translated differentially on constitutive versus p53-regulated transcripts have distinct functions in the

- p53/MDM2 and TSG101/MDM2 feedback control loops. *Mol Cell Biol.* 2007;27:111-9.
90. Barak Y, Gottlieb E, Juven-Gershon T, Oren M. Regulation of mdm2 expression by p53: alternative promoters produce transcripts with nonidentical translation potential. *Genes Dev.* 1994;8:1739-49.
 91. Oliner JD, Pietenpol JA, Thiagalingam S, Gyuris J, Kinzler KW, Vogelstein B. Oncoprotein MDM2 conceals the activation domain of tumour suppressor p53. *Nature.* 1993;362:857-60.
 92. Haupt Y, Maya R, Kazaz A, Oren M. Mdm2 promotes the rapid degradation of p53. *Nature.* 1997;387:296-9.
 93. Hock A, Vousden KH. Regulation of the p53 pathway by ubiquitin and related proteins. *Int J Biochem Cell Biol.* 2010;42:1618-21.
 94. Honda R, Yasuda H. Activity of MDM2, a ubiquitin ligase, toward p53 or itself is dependent on the RING finger domain of the ligase. *Oncogene.* 2000;19:1473-6.
 95. Fang S, Jensen JP, Ludwig RL, Vousden KH, Weissman AM. Mdm2 is a RING finger-dependent ubiquitin protein ligase for itself and p53. *J Biol Chem.* 2000;275:8945-51.
 96. Stommel JM, Wahl GM. A new twist in the feedback loop: stress-activated MDM2 destabilization is required for p53 activation. *Cell Cycle.* 2005;4:411-7.
 97. Stommel JM, Wahl GM. Accelerated MDM2 auto-degradation induced by DNA-damage kinases is required for p53 activation. *EMBO J.* 2004;23:1547-56.
 98. Iwakuma T, Lozano G. MDM2, an introduction. *Mol Cancer Res.* 2003;1:993-1000.
 99. Moll UM, Petrenko O. The MDM2-p53 interaction. *Mol Cancer Res.* 2003;1:1001-

- 8.
100. Watanabe T, Hotta T, Ichikawa A, Kinoshita T, Nagai H, Uchida T, et al. The MDM2 oncogene overexpression in chronic lymphocytic leukemia and low-grade lymphoma of B-cell origin. *Blood*. 1994;84:3158-65.
101. Chilosì M, Doglioni C, Menestrina F, Montagna L, Rigo A, Lestani M, et al. Abnormal expression of the p53-binding protein MDM2 in Hodgkin's disease. *Blood*. 1994;84:4295-300.
102. Shanmugham A, Ovaa H. DUBs and disease: activity assays for inhibitor development. *Curr Opin Drug Discov Devel*. 2008;11:688-96.
103. Guedat P, Colland F. Patented small molecule inhibitors in the ubiquitin proteasome system. *BMC Biochem*. 2007;8 Suppl 1:S14.
104. Hjerpe R, Rodriguez MS. Alternative UPS drug targets upstream the 26S proteasome. *Int J Biochem Cell Biol*. 2008;40:1126-40.
105. Daviet L, Colland F. Targeting ubiquitin specific proteases for drug discovery. *Biochimie*. 2008;90:270-83.
106. LeBlanc R, Catley LP, Hideshima T, Lentzsch S, Mitsiades CS, Mitsiades N, et al. Proteasome inhibitor PS-341 inhibits human myeloma cell growth in vivo and prolongs survival in a murine model. *Cancer Res*. 2002;62:4996-5000.
107. Kanayama H, Tanaka K, Aki M, Kagawa S, Miyaji H, Satoh M, et al. Changes in expressions of proteasome and ubiquitin genes in human renal cancer cells. *Cancer Res*. 1991;51:6677-85.
108. Kumatori A, Tanaka K, Inamura N, Sone S, Ogura T, Matsumoto T, et al. Abnormally high expression of proteasomes in human leukemic cells. *Proc Natl Acad Sci U S A*. 1990;87:7071-5.

109. Voorhees PM, Dees EC, O'Neil B, Orlowski RZ. The proteasome as a target for cancer therapy. *Clin Cancer Res.* 2003;9:6316-25.
110. Adams J, Palombella VJ, Sausville EA, Johnson J, Destree A, Lazarus DD, et al. Proteasome inhibitors: a novel class of potent and effective antitumor agents. *Cancer Res.* 1999;59:2615-22.
111. Traenckner EB, Wilk S, Baeuerle PA. A proteasome inhibitor prevents activation of NF-kappa B and stabilizes a newly phosphorylated form of I kappa B-alpha that is still bound to NF-kappa B. *EMBO J.* 1994;13:5433-41.
112. Kane RC, Farrell AT, Sridhara R, Pazdur R. United States Food and Drug Administration approval summary: bortezomib for the treatment of progressive multiple myeloma after one prior therapy. *Clin Cancer Res.* 2006;12:2955-60.
113. Kane RC, Dagher R, Farrell A, Ko CW, Sridhara R, Justice R, et al. Bortezomib for the treatment of mantle cell lymphoma. *Clin Cancer Res.* 2007;13:5291-4.
114. O'Connor OA. The emerging role of bortezomib in the treatment of indolent non-Hodgkin's and mantle cell lymphomas. *Curr Treat Options Oncol.* 2004;5:269-81.
115. Goy A, Younes A, McLaughlin P, Pro B, Romaguera JE, Hagemester F, et al. Phase II study of proteasome inhibitor bortezomib in relapsed or refractory B-cell non-Hodgkin's lymphoma. *J Clin Oncol.* 2005;23:667-75.
116. Gerecitano J, Goy A, Wright J, MacGregor-Cortelli B, Neylon E, Gonen M, et al. Drug-induced cutaneous vasculitis in patients with non-Hodgkin lymphoma treated with the novel proteasome inhibitor bortezomib: a possible surrogate marker of response? *Br J Haematol.* 2006;134:391-8.
117. Lonial S, Waller EK, Richardson PG, Jagannath S, Orlowski RZ, Giver CR, et al. Risk factors and kinetics of thrombocytopenia associated with bortezomib for

- relapsed, refractory multiple myeloma. *Blood*. 2005;106:3777-84.
118. Ding K, Lu Y, Nikolovska-Coleska Z, Wang G, Qiu S, Shangary S, et al. Structure-based design of spiro-oxindoles as potent, specific small-molecule inhibitors of the MDM2-p53 interaction. *J Med Chem*. 2006;49:3432-5.
119. Bianco R, Caputo R, Damiano V, De Placido S, Ficorella C, Agrawal S, et al. Combined targeting of epidermal growth factor receptor and MDM2 by gefitinib and antisense MDM2 cooperatively inhibit hormone-independent prostate cancer. *Clin Cancer Res*. 2004;10:4858-64.
120. Chene P, Fuchs J, Carena I, Furet P, Garcia-Echeverria C. Study of the cytotoxic effect of a peptidic inhibitor of the p53-hdm2 interaction in tumor cells. *FEBS Lett*. 2002;529:293-7.
121. Castanotto D, Li JR, Michienzi A, Langlois MA, Lee NS, Puymirat J, et al. Intracellular ribozyme applications. *Biochem Soc Trans*. 2002;30:1140-5.
122. Kaeser MD, Pebernard S, Iggo RD. Regulation of p53 stability and function in HCT116 colon cancer cells. *J Biol Chem*. 2004;279:7598-605.
123. Zhang Z, Li M, Wang H, Agrawal S, Zhang R. Antisense therapy targeting MDM2 oncogene in prostate cancer: Effects on proliferation, apoptosis, multiple gene expression, and chemotherapy. *Proc Natl Acad Sci U S A*. 2003;100:11636-41.
124. Wang H, Nan L, Yu D, Agrawal S, Zhang R. Antisense anti-MDM2 oligonucleotides as a novel therapeutic approach to human breast cancer: in vitro and in vivo activities and mechanisms. *Clin Cancer Res*. 2001;7:3613-24.
125. Shangary S, Wang S. Targeting the MDM2-p53 interaction for cancer therapy. *Clin Cancer Res*. 2008;14:5318-24.
126. Vassilev LT, Vu BT, Graves B, Carvajal D, Podlaski F, Filipovic Z, et al. In vivo

- activation of the p53 pathway by small-molecule antagonists of MDM2. *Science*. 2004;303:844-8.
127. Ding K, Lu Y, Nikolovska-Coleska Z, Qiu S, Ding Y, Gao W, et al. Structure-based design of potent non-peptide MDM2 inhibitors. *J Am Chem Soc*. 2005;127:10130-1.
 128. Kussie PH, Gorina S, Marechal V, Elenbaas B, Moreau J, Levine AJ, et al. Structure of the MDM2 oncoprotein bound to the p53 tumor suppressor transactivation domain. *Science*. 1996;274:948-53.
 129. Kojima K, Burks JK, Arts J, Andreeff M. The novel tryptamine derivative JNJ-26854165 induces wild-type p53- and E2F1-mediated apoptosis in acute myeloid and lymphoid leukemias. *Mol Cancer Ther*. 2010;9:2545-57.
 130. Newcomb EW. P53 gene mutations in lymphoid diseases and their possible relevance to drug resistance. *Leuk Lymphoma*. 1995;17:211-21.
 131. Koduru PR, Raju K, Vadmal V, Menezes G, Shah S, Susin M, et al. Correlation between mutation in P53, p53 expression, cytogenetics, histologic type, and survival in patients with B-cell non-Hodgkin's lymphoma. *Blood*. 1997;90:4078-91.
 132. Krug U, Ganser A, Koeffler HP. Tumor suppressor genes in normal and malignant hematopoiesis. *Oncogene*. 2002;21:3475-95.
 133. Mohammad RM, Mohamed AN, Smith MR, Jawadi NS, al-Katib A. A unique EBV-negative low-grade lymphoma line (WSU-FSCCL) exhibiting both t(14;18) and t(8;11). *Cancer Genet Cytogenet*. 1993;70:62-7.
 134. Al-Katib AM, Smith MR, Kamanda WS, Pettit GR, Hamdan M, Mohamed AN, et al. Bryostatins 1 down-regulates mdr1 and potentiates vincristine cytotoxicity in

- diffuse large cell lymphoma xenografts. *Clin Cancer Res.* 1998;4:1305-14.
135. al-Katib A, Mohammad R, Hamdan M, Mohamed AN, Dan M, Smith MR. Propagation of Waldenstrom's macroglobulinemia cells in vitro and in severe combined immune deficient mice: utility as a preclinical drug screening model. *Blood.* 1993;81:3034-42.
136. Wang JL, Liu D, Zhang ZJ, Shan S, Han X, Srinivasula SM, et al. Structure-based discovery of an organic compound that binds Bcl-2 protein and induces apoptosis of tumor cells. *Proc Natl Acad Sci U S A.* 2000;97:7124-9.
137. Mohammad RM, Wu J, Azmi AS, Aboukameel A, Sosin A, Wu S, et al. An MDM2 antagonist (MI-319) restores p53 functions and increases the life span of orally treated follicular lymphoma bearing animals. *Mol Cancer.* 2009;8:115.
138. Livak KJ, Schmittgen TD. Analysis of relative gene expression data using real-time quantitative PCR and the $2^{-(\Delta\Delta C(T))}$ Method. *Methods.* 2001;25:402-8.
139. Shangary S, Qin D, McEachern D, Liu M, Miller RS, Qiu S, et al. Temporal activation of p53 by a specific MDM2 inhibitor is selectively toxic to tumors and leads to complete tumor growth inhibition. *Proc Natl Acad Sci U S A.* 2008;105:3933-8.
140. Xia M, Knezevic D, Tovar C, Huang B, Heimbrook DC, Vassilev LT. Elevated MDM2 boosts the apoptotic activity of p53-MDM2 binding inhibitors by facilitating MDMX degradation. *Cell Cycle.* 2008;7:1604-12.
141. Vogelstein B, Lane D, Levine AJ. Surfing the p53 network. *Nature.* 2000;408:307-10.
142. Chene P. Inhibiting the p53-MDM2 interaction: an important target for cancer

- therapy. *Nat Rev Cancer*. 2003;3:102-9.
143. Vousden KH, Lu X. Live or let die: the cell's response to p53. *Nat Rev Cancer*. 2002;2:594-604.
 144. Tabernero J, Dirix L, Schoffski P, Cervantes A, Lopez-Martin JA, Capdevila J, et al. A phase I first-in-human pharmacokinetic and pharmacodynamic study of serdemetan in patients with advanced solid tumors. *Clin Cancer Res*. 2011;17:6313-21.
 145. Thiagarajan P, Tait JF. Binding of annexin V/placental anticoagulant protein I to platelets. Evidence for phosphatidylserine exposure in the procoagulant response of activated platelets. *J Biol Chem*. 1990;265:17420-3.
 146. Pishas KI, Al-Ejeh F, Zinonos I, Kumar R, Evdokiou A, Brown MP, et al. Nutlin-3a is a potential therapeutic for ewing sarcoma. *Clin Cancer Res*. 2011;17:494-504.
 147. Drakos E, Atsaves V, Schlette E, Li J, Papanastasi I, Rassidakis GZ, et al. The therapeutic potential of p53 reactivation by nutlin-3a in ALK+ anaplastic large cell lymphoma with wild-type or mutated p53. *Leukemia*. 2009;23:2290-9.
 148. Drakos E, Singh RR, Rassidakis GZ, Schlette E, Li J, Claret FX, et al. Activation of the p53 pathway by the MDM2 inhibitor nutlin-3a overcomes BCL2 overexpression in a preclinical model of diffuse large B-cell lymphoma associated with t(14;18)(q32;q21). *Leukemia*. 2011.
 149. Patton JT, Mayo LD, Singhi AD, Gudkov AV, Stark GR, Jackson MW. Levels of HdmX expression dictate the sensitivity of normal and transformed cells to Nutlin-3. *Cancer Res*. 2006;66:3169-76.
 150. Gu L, Zhu N, Findley HW, Zhou M. MDM2 antagonist nutlin-3 is a potent inducer of apoptosis in pediatric acute lymphoblastic leukemia cells with wild-type p53

- and overexpression of MDM2. *Leukemia*. 2008;22:730-9.
151. Wade M, Rodewald LW, Espinosa JM, Wahl GM. BH3 activation blocks Hdmx suppression of apoptosis and cooperates with Nutlin to induce cell death. *Cell Cycle*. 2008;7:1973-82.
 152. Shen H, Moran DM, Maki CG. Transient nutlin-3a treatment promotes endoreduplication and the generation of therapy-resistant tetraploid cells. *Cancer Res*. 2008;68:8260-8.
 153. Laurie NA, Donovan SL, Shih CS, Zhang J, Mills N, Fuller C, et al. Inactivation of the p53 pathway in retinoblastoma. *Nature*. 2006;444:61-6.
 154. Rinaldo C, Prodosmo A, Siepi F, Moncada A, Sacchi A, Selivanova G, et al. HIPK2 regulation by MDM2 determines tumor cell response to the p53-reactivating drugs nutlin-3 and RITA. *Cancer Res*. 2009;69:6241-8.
 155. Murray-Zmijewski F, Slee EA, Lu X. A complex barcode underlies the heterogeneous response of p53 to stress. *Nat Rev Mol Cell Biol*. 2008;9:702-12.
 156. Krajewski M, Ozdowy P, D'Silva L, Rothweiler U, Holak TA. NMR indicates that the small molecule RITA does not block p53-MDM2 binding in vitro. *Nat Med*. 2005;11:1135-6; author reply 6-7.
 157. Kojima K, Konopleva M, Samudio IJ, Shikami M, Cabreira-Hansen M, McQueen T, et al. MDM2 antagonists induce p53-dependent apoptosis in AML: implications for leukemia therapy. *Blood*. 2005;106:3150-9.
 158. Stuhmer T, Chatterjee M, Hildebrandt M, Herrmann P, Gollasch H, Gerecke C, et al. Nongenotoxic activation of the p53 pathway as a therapeutic strategy for multiple myeloma. *Blood*. 2005;106:3609-17.
 159. Kitagawa M, Aonuma M, Lee SH, Fukutake S, McCormick F. E2F-1

transcriptional activity is a critical determinant of Mdm2 antagonist-induced apoptosis in human tumor cell lines. *Oncogene*. 2008;27:5303-14.

160. Logan IR, McNeill HV, Cook S, Lu X, Lunec J, Robson CN. Analysis of the MDM2 antagonist nutlin-3 in human prostate cancer cells. *Prostate*. 2007;67:900-6.

ABSTRACT**HDM2 SMALL-MOLECULE INHIBITORS FOR THERAPEUTIC INTERVENTION IN B-CELL LYMPHOMA**

by

ANGELA M. SOSIN**December 2012****Advisor:** Ayad M. Al-Katib, M.D.**Major:** Cancer Biology**Degree:** Doctor of Philosophy

Lymphomas frequently retain wild-type (wt) p53 function but overexpress HDM2, compromising p53 activity. Therefore, lymphoma is a suitable model for studying therapeutic value of disrupting HDM2-p53 association by small-molecule inhibitors (SMIs). HDM2 SMIs have been developed and are currently under various stages of preclinical and clinical investigation. This study examined various molecular mechanisms associated and biological effects of two different classes of HDM2 SMIs: the spiro-oxindoles (MI-219) and *cis*-imidazoline (Nutlin-3) in lymphoma cell lines and patient-derived B-lymphoma cells. Surprisingly, results revealed significant quantitative and qualitative differences between these two agents. At the molecular level, effect of Nutlin-3 was generally more delayed (48h) and was notable for inducing cell cycle arrest. These findings indicate a response to a low level cellular stress and are supported by lower levels of p53 expression in Nutlin-3-treated cells. In contrast, MI-219 triggered an earlier response (12-24h), predominantly in the form of cell death associated with higher levels of p53 expression. Neither agent interfered with the E3 ligase function of HDM2, as confirmed in a cell-free autoubiquitination assay.

Interestingly, these results report for the first time a novel mechanism of HDM2 antagonism by MI-219 in wt-p53 lymphoma cells that stimulates HDM2 self-ubiquitination. Additionally, it corresponds with biological response of anti-lymphoma activity and may provide an explanation for the differences in efficacy between MI-219 and Nutlin-3. This study indicates that p53-HDM2 interaction and methods of its disruption are more complex than is currently realized and suggests that stimulation of HDM2 self-ubiquitinating activity may be a novel treatment strategy for lymphoma.

AUTOBIOGRAPHICAL STATEMENT

Angela M. Sosin

Education:

- 2012 Ph.D. in Cancer Biology-Wayne State University School of Medicine, Detroit, MI (Minor: Pharmacology)
- 2005 B.S. in Microbiology and Molecular Genetics-Michigan State University, East Lansing, MI (Area of concentration: Cell and Molecular Biology; Medical Microbiology and Immunology)

Additional Training:

- 2011 Principals in Clinical Pharmacology-National Institute of Health, Bethesda, MD (Course consisting of 31 lectures on the fundamentals of clinical pharmacology as a translational scientific discipline emphasizing rational drug development and exploitation in therapeutics.)

Awards:

- 2010 & 2011 Cancer Biology Travel Grant Award, Wayne State University School of Medicine/Karmanos Cancer Institute
- 2007-2010 Interdisciplinary Biological Sciences Competitive Stipend, Wayne State University School of Medicine
- 2008 Departmental Housing Award, Wayne State University School of Medicine
- 2005 Honorable Mention-Student Employee of the Year (nominated), MSU
- 2002 Dean's List, Two-time recipient, College of Natural Science, Michigan State University

Publications:

1. **Sosin AM**, Hwang C, Heath EI. Clinical translation of angiogenesis inhibitors in renal cell carcinoma. In: Cancer Biology Review: A Case Based Approach. Stadler, W. and Winters, R. (Eds.), Demos Medical Publishing, New York, NY (expected in press: Winter 2013)
2. Shalhout S, **Sosin A**, Martin A, Holland T, Al-Katib A, Bhagwat AS. Germinal center derived B-cell lymphomas contain extensive DNA damage. (*in preparation*)
3. **Sosin AM**, Zhou W, Bluth MH. PDGF isoforms are differentially expressed in peripheral blood mononuclear cellular subsets. (*in preparation*)
4. **Sosin AM**, Burger AM, Siddiqi A, Abrams J, Mohammad RM, Al-Katib A. HDM2 antagonist MI-219 (spiro-oxindole), compared to Nutlin-3 (cis-imidazoline), regulates p53 through enhanced HDM2 autoubiquitination and degradation in human malignant B-cell lymphomas. *Journal of Hematology and Oncology*, 2012, 5: 57
5. Arnold AA, Aboukameel A, **Sosin A**, Smith P, Goustin AS, Mohammad RM, Al-Katib A. I-Kappa-Kinase-2 (IKK-2) inhibition potentiates vincristine cytotoxicity in non-Hodgkin's lymphoma. *Molecular Cancer*, 2010, 9: 228
6. Mohammad RM, Wu J, Azmi AS, Aboukameel A, **Sosin A**, Wu S, Yang D, Wang S., Al-Katib AM. An MDM2 antagonist (MI-319) restores functions and increases the life span of orally treated follicular lymphoma bearing animals. *Molecular Cancer*, 2009. 8: 115